A STUDY OF THE GAMMA DECAY OF EXCITED LEVELS OF ^{51}Ti

by

George Paul Lamaze

Department of Physics
Duke University

Date: Jan. 18, 1972

Approved:

N. Russell Roberson, Supervisor

Carl M. Rose

Richard Scott

An abstract of a dissertation submitted in partial fulfillment of the requirements for the degree of Doctor of Philosophy in the Department of Physics in the Graduate School of Arts and Sciences of Duke University

1971

ABSTRACT

(Physics)

A STUDY OF THE GAMMA DECAY OF EXCITED LEVELS OF ^{51}Ti

by

George Paul Lamaze

Department of Physics
Duke University

Date: _____

Approved:

_____
N. Russell Roberson, Supervisor

_____

_____

_____

_____

An abstract of a dissertation submitted in partial fulfillment of the requirements for the degree of Doctor of Philosophy in the Department of Physics in the Graduate School of Arts and Sciences of Duke University

1971

A STUDY OF THE GAMMA DECAY OF EXCITED LEVELS OF ^{51}Ti

by

George Paul Lamaze

The excited states of ^{51}Ti populated with the reaction ^{50}Ti(d,pγ)^{51}Ti have been studied with the angular-correlation method which utilizes a geometry of axial symmetry. The observed protons were detected in an annular semiconductor counter positioned at 180° relative to the beam direction. From the analysis of the experimental angular correlations, and in conjunction with known ℓ_n values for ^{51}Ti, a spin and parity assignment of $9/2^+$ was established for the level at 3774 keV. Correlations for other levels did not yield unique spin assignments. Branching ratios were measured for the levels at 1167, 2144, 2198, 2907, 3174, 4162, 4592, 4747, 4810, 4882, 5139, 5214, and 5440 keV. New levels were observed at 2346 keV and 5440 keV.

The reaction ^{48}Ca(α,nγ)^{51}Ti was also used to populate many levels of ^{51}Ti. The resultant decays were studied with n-γ coincidence techniques using a 30 cm^3 Ge(Li) detector, and with γ-γ coincidence techniques using 30 cm^3 and 80 cm^3 Ge(Li)

detectors. Five previously unreported levels were observed at 2733, 2755, 2922, 3235, and 3636 keV. Additionally, tentative assignment of three previously unreported levels was made. These levels are at 3473, 3619, and 5785 keV excitation.

The decay scheme of ^{51}Ti is compared with the other N = 29 nuclei (^{49}Ca, ^{53}Cr, ^{55}Fe, and ^{57}Ni). Comparisons are also made with model predictions of Ohnuma (1966) and Divadeenam (1971). These calculations succeed in accounting for the number of new levels seen.

ACKNOWLEDGMENTS

I wish to express my gratitude to Dr. N.R. Roberson who suggested this project and has given his continued interest and support during all phases of this work. I am indebted to Dr. D.R. Tilley for many helpful discussions related to both the measurements and the analysis of the data. I wish to thank Dr. C.R. Gould for our many discussions concerning experimental problems, for his help with computer programming, and for his assistance in taking data.

The assistance of Mr. E.C. Hagen in taking the data is deeply appreciated. I would like to thank Mr. S.E. Edwards for his help with the electronics and computers. I would like to thank Mr. R.L. Rummel and Mr. M.T. Smith for keeping the accelerator in excellent running condition. Thanks are also due to Mr. A.W. Lovette and Mr. E.P. Harris for many helpful discussions concerning the design of the angular correlation chamber.

I would like to thank Dr. D.J. Church for the use of his angular correlation code and Dr. S.M. Shafroth for the use of his target chamber and 80 cm^3 Ge(Li) detector for the γ-γ coincidence measurements. I am grateful to Drs. H.W. Newson and

E.G. Bilpuch for providing me with the research assistantship. Most of all I thank my wife, Catherine, for her continuous encouragement during all phases of my graduate education.

This work supported in part by the Atomic Energy Commission.

G. P. L.

CONTENTS

LIST OF FIGURES

LIST OF TABLES

A STUDY OF THE GAMMA DECAY OF EXCITED LEVELS OF ^{51}Ti

Chapter I

INTRODUCTION

A) Historical Background

The odd atomic mass nuclei ^{49}Ca, ^{51}Ti, ^{53}Cr, and ^{55}Fe with N = 29 have been studied extensively. The interest arises from the nearness of these nuclei to the shell model closure at N = 28.

Since the nucleus ^{48}Ca is doubly magic (Z = 20), the earlier studies of the low-lying levels of ^{49}Ca assumed the simple shell model picture of a single neutron in the $2p_{3/2}$, $2p_{1/2}$, or $1f_{5/2}$ shell. Kashy et al. (1962) using the reaction $^{48}Ca(d,p)^{49}Ca$ obtained ℓ-values and spectroscopic factors for many of the low-lying levels of ^{49}Ca. For the ground and first excited states $\left(1p_{3/2}, \text{ and } 1p_{1/2} \text{ shell model configurations}\right)$ spectroscopic factors of 1.03 and 1.33 respectively were obtained. These values are very close to the shell model predictions of 1.0. However, these authors found that the $1f_{5/2}$ level is fragmented into at least three levels which indicates the influence of ^{48}Ca core excitations.

The other nuclei in this series $\left(^{51}Ti, ^{53}Cr, \text{ and } ^{55}Fe\right)$ are more complex. Each of these nuclei have one neutron outside

the closed $1f_{7/2}$ shell and 2, 4, or 6 protons respectively in the $1f_{7/2}$ shell. In principal, a pure shell model calculation could be made for these N = 29 muclei which considered only those particles outside the inert ^{48}Ca core. A calculation of this type has been made by McGrory et al. (1970) for the structure of the $^{42-50}Ca$ isotopes. In this calculation, the ^{40}Ca core was assumed to be inert and the remaining neutrons were considered to be in the $1f_{7/2}$, $2p_{3/2}$, $2p_{1/2}$, or $1f_{5/2}$ orbits. Initial calculations were made using an effective interaction derived by Kuo and Brown (1968). This interaction was then modified to obtain results in better agreement with experiment. In this latter calculation, only those configurations with no more than two neutrons in the $2p_{1/2}$ and $1f_{5/2}$ orbits were allowed. With these modifications, the observed energy levels of the $1f_{7/2}$ states and of the strong $2p_{3/2}$ single particle states in $^{42-49}Ca$ are quite well reproduced, as are measured binding energies of the ground states with respect to ^{40}Ca. The calculated spectroscopic factors for $1f_{7/2}$ neutron transfers between the various calcium isotopes are also in good agreement with experiment. However, there are no calculated levels that correspond with the observed second 0^+ and 2^+ states in ^{42}Ca, ^{44}Ca, and ^{46}Ca. The authors suggest that these levels are due to core excitations.

Although McGrory et al.(1970) had very good success with shell model calculations, the calculations were very complicated and the number of possible configurations that could be treated was necessarily limited. In order to make the calculations more

manageable several authors have proposed models that make simplifying approximations.

Maxwell and Parkinson (1964), Vervier (1965), and Ohnuma (1966) all used similar shell model descriptions to explain the spectra of ^{51}Ti, ^{53}Cr, and ^{55}Fe. The simplifying assumption made by all of these authors was that the proton part of the shell model wave functions could be approximated by the ^{50}Ti, ^{52}Cr, and ^{54}Fe cores respectively. The ^{48}Ca core was assumed closed and a single neutron in the $2p_{3/2}$, $2p_{1/2}$, or $1f_{5/2}$ orbit was coupled to the possible $\left(1f_{7/2}\right)^n$ core states. The authors obtained the effective proton-proton interaction from the experimental spectra of ^{50}Ti, ^{52}Cr, and ^{54}Fe. Core states having configurations different from $\left(1f_{7/2}\right)^n$ were ignored. The three papers differed in their treatment of the neutron-proton interaction. Maxwell and Parkinson (1964) chose a neutron-proton interaction potential with a Gaussian radial dependence

$$V_{np} = V_0 \, e^{-r_{np}^2/r_0^2}\left(W + BP_\sigma + HP_\sigma P_r + MP_r\right)$$

where the P_σ and P_r are the spin exchange and space exchange operators, respectively. The coefficients W, B, H, and M give the strength of the various exchange potentials.

Both Vervier (1965) and Ohnuma (1966) assumed an interaction potential of the form

$$V_{np} = \left(V_0 + V_1(\sigma_n \cdot \sigma_p)\right) f(r_{np})$$

where σ_n and σ_p denote the spin of the neutron and proton respectively. Vervier (1965) assumed $f\left(r_{np}\right)$ to be a δ function while Ohnuma employed a Gaussian radial dependence for $f\left(r_{np}\right)$.

All three authors claimed quantitative agreement with experiment for the energy spectra and spectroscopic factors of levels below 2 MeV excitation. Above that energy the model appears to be inadequate. Maxwell and Parkinson (1964) discussed only levels with $J \leq 5/2$, Vervier (1965) those with $J \leq 7/2$, and Ohnuma those with $J \leq 15/2$.

Ramavataram (1963) interpreted the properties of the low-lying levels of ^{51}Ti, ^{53}Cr, and ^{55}Fe in terms of the unified model. In this model, the lowest shell model states for the odd neutron, in this case the $2p_{3/2}$, $2p_{1/2}$, and $1f_{5/2}$, were coupled to the ^{50}Ti, ^{52}Cr, and ^{54}Fe cores, respectively. The model assumed that the core excitations were collective in nature. The core was considered capable of performing quadrupole oscillations and the core-to-particle coupling was considered intermediate rather than weak (nuclei near double closed shells) or strong (deformed nuclei). States of up to three phonons were included in the calculations. The phonon energy of the vibrations was taken as a parameter rather than from the experimental spectra of the even cores. The strength of the core-particle interaction as well as the $2p_{1/2}$ - $2p_{3/2}$ and $1f_{5/2}$ - $2p_{3/2}$ single particle level distances were considered as free parameters which were allowed to vary for each nucleus. Qualitative agreement was obtained for the energy spectra and spectroscopic factors

of the low-lying levels of ^{51}Ti, ^{53}Cr, and ^{55}Fe. Only levels with $J \leq 7/2$ were considered.

Carola and Ohnuma (1971) also used the unified model to describe the low-lying levels of ^{53}Cr and ^{55}Fe. Energy levels, electromagnetic transition rates, branching ratios, mixing ratios, lifetimes and spectroscopic factors were calculated and compared with experimental results. Shell model calculations were also made in the same manner as Ohnuma (1966). The two approaches were compared and the authors concluded that both models yielded comparable results and were both in fair agreement with experimental data up to 2.5 MeV excitation.

Divadeenam and Beres (1969) have used the excited-core model as developed by Thankappan and True (1964) to predict properties of the low-lying levels of ^{51}Ti. In this model, a single nucleon was coupled to the even A core. The core to particle coupling was considered intermediate. The Hamiltonian takes the form

$$H = H_c + H_p + H_{int}$$

where H_c is the Hamiltonian describing the core. H_p is the Hamiltonian describing the particle moving in the average potential generated by the core, and H_{int} is the core to particle interaction. The form of H_{int} was assumed to be

$$H_{int} = -\xi\left(J_c^{(1)} \cdot j_p^{(1)}\right) - \eta\left(Q_c^{(2)} \cdot Q_p^{(2)}\right),$$

where J_c and j_p are, respectively, the total angular momentum operators for the core and particle, Q_c and Q_p are, respectively, the mass quadrupole moment operators of the core and particle, and ξ and η are parameters describing the strength of the interactions. The exact nature of the core states was not specified and the reduced matrix elements $\langle J_c' || Q_c || J_c \rangle$ for various J_c' and J_c were treated as parameters. The single particle energies $\left(2p_{3/2}, 2p_{1/2}, 1f_{1/2}, \text{and } 1g_{9/2}\right)$ were taken from the results of the $^{50}Ti(d,p)^{51}Ti$ experiment and the energy of the excited core states from the experimental energy spectra of ^{50}Ti.

Divadeenam and Beres (1969) account for the second $7/2^-$ level in ^{51}Ti by specifically including two neutron particle-one neutron hole states in their calculations. The core plus neutron--two particle-one hole matrix elements were treated as parameters. The authors obtain good agreement with experiment for energies and spectroscopic factors of most levels below 3.0 MeV excitation. The agreement between the calculated and experimental energy levels for the $5/2^-$ levels is only fair.

Each of the above models agrees to some extent with the known experimental data for ^{51}Ti, ^{53}Cr, and ^{55}Fe. However, the spins, mixing ratios, branching ratios, and lifetimes of many of the low-lying levels of these nuclei (^{51}Ti in particular) are still unknown. Much more experimental information is needed so that further comparisons with model predictions may be made.

B) Objectives of the Present Study and Notes on ^{51}Ti

The experimental work reported in this thesis was undertaken to determine spectroscopic information (excitation energies, branching ratios, spins, and mixing ratios) for some of the excited states of ^{51}Ti below 5.5 MeV. Figure 1 summarizes earlier information about ^{51}Ti. Ramavataram (1963) and Barnes et al. (1964) have used the reaction ^{50}Ti(d,p)^{51}Ti to obtain the excitation energies, ℓ-values and spectroscopic factors for many of the low-lying levels. Glover et al. (1968) employed the same reaction as well as the reaction ^{49}Ti(t,p)^{51}Ti to obtain ℓ-values and spectroscopic factors. Cosman et al. (1969) using the reaction ^{50}Ti(p,p')^{50}Ti studied the analog states of ^{51}Ti. Bizzeti-Sona et al. (1966) have observed the β decay of ^{51}Sc. Two excited states of ^{51}Ti were seen in this latter experiment. More recently Tenenbaum et al. (1971) as well as Tripathi et al. (1969) have used the reaction ^{50}Ti(n,γ)^{51}Ti to look at the γ-ray decays of the excited levels of ^{51}Ti. Unfortunately, the ^{50}Ti(n,γ)^{51}Ti reaction populated only a limited number of levels.

In the present investigation the levels of ^{51}Ti were first studied with the ^{50}Ti(d,pγ)^{51}Ti reaction. Particle--gamma-ray correlations were measured with a method which employed a collinear geometry. This correlation procedure was described in detail by Litherland and Ferguson (1961), but Biedenharn et al. (1951) first pointed out the simplifications which are brought about by axial symmetry. Because of the spin of the deuteron, the number of rigorous spin assignments that

Figure 1. The Level Scheme Containing Information Available on ^{51}Ti Prior to this Experiment. Energies are given in keV. Gamma rays on the left are those measured in the β-decay of ^{51}Sc by Bizzeti-Sona et al. (1966). Gamma rays on the right are those measured in the ^{50}Ti(n,γ)^{51}Ti reaction by Tenenbaum et al. (1971), who assigned a spin of 1/2 to the neutron capture level at 6377-keV. Recent work by Prochnow (1971) has shown the spin of the 1167-keV level to be $1/2^-$. The spin assignments of the ground state, 1429, 2189, and 2690-keV levels are from Glover et al. (1968). Other spin values are taken from Barnes et al. (1964).

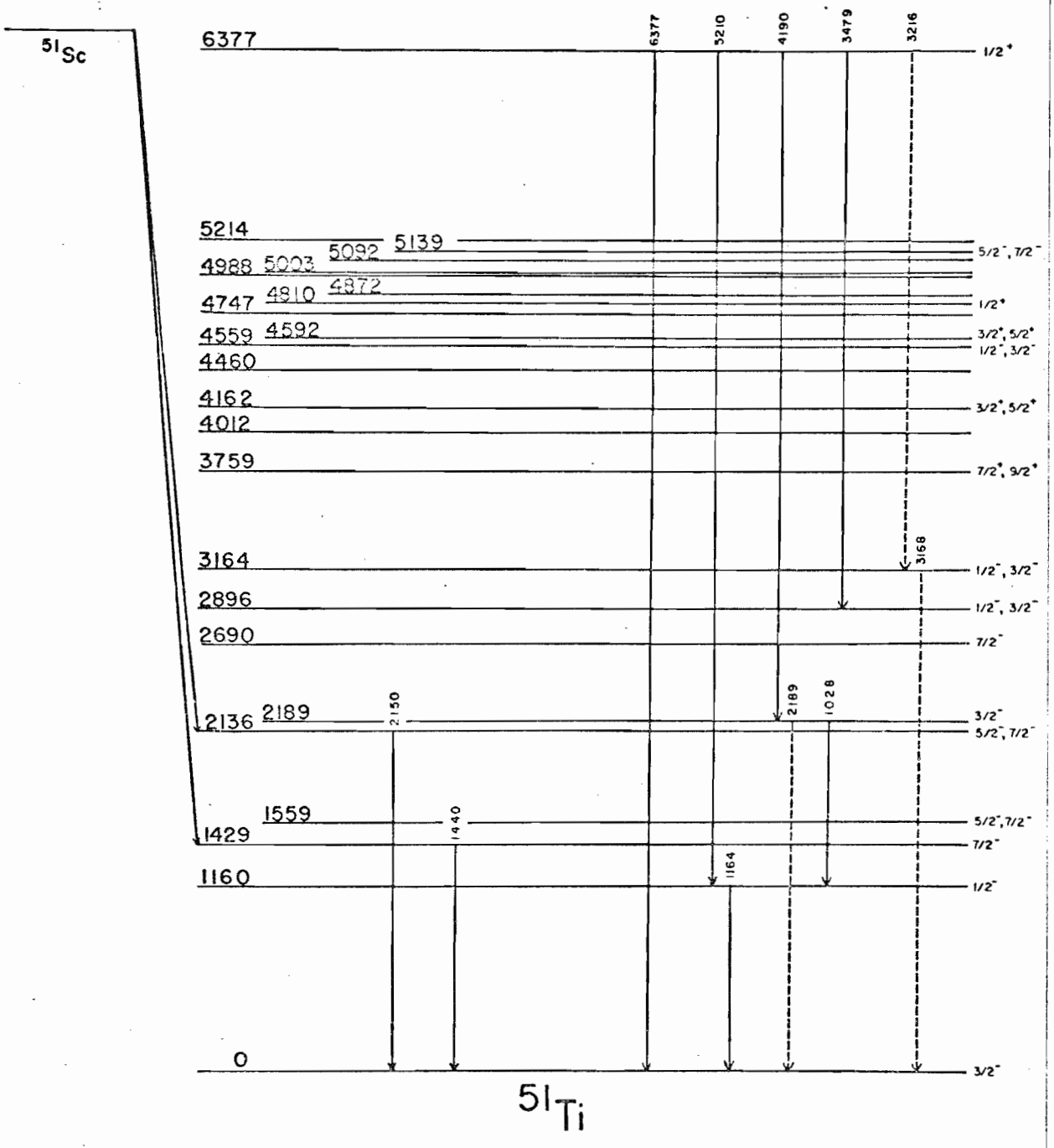
51Sc
6377
5214
4988
5003
5092
5139
4747
4810
4872
4559
4592
4460
4162
4012
3759
3164
2896
2690
2136
2189
2150
1559
1440
1429
1160
1164
0
6377
3210
4190
3479
3216
3168
2189
1028
1/2+
5/2-, 7/2-
1/2+
3/2+, 5/2+
1/2-, 3/2-
3/2+, 5/2+
7/2+, 9/2+
1/2-, 3/2-
1/2-, 3/2-
7/2-
3/2-
5/2-, 7/2-
5/2-, 7/2-
7/2-
1/2-
3/2-
51Ti

can be made with the (d,p) reaction is somewhat limited (see Chapter III).

In order to confirm the γ-rays observed in the $^{50}Ti(d,p\gamma)^{51}Ti$ work and to investigate the possibility of a new level at 2346-keV, the γ-rays produced by the $^{48}Ca(\alpha,n\gamma)^{51}Ti$ reaction were studied via both n-γ and γ-γ coincidence measurements. These measurements yielded accurate excitation energies and allowed the identification of five new levels in ^{51}Ti below 5.0 MeV. Unfortunately, it was not possible to perform n-γ correlation measurements with axial symmetry. To obtain sufficient yield, a thick target and a high bombarding energy (>7 MeV) were necessary. Gamma-ray cascades from higher levels through the lower levels precluded an accurate analysis of any correlation data.

A comparison of the measurements made during the present investigation will be made in Chapter V with the various model predictions for ^{51}Ti. Since many of the theoretical studies have not dealt with levels with $J^{\pi} > 7/2^{-}$, new calculations have been carried out with the help of M. Divadeenam. These new calculations are useful in providing physical insight into the level structure of ^{51}Ti.

Chapter II

EXPERIMENTAL PROCEDURE

A) $^{50}Ti(d,p\gamma)^{51}Ti$ Angular Correlations

1) Targets

Self-Supporting ^{50}Ti targets were prepared from enriched Ti metal (69.7% ^{50}Ti, 22.8% ^{48}Ti, 3.1% ^{46}Ti, 2.4% ^{47}Ti and 2% ^{49}Ti). The Titanium along with Cesium Iodide crystals was placed in a Tantalum boat in a bell jar. After the bell jar was evacuated, the boat was slowly heated until the CsI evaporated onto glass slides. The boat temperature was then raised to about 2200°C, and the Titanium was evaporated onto the same slides. When removed from the bell jar, the Ti foils were cut and then floated on water. The CsI acted as a release agent when the glass slides were slowly immersed in water. The targets were then picked up on target rings and dried. The targets used in this experiment ranged in thickness from 200 to 500 $\mu g/cm^2$. Similar targets were prepared from natural Ti and Ti enriched to 99% ^{48}Ti.

2) Beams

Deuteron beams from the TUNL Tandem van de Graaff were used at bombarding energies between 5.35 and 6.8 MeV. Excitation

functions over this range for the proton groups leading to many of the low-lying states were performed with an annular detector placed at 180° with respect to the beam axis. Guided by the information obtained from these excitation functions, correlation measurements were made at 5.4 and 6.0 MeV deuteron energies. Additionally, a $^{48}Ti(d,p\gamma)^{49}Ti$ coincident measurement was made at E_d = 6.0 MeV.

3) Chamber

The target chamber used in this experiment is shown in figure 2. The detector holder and collimator assembly can be removed completely from the chamber for ease of mounting and alignment of the surface barrier detectors. Two 3/16" collimators were located 10.5 cm. apart as shown in figure 2. The detector used was a 2000 μm annular silicon surface barrier detector placed at 180° with respect to the beam axis and at a distance of 4.45 cm. from the target. The detector was cooled during the experiment with a cold finger immersed in a dry ice-acetone mixture. This cooling lowered the reverse bias current from 2.0 μA to approximately 0.1 μA. As many as eight targets could be placed in the chamber at one time and then rotated into position as needed. Normally, one target is replaced by an ^{241}Am source for calibrating the particle detector.

Gamma-rays were detected with two 7.62 by 7.62 cm. NaI(Tl) detectors mounted on RCA 8575 photomultiplier tubes. The detectors were placed on opposite sides of the chamber so that two

Figure 2. Target Chamber Used for Particle-gamma Correlation Measurements.

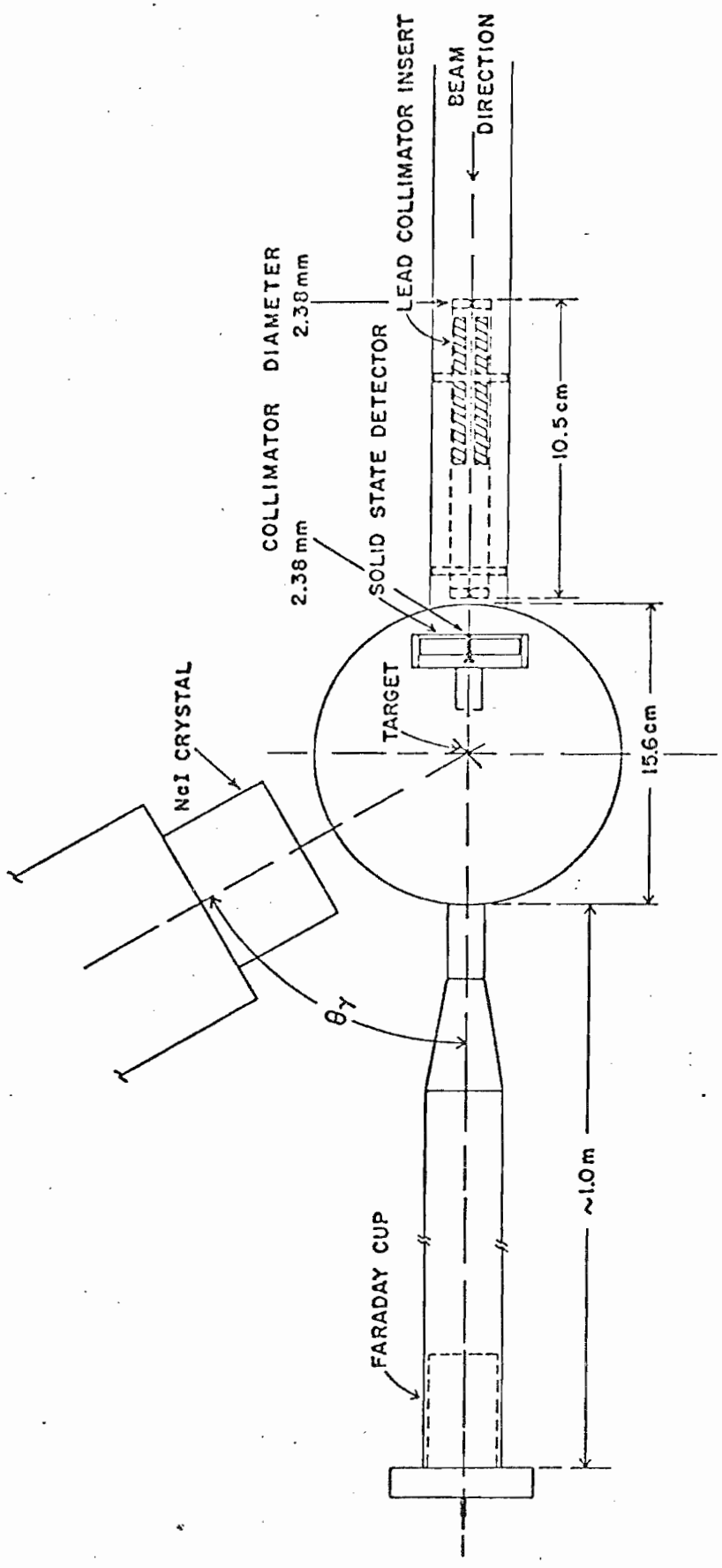

TOP VIEW OF CORRELATION CHAMBER

correlations could be measured simultaneously. Fast negative signals were taken from the anode for use as timing signals. The linear signal was taken from the ninth dynode.

4) Electronics and Software

The circuit diagram for the particle-γ coincidence measurements is shown in figure 3. Briefly, the fast signals were sent to a time to amplitude converter (TAC). The TAC signal was fed to a single channel analyzer (SCA) which was used to generate a gate which indicated the presence of a valid coincidence event. Pile-up rejection of the γ-ray signals was performed through leading edge-crossover timing. If a coincidence requirement between the delayed leading edge signal and the crossover signal was met, the event was considered valid and a gate was generated. For a pile-up event, the crossover signal arrived too late and no gate was generated. The TAC gate and the pile-up rejection gate were fed to a coincidence circuit and the output was used to open all the linear gates and to control the analog-to-digital converters (ADC).

For each coincidence event, four digital words were generated, corresponding to the γ-ray energy (10 bits), the time signal (7 bits), the particle energy (10 bits), and a two bit word containing the routing information indicating which NaI(Tl) detector received the event. A DDP-224 computer system was used to collect the digitized information which was then stored, event by event, on magnetic tape. Additionally, a particle

Figure 3. Electronic Circuit Diagram for Particle-gamma Correlation Measurements

The following abbreviations are used:

AMP ---- Amplifier

G.S. --- Gated Stretcher

ADC ---- Analog-to-Digital-Converter

B A ---- Biased Amplifier

T P ---- Time Pickoff

U.D. --- Updating Discriminator

TAC ---- Time-to-Amplitude-Converter

TFA ---- Timing Filter Amplifier

SCA ---- Single Channel Analyzer

L.S. --- Logic Shaper and Delay

TSCA --- Timing Single Channel Analyzer

Coin. -- Coincidence Unit

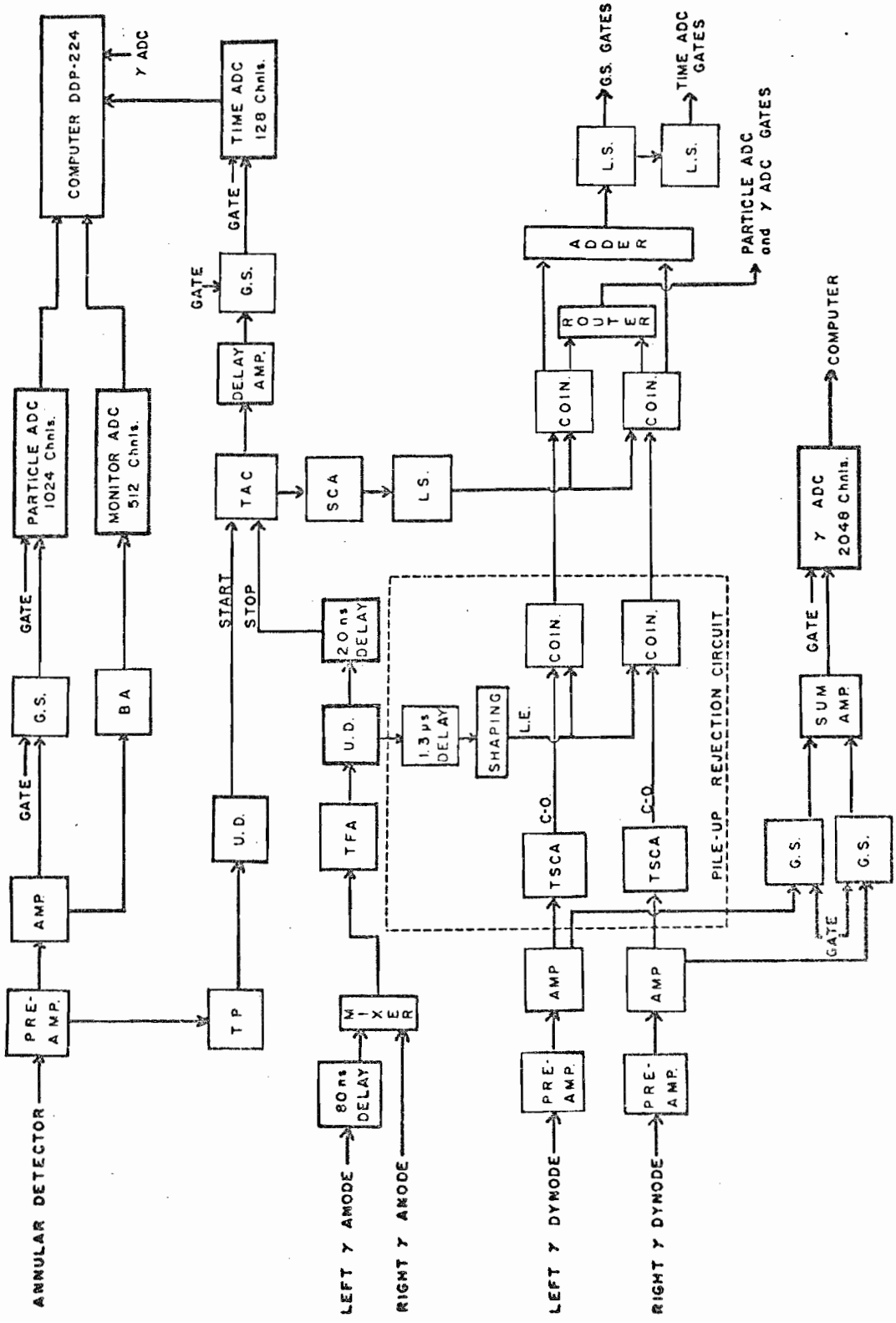
ANNULAR DETECTOR
PRE-AMP.
AMP
G.S.
BA
GATE
GATE
PARTICLE ADC 1024 Chnls.
MONITOR ADC 512 Chnls.
COMPUTER DDP-224
Y ADC
T P
U.D.
START
STOP
TAC
DELAY AMP.
GATE
G.S.
GATE
TIME ADC 128 Chnls.
SCA
LS
20ns DELAY
U.D.
TFA
80ns DELAY
MIXER
LEFT Y AMODE
RIGHT Y ANODE
1.3μs DELAY
SHAPING
L.E.
C-O
TSCA
PRE-AMP.
AMP
LEFT Y DYMODE
RIGHT Y DYMODE
COIN.
ROUTER
ADDER
L.S.
G.S. GATES
TIME ADC GATES
PARTICLE ADC and Y ADC GATES
PILE-UP REJECTION CIRCUIT
Y ADC 2048 Chnls.
COMPUTER
SUM AMP.
GATE

singles spectrum was accumulated in the computer and written on magnetic tape at the end of each run.

By giving instructions to the analysis program, either a particle, time or γ-ray spectrum could be obtained from the data tape. A sample particle spectrum is shown in figure 4. Setting appropriate windows on the particle and time (width less than 15ns.) spectra produced the coincident γ-ray spectra. Peaks of the γ-ray spectra were summed after fitting the background with a straight line or an exponential curve. For most of the correlations, only the photopeak was measured. Normalization for each run was obtained by summing a particular peak in the particle singles spectrum. Since correlations could be performed only for the principal decay branch for each level, branching ratios were obtained by summing the data at five angles. Background was then subtracted from these sum spectra and the photopeak for each transition was summed. Appropriate corrections for detector efficiency and absorption in the target chamber walls were made.

B) $^{48}Ca(\alpha,n\gamma)^{51}Ti$ Measurements

1) Targets

Since ^{48}Ca is a relatively rare isotope, a procedure was chosen to insure maximum use of the enriched calcium (97% ^{48}Ca). ^{48}Ca in the form of $^{48}CaCO_3$ was carefully weighed and then dissolved in a measured amount of 0.2N solution of HNO_3 according

Figure 4. Particle Spectrum Coincident with Gamma-rays taken at 6.0 MeV Deuteron Energy. Excitation energies are given in MeV. The three small peaks near 7.9 MeV proton energy are, left to right, the 1.568 MeV level of ^{51}Ti, the 3.260 MeV level of ^{49}Ti, and the 1.438 MeV level of ^{51}Ti. The peak near 4.1 MeV proton energy has not been identified.

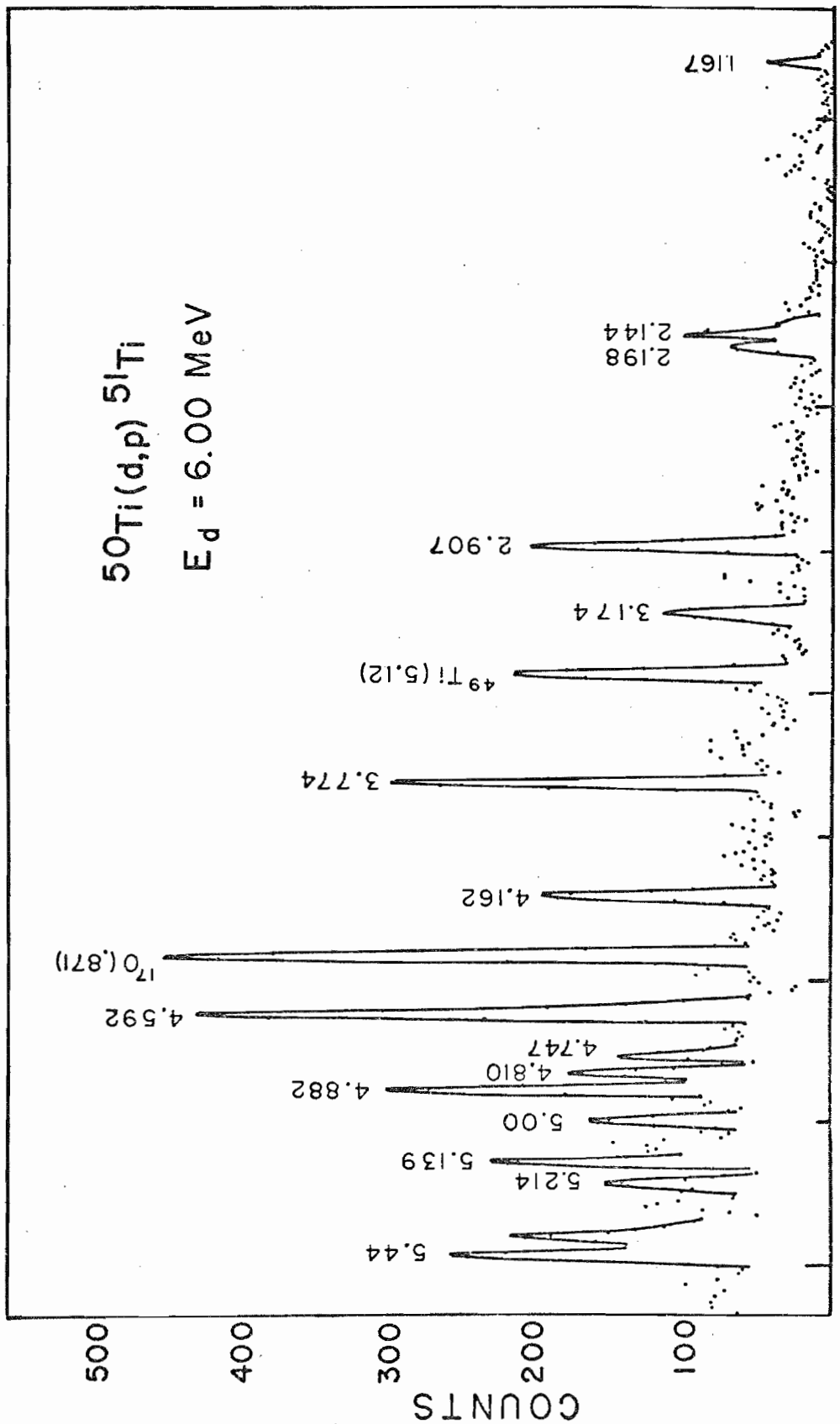
$^{50}Ti(d,p)\,^{51}Ti$
E_d = 6.00 MeV
COUNTS
100
200
300
400
500
4.0
5.0
6.0
7.0
8.0
E_p (MeV)
5.44
5.214
5.139
5.00
4.882
4.810
4.747
4.592
^{17}O (.871)
4.162
3.774
^{49}Ti (5.12)
3.174
2.907
2.198
2.144
1.167

to the equation

$$^{48}CaCO_3 + 2HNO_3 \rightarrow {}^{48}Ca(NO_3)_2 + H_2O + CO_2$$

The solution was gently heated to evaporate the water and the residue was dissolved in alcohol. The nitrate form was used in this method since it dissolves readily in alcohol while $CaCO_3$ and CaO are relatively insoluble in alcohol. This solution was then dripped onto a heated gold disc and the alcohol evaporated leaving a residue of $Ca(NO_3)_2$. Target thickness was estimated to be about 3 mg./cm.^{2} of $^{48}Ca(NO_3)_2$.

2) Beams

Alpha particle beams from the TUNL Tandem van de Graaff were used at bombarding energies between 5.5 and 11.0 MeV. Beam currents were restricted from 30 to 60 n.A. Gamma-ray spectra were taken at many energies while most of the n-γ and γ-γ coincident runs were made at 8.1 MeV.

3) Target Chambers

a) The n-γ Coincidence Measurements

The target chamber used for the n-γ coincidence measurements is shown in figure 5. Neutrons were detected at 0° in a 12.70 cm. by 10.16 cm. NE213 liquid scintillator mounted on an Amperex XP1040 photomultiplier tube. Fast negative signals were taken from the anode for use as timing signals. The linear signal was taken from the tenth dynode. Gamma-rays were detected

Figure 5. The Target Chamber Used for Neutron-gamma Coincidence Measurements.

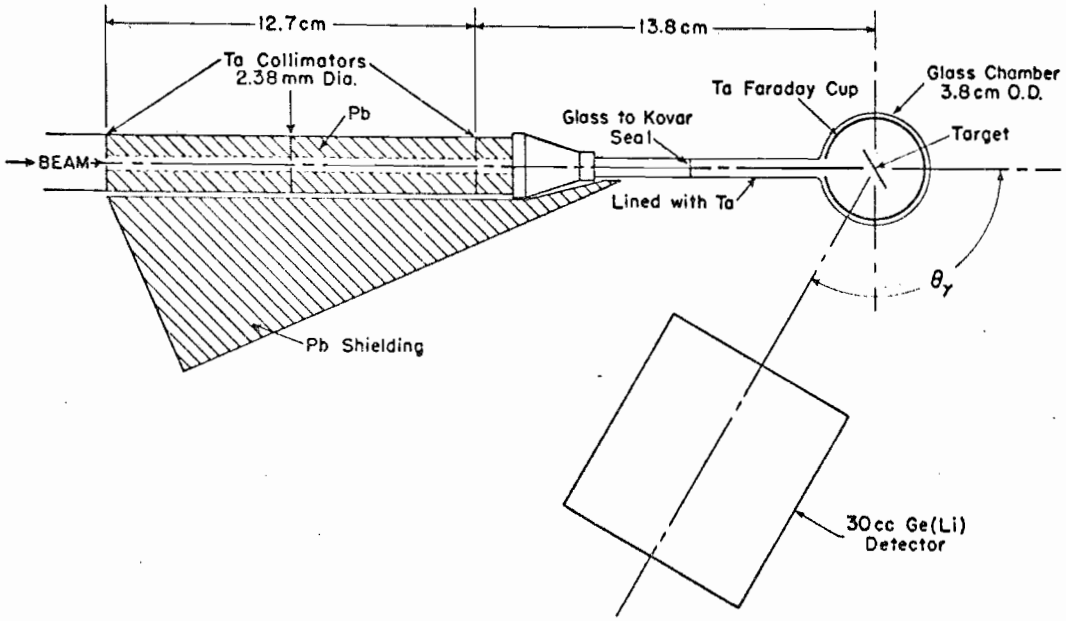
12.7cm
13.8cm
Ta Collimators
2.38mm Dia.
Pb
Glass to Kovar
Seal
Ta Faraday Cup
Glass Chamber
3.8cm O.D.
Target
BEAM
Lined with Ta
θ_γ
Pb Shielding
30cc Ge(Li)
Detector

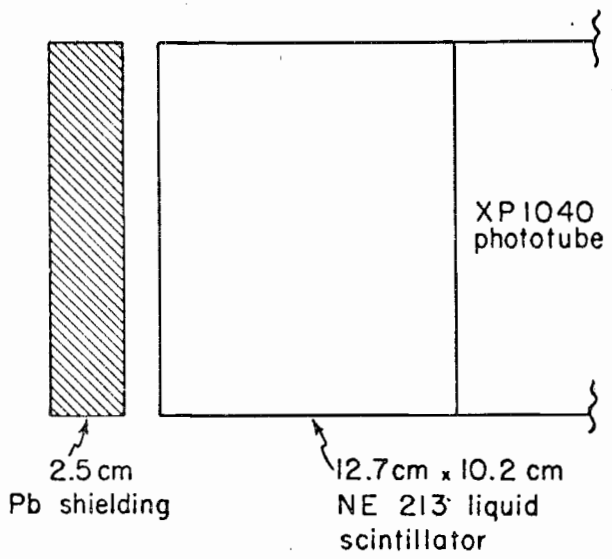
XP1040
phototube
2.5cm
Pb shielding
12.7cm x 10.2 cm
NE 213 liquid
scintillator

with a 30 cm^3 Lithium-drifted Germanium detector (Ge(Li)) which could be rotated from 42° to 143° relative to the beam direction. The NE213 detector was calibrated by measuring the relative pulse height of the Compton edges of ^{60}Co and ^{137}Cs γ-ray sources. The equivalent neutron energies for these pulse heights were obtained from Stammbach (1969). The ^{137}Cs Compton edge was taken to correspond to a 1800 keV neutron and the ^{60}Co Compton edge to a 3500 keV neutron. A straight line was extrapolated through these two points which is a good approximation for neutrons of less than 5000 keV energy and a somewhat poorer one for neutrons of greater than 5000 keV energy. The Ge(Li) detector was calibrated before and after each run with ^{56}Co, ^{60}Co, and ^{137}Cs sources.

b) The γ-γ Coincidence Measurements

The target chamber for γ-γ coincidence consisted of a T-shaped piece of beam pipe with two mylar windows at 90° relative to the beam direction on opposite sides of the beam pipe. Two Ge(Li) detectors (30 cm^3 and 80 cm^3) were placed close to the mylar windows and the distances adjusted to obtain approximately equal count rates in each detector. Beam pipe supports prevented the placing of the detectors at angles other than 90°. The 90°-90° geometry made analysis of γ-rays of less than 511 keV difficult due to the large number of coincidence events from annihilation γ-rays. Future γ-γ coincidence experiments performed here will be performed in a chamber better suited to this experiment.

4) Electronics and Software

a) The n-γ Coincidence Measurements

The circuit diagram for the n-γ coincidence measurements is shown in figure 6. A timing signal was obtained for the Ge(Li) events by amplifying fast components of the preamp signal and sending it to a constant fraction discriminator. This signal together with the timing signal from the neutron detector was sent to a TAC. The TAC signal was used to generate a gate. Pulse shape discrimination (PSD) was used to differentiate between γ-ray and neutron events in the NE213 scintillator. This was accomplished through the use of leading edge-crossover timing. The γ-ray crossover occurs before the neutron crossover and when the leading edge and crossover signals are sent to a TAC, two distinct peaks are observed.

For each coincidence event four digital words were generated, corresponding to the γ-ray energy (12 bits), the neutron energy (8 bits), the time signal (7 bits) and the PSD signal (7 bits). A DDP-224 computer system was used to collect the digitized information which was then stored, event by event, on magnetic tape.

The analysis program displays a two dimensional contour plot of neutron energy vs. PSD with the z-axis being counts. The neutron group was well separated from the γ-ray group and this area could be designated with a light pen as a window for reading back the Ge(Li) spectra. A window was also set on the

Figure 6. Electronic Circuit Diagram for Neutron-gamma Coincidence Measurements.

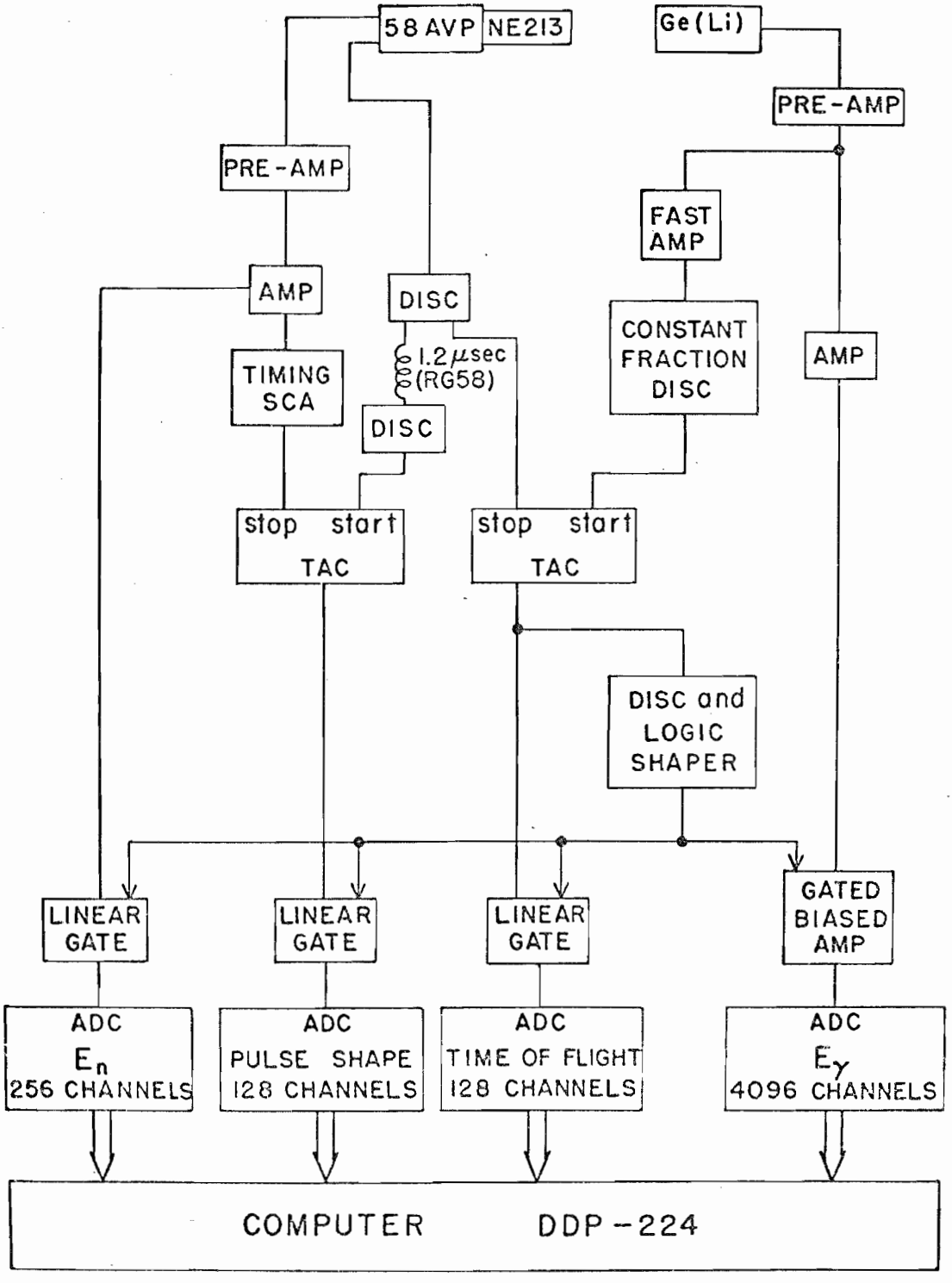

Abbreviations: SCA - SINGLE CHANNEL ANALYZER
TAC - TIME TO PULSE HEIGHT CONVERTER
ADC - ANALOG TO DIGITAL CONVERTER

peak of the time spectra and another window on the flat part of the spectra to subtract random coincidence events. The coincident γ-ray spectra could be written on magnetic tape for further analysis by other programs. These programs fit exponential or straight line backgrounds and calculated centroids and areas of peaks.

b) The γ-γ Coincidence Measurements

The circuit diagram for the γ-γ coincidence measurements is shown in figure 7. The timing signal from one Ge(Li) detector was obtained as discussed above. Timing for the other detector was obtained by using a leading edge differential discriminator. The linear signal for each detector was sent to a 4096 channel ADC. The data was stored on tape as three digital words, corresponding to the two γ-ray energies (12 bits each) and the time signal (7 bits).

To obtain a coincident γ-ray spectrum with the analysis program, four digital windows were set. A window was set on the peak of interest in the γ-ray spectrum in one detector and a window of equal width was set on a flat part of the spectrum near the peak of interest. This second window was used to subtract the γ-rays in coincidence with events in the Compton distribution. The other two windows were set on the time peak and a flat portion of the time spectrum to subtract randoms. The coincident γ-ray spectra were then analyzed with a program that fitted exponential or straight line backgrounds and calculated centroids and areas of peaks.

Figure 7. Electronic Circuit Diagram for Gamma-gamma Coincidence Measurements.

The following abbreviations are used:

AMP. --------- Amplifier

GeLi --------- Lithium Drifted Germanium Detector

R.R. --------- Restorer-Rejector

B.A. --------- Biased Amplifier

TFA ---------- Timing Filter Amplifier

Diff. Disc. -- Differential Discriminator

CFD ---------- Constant Fraction Discriminator

U D ---------- Updating Discriminator

SCA ---------- Single Channel Analyzer

G.S. --------- Gated Stretcher

L.S. --------- Logic Shaper and Delay

ADC ---------- Analog-to-Digital-Converter

TAC ---------- Time-to-Amplitude-Converter

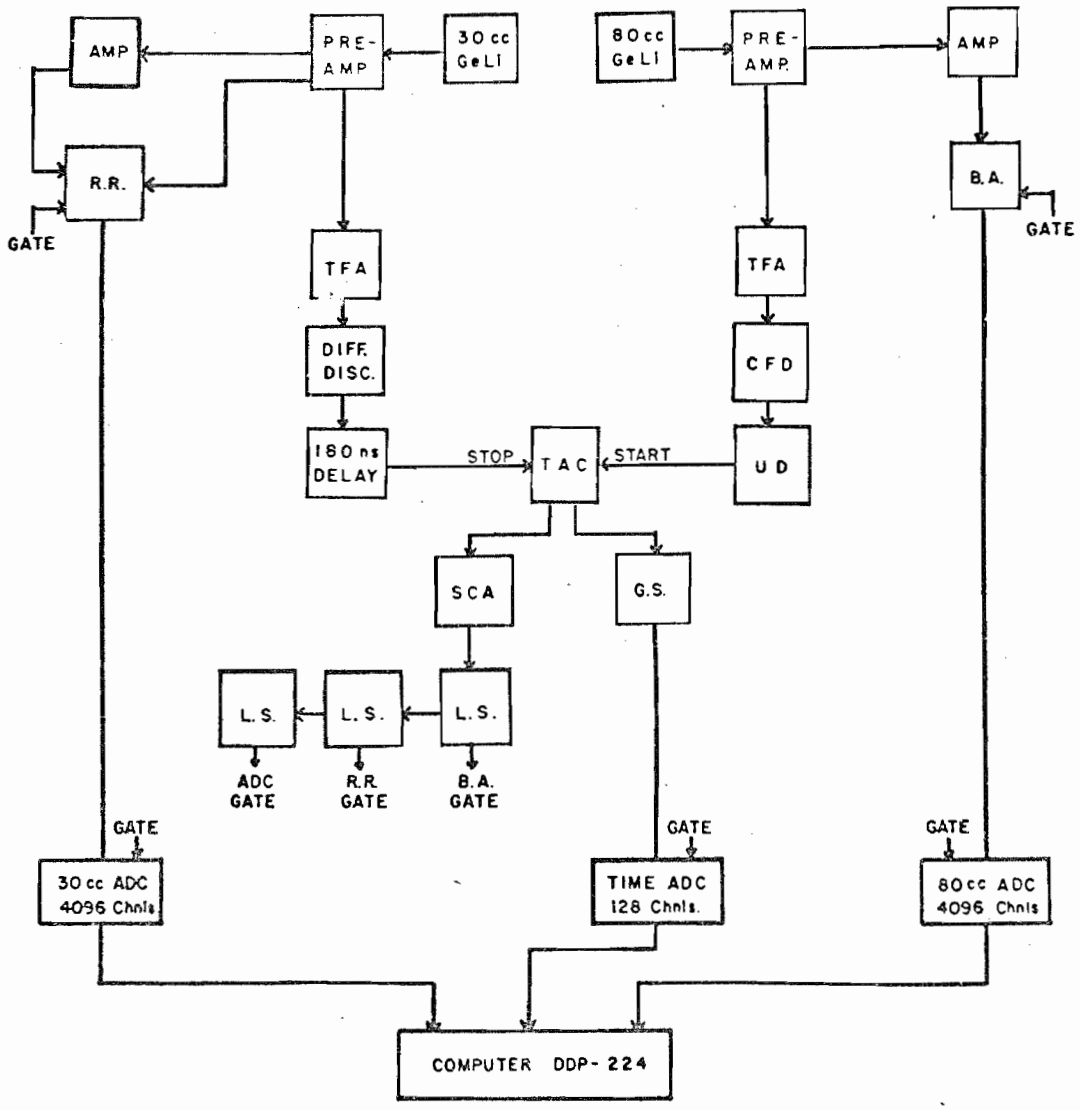
AMP
PRE-AMP
30 cc GeLi
80 cc GeLi
PRE-AMP.
AMP
R.R.
B.A.
GATE
GATE
TFA
TFA
DIFF. DISC.
CFD
180 ns DELAY
STOP
T A C
START
U D
SCA
G.S.
L. S.
L. S.
L. S.
ADC GATE
R.R. GATE
B.A. GATE
GATE
GATE
GATE
30 cc ADC 4096 Chnls
TIME ADC 128 Chnls.
80 cc ADC 4096 Chnls
COMPUTER DDP-224

Chapter III

Analysis of Angular Correlations

The theory of angular correlations has been discussed in detail by many authors. Devons and Goldfarb (1957) discuss the general theory of directional correlations and its applications to many different types of experiments. Litherland and Ferguson (1961) discuss two procedures for the measurement and analysis of angular correlations of gamma radiation from nuclear reactions. Their methods involve limiting the number of unknown parameters by making the reacting system axially symmetric. Rose and Brink (1967) derive the angular distribution formulas directly from perturbation theory and explicitly define all quantities. If the convention of Rose and Brink (1967) is followed, the sign of the mixing ratio is unambiguously determined, and the mixing ratio can then be compared in both magnitude and sign with the predictions of nuclear models. The following treatment will give a brief outline of the method of analysis used in this work.

When an excited state of a nucleus having an angular momentum $\vec{J}_1$ and a z component M_1 decays by γ-ray emission* to a

---

*Gamma-ray emission is allowed unless $J_1 = J_2 = 0$.

lower level having an angular momentum $\vec{J}_2$ and a z component M_2, the γ-ray carries away orbital angular momentum $L \geq 1$ with z component M given by

$$\vec{J}_1 = \vec{J}_2 + \vec{L} \qquad (1a)$$

$$M_1 = M_2 + M \quad . \qquad (1b)$$

The value of 2^L defines the multipole order of the radiation which can be of two types: electric or magnetic. Electric radiation has parity of $(-1)^L$ and magnetic radiation has parity of $(-1)^{L+1}$.

In a nuclear reaction of the type A(b,cγ)D, excited states of nucleus D are populated and the γ-ray decays are observed. If the nuclei are randomly oriented (as in β decay) or the magnetic substates are equally populated, an isotropic distribution of γ-rays should be observed. In order to achieve alignment and restrict the number of magnetic substates populated, Method II correlations (Litherland and Ferguson, 1961) were performed. In this method, the γ-rays are detected in coincidence with the outgoing particles c at 0° or 180° with respect to the incoming particles b. Since the momentum vector $\vec{p}$ is parallel with the beam axis, then the angular momentum vector $\vec{\ell} = \vec{r} \times \vec{p}$ must be perpendicular to the beam axis (designated as the z-axis) and hence its z component $m_\ell = 0$. For a particular excited level of nucleus D, the z component of the angular momentum, M_1, is obtained from considering the projections of the intrinsic spins of particles A, b, and c.

$$M_1 = m_s(A) + m_s(b) - m_s(c) \tag{2a}$$

or

$$M_1 \leq |\vec{S}(A) + \vec{S}(b) + \vec{S}(c)| \tag{2b}$$

where S designates the intrinsic spin and m_s its projection along the z-axis. If the beam and target nuclei are unpolarized and if $\vec{J}_1$ has definite parity, then both positive and negative substates are equally populated.

$$P(M_1) = P(-M_1) \tag{3}$$

where $P(M_1)$ is the probability that the system has z component M_1 and is called the population parameter. The population parameters are normalized such that

$$\sum_{M_1} P(M_1) = 1 \quad . \tag{4}$$

For the reaction $^{50}Ti(d,p)^{51}Ti$, $S(^{50}Ti) = 0$, $S(d) = 1$ and $S(p) = 1/2$ so that M_1 is restricted to the values of $\pm 1/2$ and $\pm 3/2$.

The angular distribution of the gamma radiation following the decay of the initial level with spin J_1 to a level with spin J_2 is given in the notation of Poletti and Warburton (1965) as:

$$W(\theta_\gamma) = \sum_k \rho_k(J_1) F_k(J_1 J_2 x) Q_k P_k(\cos\theta_\gamma) \tag{5}$$

where the summation goes over all even integers $0 \leq k \leq 2J_1$. θ_γ is the angle of emission of the observed γ-rays with respect to the beam axis. The $\rho_k(J_1)$ are statistical tensors describing the alignment of the initial state and are given by

$$\rho_k(J_1) = \sum_{M_1 \geq 0} P(M_1) \left[2 - \delta_{M_1 0}\right] \frac{\langle J_1 M_1 J_1 - M_1 | k0 \rangle}{\langle J_1 M_1 J_1 \quad M_1 | 00 \rangle} \tag{6}$$

where since $P(M_1) = P(-M_1)$, it is convenient to sum over values of $M_1 \geq 0$. The $F_k(J_1 M_1 x)$ are coefficients describing the γ-ray cascade. If only the two lowest multipolarities (L and L' = L + 1) are allowed, then these coefficients are given by

$$F_k(J_1 M_1 x) = \frac{F_k(LLJ_2J_1) - 2x(-1)^p F_k(LL'J_2J_1) + x^2 F_k(L'L'J_2J_1)}{1 + x^2} \tag{7}$$

In the Rose and Brink phase convention (used in this analysis), p is chosen to be zero. The quantity x is the mixing ratio and is given by a ratio of the reduced matrix elements of the two lowest allowed competing multipolarities:

$$x = \frac{\langle J_1 || L' \pi' || J_2 \rangle}{\langle J_1 || L \; \pi \; || J_2 \rangle} \tag{8}$$

The $F_k(LL'J_2J_1)$ are given by

$$F_k(LL'J_2J_1) = (-1)^{J_2 - J_1 - 1} \left[(2L+1)(2L'+1)(2J_1+1)\right]^{\frac{1}{2}} \langle L1L'-1 | k0 \rangle \; W(J_1 J_1 LL', kJ_2) \; . \tag{9}$$

The Q_k are attenuation coefficients which are functions of the size and position of the detector and the energy of the γ-ray involved.

The data was analyzed using the computer code M_2 (Church, 1970). To each experimental correlation a least squares fit directly to the data of equation 5 for a discrete set of values

of arctan x between -90° and +90° was made assuming different values of J_1 and J_2. If the population parameter $P(M_1)$ for a reaction is not fixed, as is the case for $^{50}Ti(d,p\gamma)^{51}Ti$, $P(M_1)$ is varied from 0 to 1 to obtain the best fit for each value of the mixing ratio. Another unknown in this procedure is the overall normalization to the experimental curve. The best fit for a certain value of x, J_1, and J_2 is determined by the values of P(1/2)* and the normalization which minimizes the value of χ^2 where

$$\chi^2 = \frac{1}{N}\sum_i \left[\frac{W(\theta_{\gamma i}) - Y(\theta_{\gamma i})}{EY(\theta_{\gamma i})}\right]^2 \qquad (10)$$

$W(\theta_{\gamma i})$ is the theoretical distribution at $\theta_{\gamma i}$ and $Y(\theta_{\gamma i})$ is the measured value with error $EY(\theta_{\gamma i})$. The sum is over all angles at which measurements were made. N is the number of degrees of freedom and is equal to the number of angles at which measurements were made (in this case five) minus the number of unknowns in $W(\theta_\gamma)$ which in this case is three (the mixing ratio, the normalization and the population parameter).

---

*Since $P(M_1) = P(-M_1)$ and $\sum_{M_1} P(M_1) = 1$, selecting a value of P(1/2) automatically selects values for P(-1/2), P(3/2), and P(-3/2).

Chapter IV

RESULTS

A) The $^{50}Ti(d,p\gamma)^{51}Ti$ Measurements

1) The 1167-keV Level

The summed γ-ray spectrum measured in coincidence with the particles leading to the first excited state of ^{51}Ti is shown in Figure 8. Figure 9 shows the isotropic angular correlation on the left and on the right the χ^2 fits to the ground state transition. Although a unique spin assignment cannot be made, the correlation is consistent with the $J^{\pi} = 1/2^-$ assignment to this level as deduced from a j-dependence study of the $^{50}Ti(d,p)^{51}Ti$ reaction by Lee and Schiffer (1967). While spins determined by j-dependence are non-rigorous, Prochnow (1971) has recently assigned $J^{\pi} = 1/2^-$ to the analog state in ^{51}V, and confirmed $J^{\pi} = 1/2^-$ for the 1167-keV level in ^{51}Ti.

This result is in agreement with the $\ell_n = 1$ $^{50}Ti(d,p)^{51}Ti$ angular distribution corresponding to population of this level by Barnes et al. (1964) in an earlier study, and with the L = 4 (t,p) angular distribution determined by Glover et al. (1968) using the $^{49}Ti(t,p)^{51}Ti$ reaction.

Figure 8. The γ-ray Spectrum in Coincidence with the Particles Leading to the ^{51}Ti 1167-keV Level. This spectrum is the sum of spectra taken at five angles. The solid line is meant only to guide the eye. Energies are given in keV. As expected, only a ground state decay is observed. The energy of the 1167-keV γ-ray is that obtained in the ^{48}Ca(α,nγ)^{51}Ti experiment.

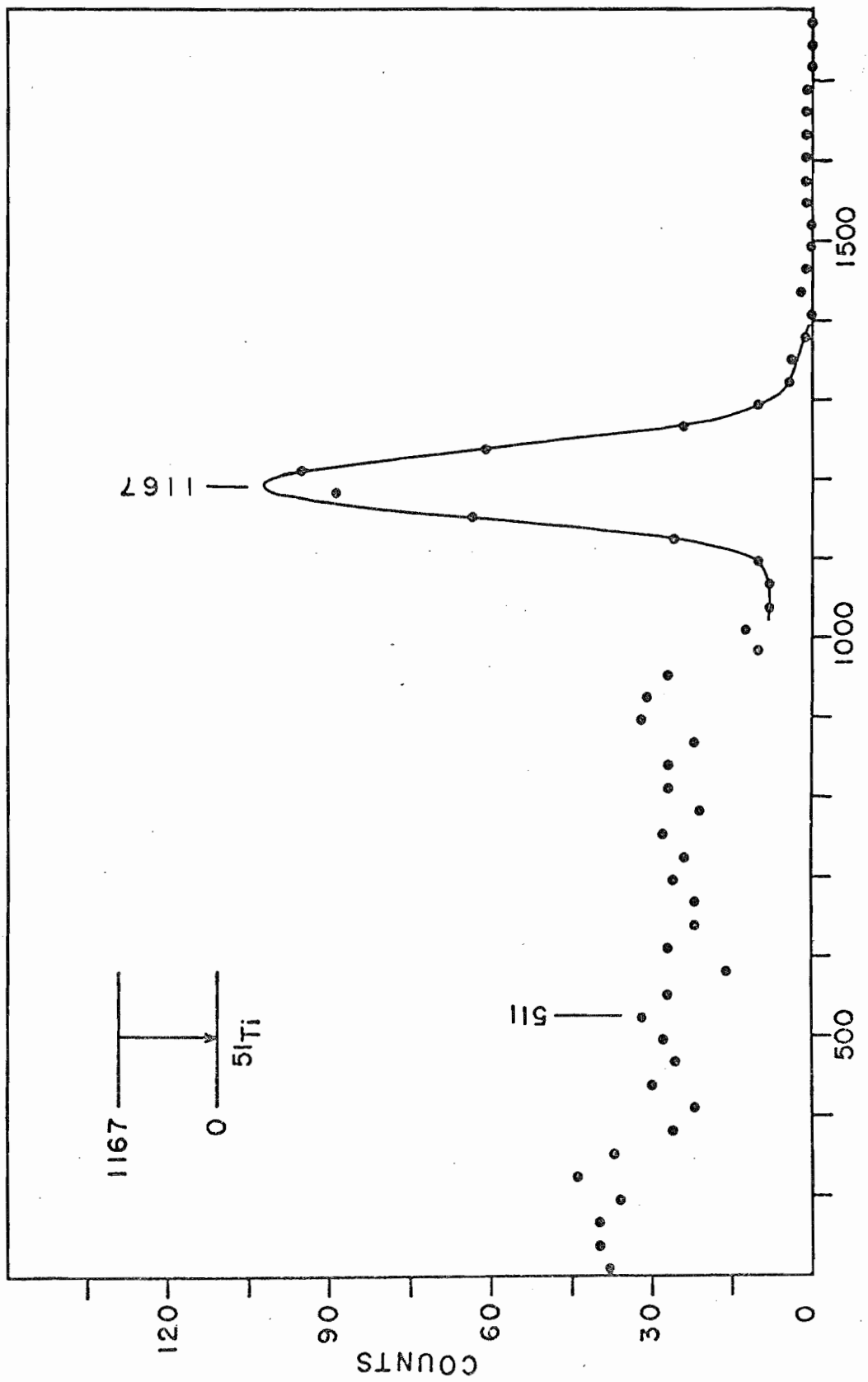
1167
511
1167
0
51Ti
COUNTS
0
30
60
90
120
500
1000
1500
Eγ (keV)

Figure 9. a) The Angular Correlation for the Photopeak of the 1167-keV γ-ray is Shown. The curve was calculated with the parameters for J = 1/2. The data are plotted as a function of $\cos^2\theta$. The correlation was performed at E_d = 5.4 MeV.

b) Plots of χ^2 Versus Arctan x for J = 1/2, 3/2, 5/2, and 7/2 are Shown. An ℓ = 1 assignment by Barnes et al. (1964) rules out all but J = 1/2 and 3/2. Recent work by Prochnow (1971) has shown J = 1/2 for this level.

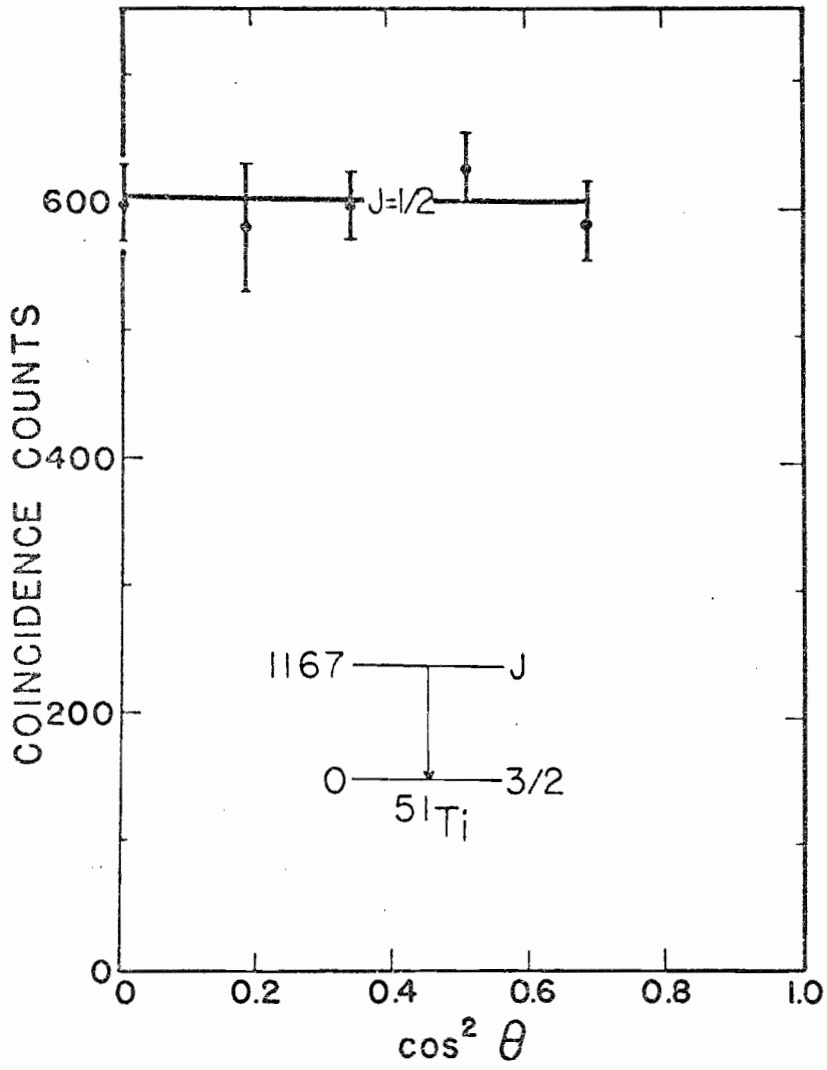
COINCIDENCE COUNTS
600
400
200
0
J=1/2
1167
J
0
3/2
51Ti
0
0.2
0.4
0.6
0.8
1.0
cos² θ

(a)

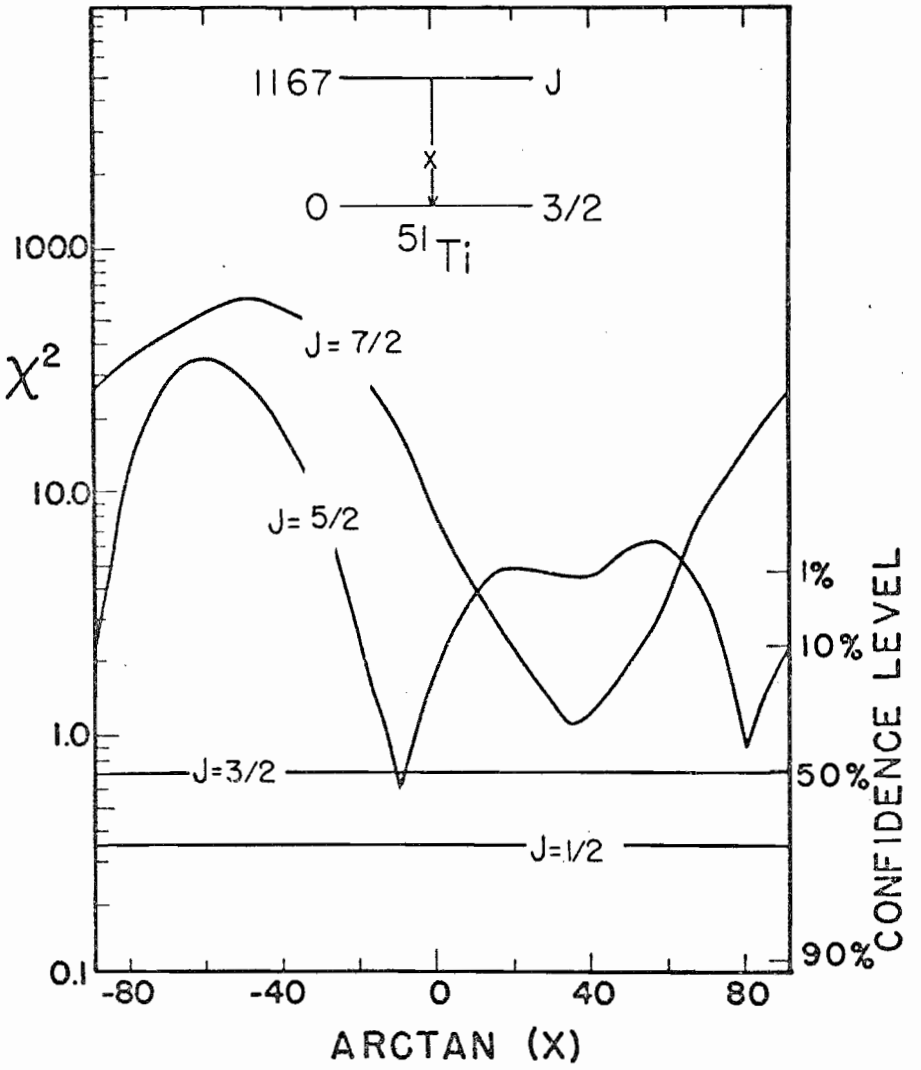
1167
J
X
0
3/2
51Ti
1000
χ²
10.0
1.0
0.1
J= 7/2
J= 5/2
J=3/2
J=1/2
-80
-40
0
40
80
ARCTAN (X)
1%
10%
50%
90%
CONFIDENCE LEVEL

(b)

2) The 1438- and 1568-keV Levels

The 1438- and 1568-keV levels are not strongly populated with the (d,p) reaction. Additionally, the proton peaks corresponding to these levels were obscured by peaks coming from the 3260- and 3176-keV levels of ^{49}Ti. The decay spectrum of the 3260-keV level has a 1380-keV γ-ray and the spectrum of the 3176-keV level has a 1550-keV γ-ray. Hence, no correlation could be performed on these two levels of ^{51}Ti.

The 1438-keV level has been assigned $J^{\pi} = 7/2^{-}$ by Glover et al. (1968), who determined an L = 0 (t,p) angular distribution corresponding to the population of this level with the ^{49}Ti(t,p)^{51}Ti reaction.

3) The 2144-keV Level

Figure 10 shows the summed γ-ray spectrum measured in coincidence with the proton group corresponding to the 2144-keV level. This level decays with a 90% branch to the ground state and a 10% branch to the 1568-keV level. A correlation was measured for the ground state decay, and the results are shown in Figure 11. An ℓ_n-value of 3 has been assigned by Barnes et al. (1964) to the proton distribution leading to this level. The results of the present experiment are consistent with this assignment. If J = 5/2 then the E2/M1 mixing ratio is $\pm\infty$ or -0.21 ± 0.07. If J = 7/2 then the M3/E2 mixing ratio is $0.3^{+0.5}_{-0.4}$.

Figure 10. The γ-ray Spectrum in Coincidence with the Particles Leading to the ^{51}Ti 2144-keV Level. This spectrum is the sum of spectra taken at five angles. The solid lines are meant only to guide the eye. Decays are observed to both the ground state and the 1568-keV level. The subsequent decay of the 1568-keV level is obscured by the first escape peak of the 2144-keV gamma-ray. All energies are given in keV. The energies of the γ-rays are those obtained in the ^{48}Ca(α,nγ)^{51}Ti experiment.

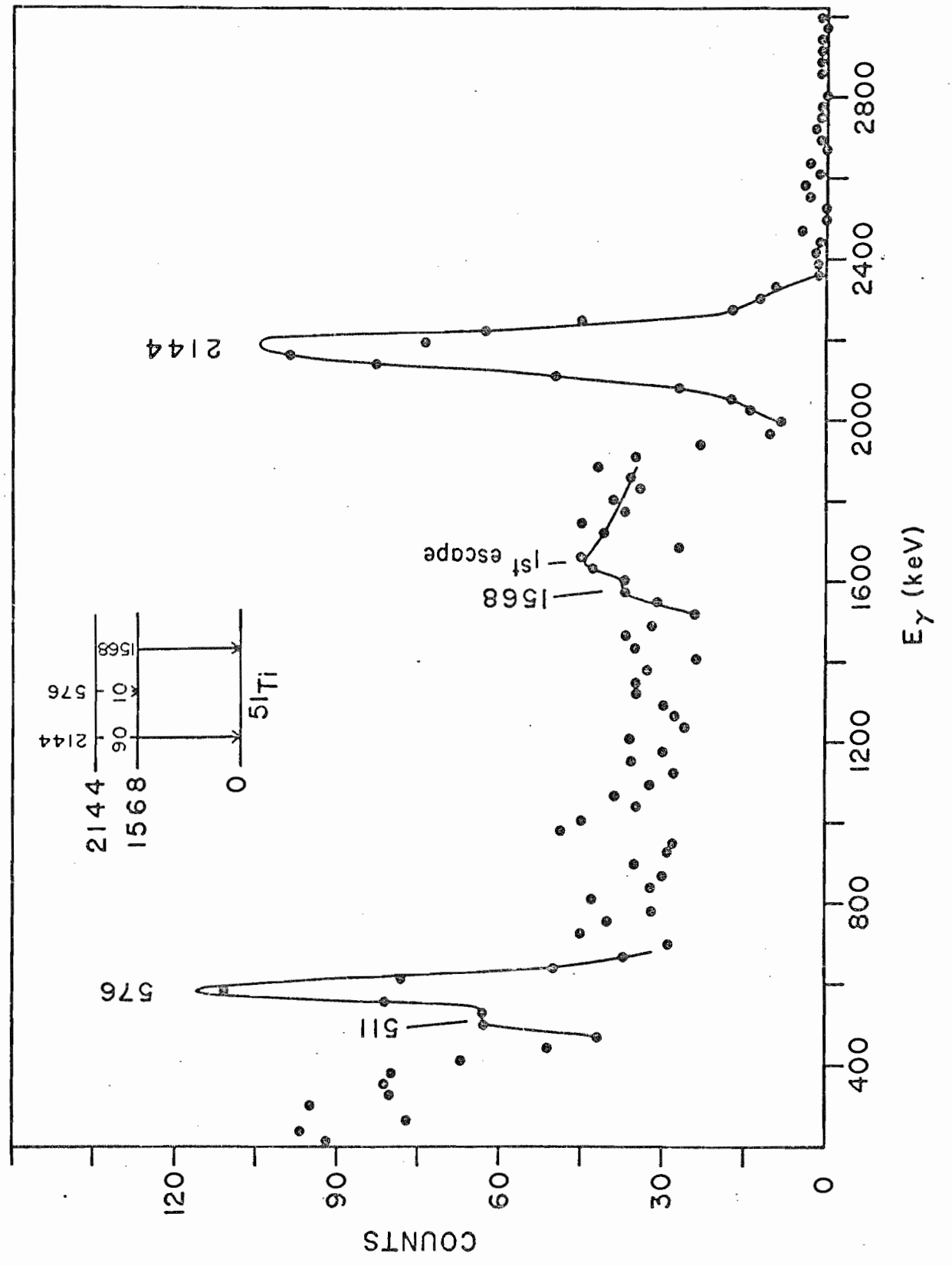
COUNTS
0
30
60
90
120
400
800
1200
1600
2000
2400
2800
E_γ (keV)
511
576
1568
1st escape
2144
^{51}Ti
2144
1568
576
511
0

Figure 11. a) The Angular Correlation for the Photopeak of the 2144-keV γ-ray is Shown. The curves were calculated with the parameters corresponding to the minima of χ^2 shown in (b) with J = 5/2 and 7/2. The data are plotted as a function of $\cos^2\theta$. The correlation was performed at E_d = 6.0 MeV.

b) Plots of χ^2 Versus Arctan x for J = 1/2, 3/2, 5/2, and 7/2 are Shown. An ℓ = 3 assignment by Barnes et al. (1964) rules out all but J = 5/2 and 7/2. No choice between the two is possible in this work.

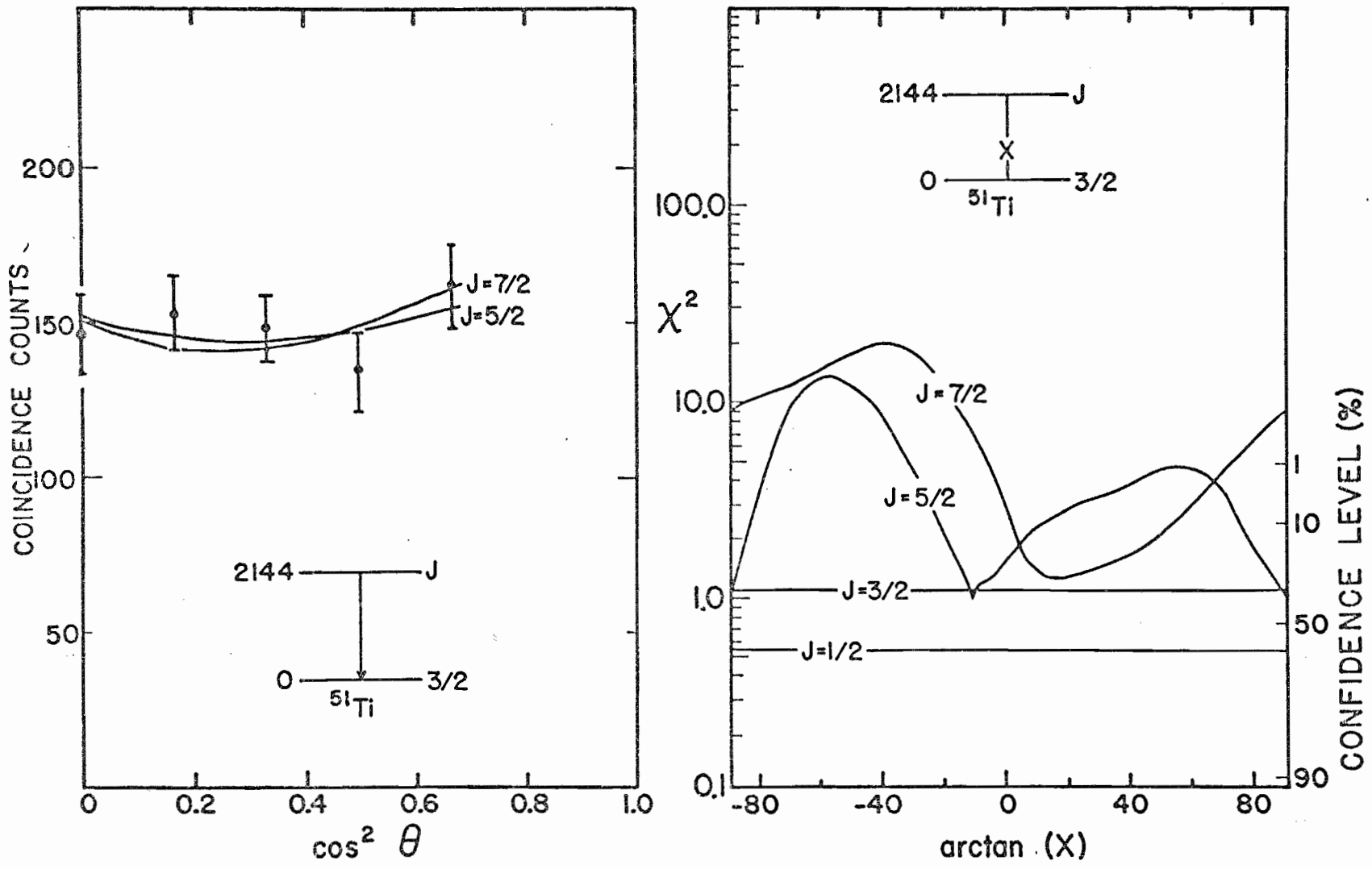
COINCIDENCE COUNTS
200
150
100
50
J=7/2
J=5/2
2144
J
0
3/2
51Ti
0
0.2
0.4
0.6
0.8
1.0
cos² θ
(a)
χ²
100.0
10.0
1.0
0.1
2144
J
X
0
3/2
51Ti
J=7/2
J=5/2
J=3/2
J=1/2
-80
-40
0
40
80
arctan (X)
CONFIDENCE LEVEL (%)
1
10
50
90
(b)

4) The 2198-keV

The summed γ-ray spectrum in coincidence with the proton group leading to the 2198-keV level is shown in Figure 12. This level decays with a 72% branch to the ground state, a 16% branch to the first excited state, a 12% branch to the third excited state. The possibility of a branch (< 3%) to the 1438-keV level also exists. While there is no evidence of a ^{49}Ti proton group appearing at the same energy as the 2198-keV proton group, the unexplained γ-ray in the coincidence spectrum at ≈1350 keV could be the decay of the first excited state of ^{49}Ti. Only the 2198-, 1031-, and 630-keV γ-rays were observed in the ^{48}Ca(α,nγ)^{51}Ti experiment.

A correlation was performed on the ground state branch and the result is shown in Figure 13. The differentiation between 1/2 and 3/2 cannot be made, and because of the unknown population parameter, a mixing ratio for this transition could not be determined. An ℓ_n-value of 1 has been assigned to the proton distribution leading to this level in the ^{50}Ti(d,p)^{51}Ti reaction (Barnes et al., 1964), and Glover et al. (1968) using the reaction ^{49}Ti(t,p)^{51}Ti assign L = 2 to the protons leading to the 2198-keV level of ^{51}Ti. The latter value rules out the 1/2 spin assignment and a $3/2^-$ assignment may be made to this level.

5) The 2907-keV Level

The proton group associated with this level was not completely resolved from the proton group from the 4660-keV level

Figure 12. The γ-ray Spectrum in Coincidence with the Particles Leading to the ^{51}Ti 2198-keV Level. This spectrum is the sum of spectra taken at four angles. The solid lines are meant only to guide the eye. Energies are given in keV. Decays are observed to the ground state, the 1167-keV level, and the 1568-keV level. The subsequent decays of these levels are also seen. The possibility of a weak branch to the 1438-keV level also exists. The energies of the γ-rays were taken from the results of the ^{48}Ca(α,nγ)^{51}Ti experiment.

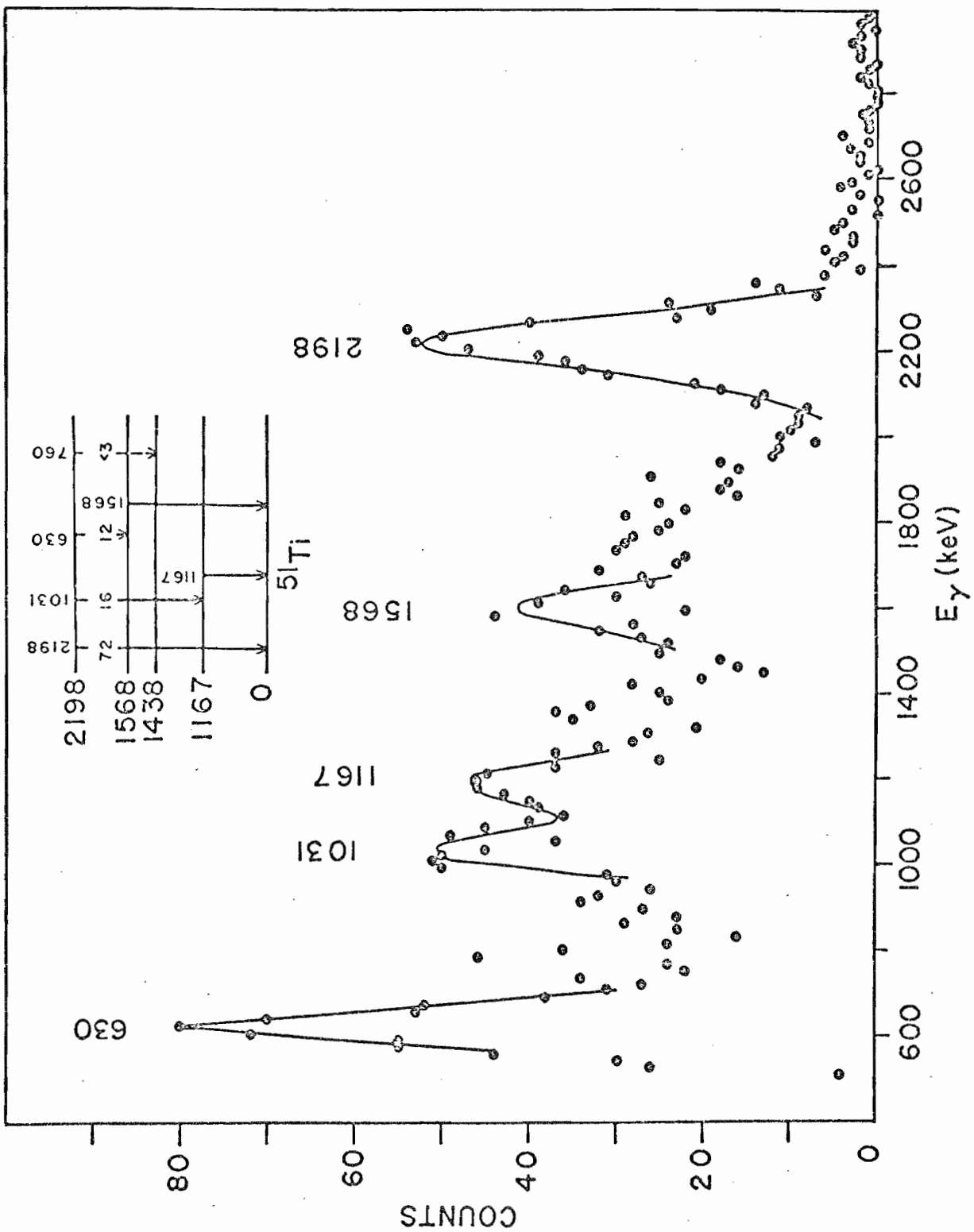
630
1031
1167
1568
2198
COUNTS
E_γ (keV)
^{51}Ti
2198
1568
1438
1167
0
760
630
1031
2198
1568
1167
72
16
12
<3

Figure 13. a) The Angular Correlation for the Photopeak of the 2198-keV γ-ray from the 2198-keV Level is Shown. The curves were calculated with the parameters corresponding with J = 1/2 and 3/2. The data are plotted as a function of $\cos^2\theta$. The correlation was performed at E_d = 5.4 MeV.

b) Plots of χ^2 Versus Arctan x for J = 1/2, 3/2, 5/2, and 7/2 are Shown. An ℓ = 1 assignment by Barnes et al. (1964) rules out all but J = 1/2 and 3/2. An L = 2 assignment by Glover et al. (1968) using the reaction $^{49}Ti(t,p)^{51}Ti$ requires $J \geq 3/2$. The spin of this level is therefore 3/2. Because of the unknown population parameter, no mixing ratio could be determined for this transition.

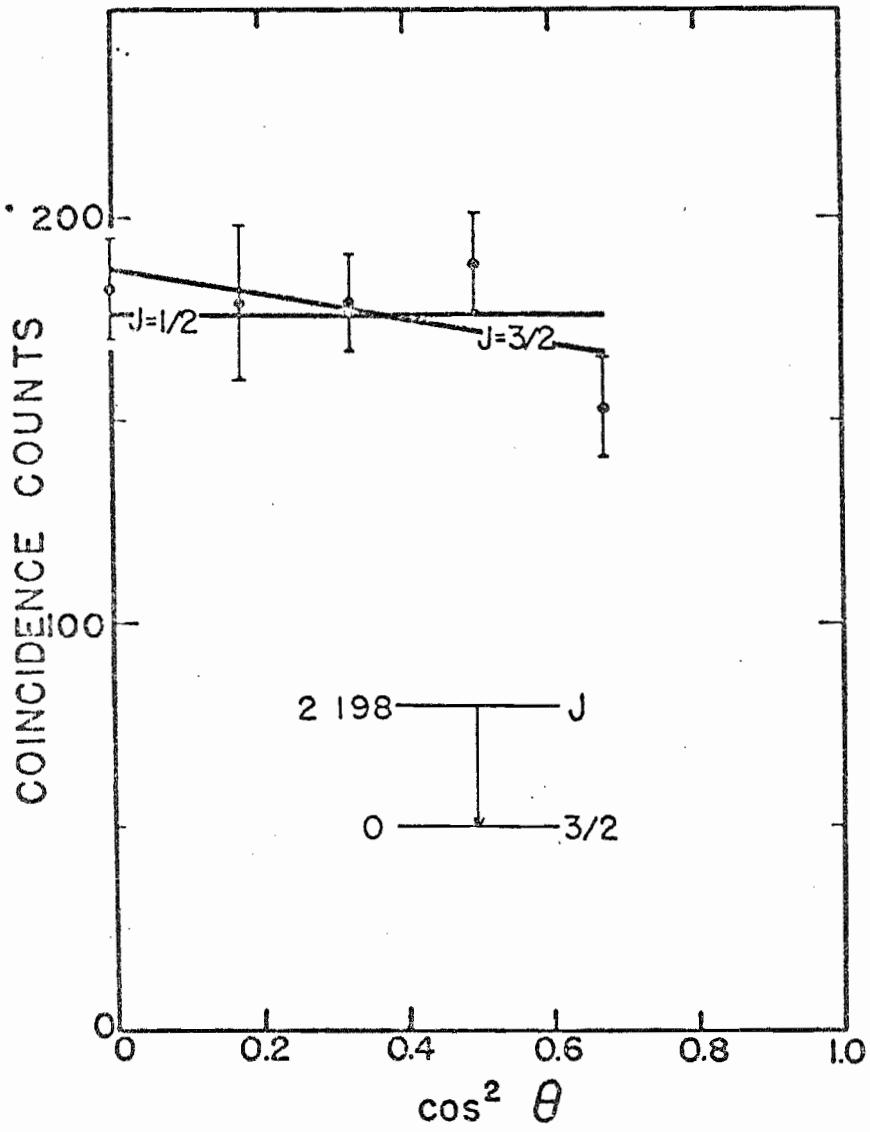
COINCIDENCE COUNTS
200
100
0
J=1/2
J=3/2
2 198
J
0
3/2
0
0.2
0.4
0.6
0.8
1.0
cos² θ

(a)

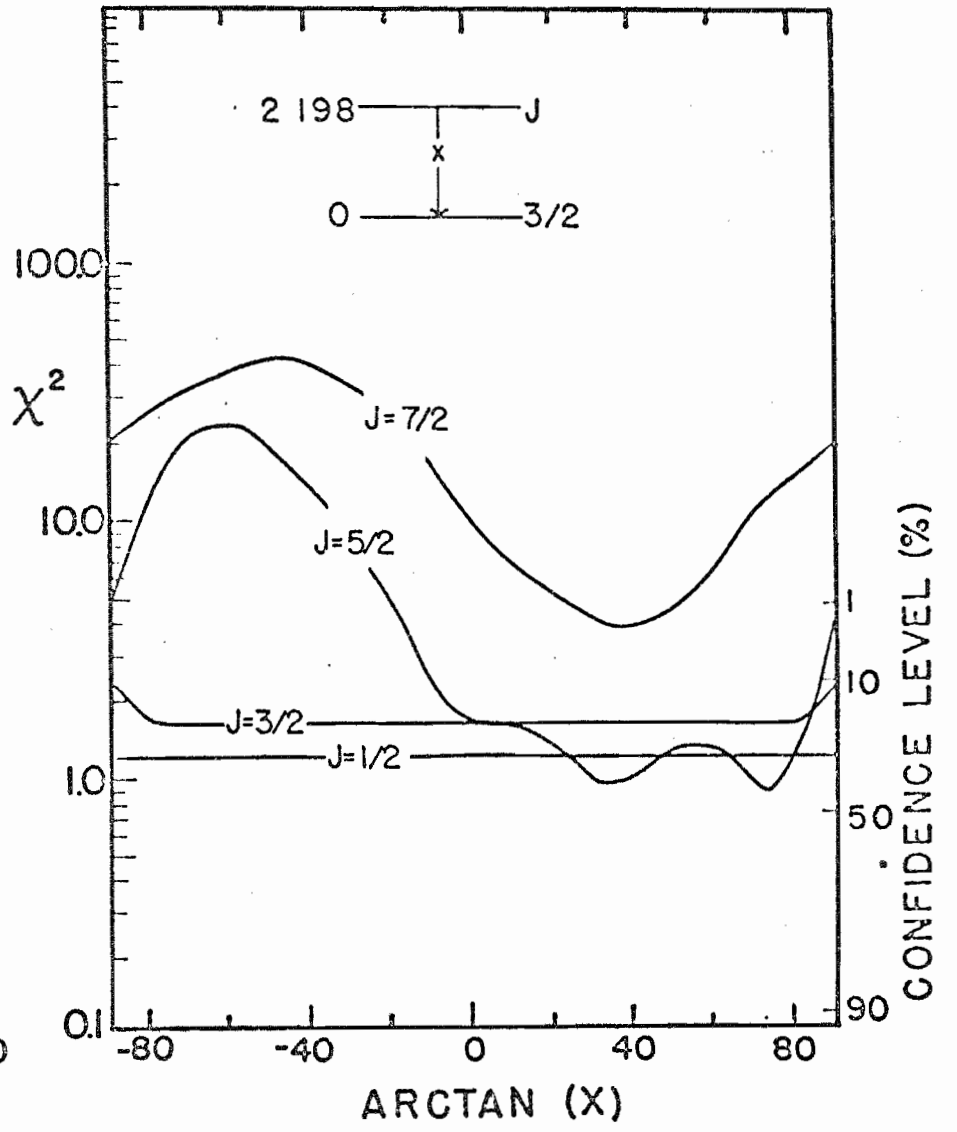
2 198
J
X
0
3/2
100.0
10.0
1.0
0.1
χ²
J=7/2
J=5/2
J=3/2
J=1/2
-80
-40
0
40
80
ARCTAN (X)
CONFIDENCE LEVEL (%)
10
50
90

(b)

of ^{49}Ti. Only γ-rays in coincidence with one-half of the total proton peak could be analyzed. The yield then became too small to obtain a reliable correlation. The sum spectrum (Figure 14) did yield a branching ratio of 60% to the first excited state, 23% to the 2198-keV level, and 17% to the ground state.

6) The 3174-keV Level

The particle group for this level was contaminated by the proton group from the 4897-keV level of ^{49}Ti. The 4897-keV level has a 3177-keV γ-ray (4897→1720) and a 340-keV γ-ray (1720→1380). By comparing the relative intensities of these γ-ray peaks obtained from the reaction ^{48}Ti(d,pγ)^{49}Ti with those seen in the ^{51}Ti spectrum, it could be determined that about one-half of the 3170-keV γ-rays came from the 3174-keV level of ^{51}Ti and about one-half from the 4897-keV level of ^{49}Ti. The γ-ray spectrum in coincidence with the proton groups corresponding to these two levels is shown in Figure 15. No correlation could be performed and only a ground state decay from the 3174-keV level of ^{51}Ti was observed.

7) The 3774-keV Level

The summed γ-ray spectrum measured in coincidence with particles leading to the 3774-keV level is shown in Figure 16. The 908-keV γ-ray could not be explained by a transition between any of the previously known levels of ^{51}Ti. Two possible decay schemes were proposed: a 908-keV γ-ray decay from the 3774-keV level to a new level at 2866-keV which in turn decayed to the 1438-keV level by emitting a 1428-keV γ-ray or a 1428-keV

Figure 14. The γ-ray Spectrum in Coincidence with the Particles Leading to the 2907-keV Level. This spectrum is the sum of spectra taken at five angles. The solid lines are meant only to guide the eye. Decays are observed to the ground state, the 1167-keV level, and the 2198-keV level. The subsequent ground state decays of the latter two levels are also observed. All energies are given in keV. The energies of the γ-rays are those obtained in the $^{48}Ca(\alpha,n\gamma)^{51}Ti$ experiment.

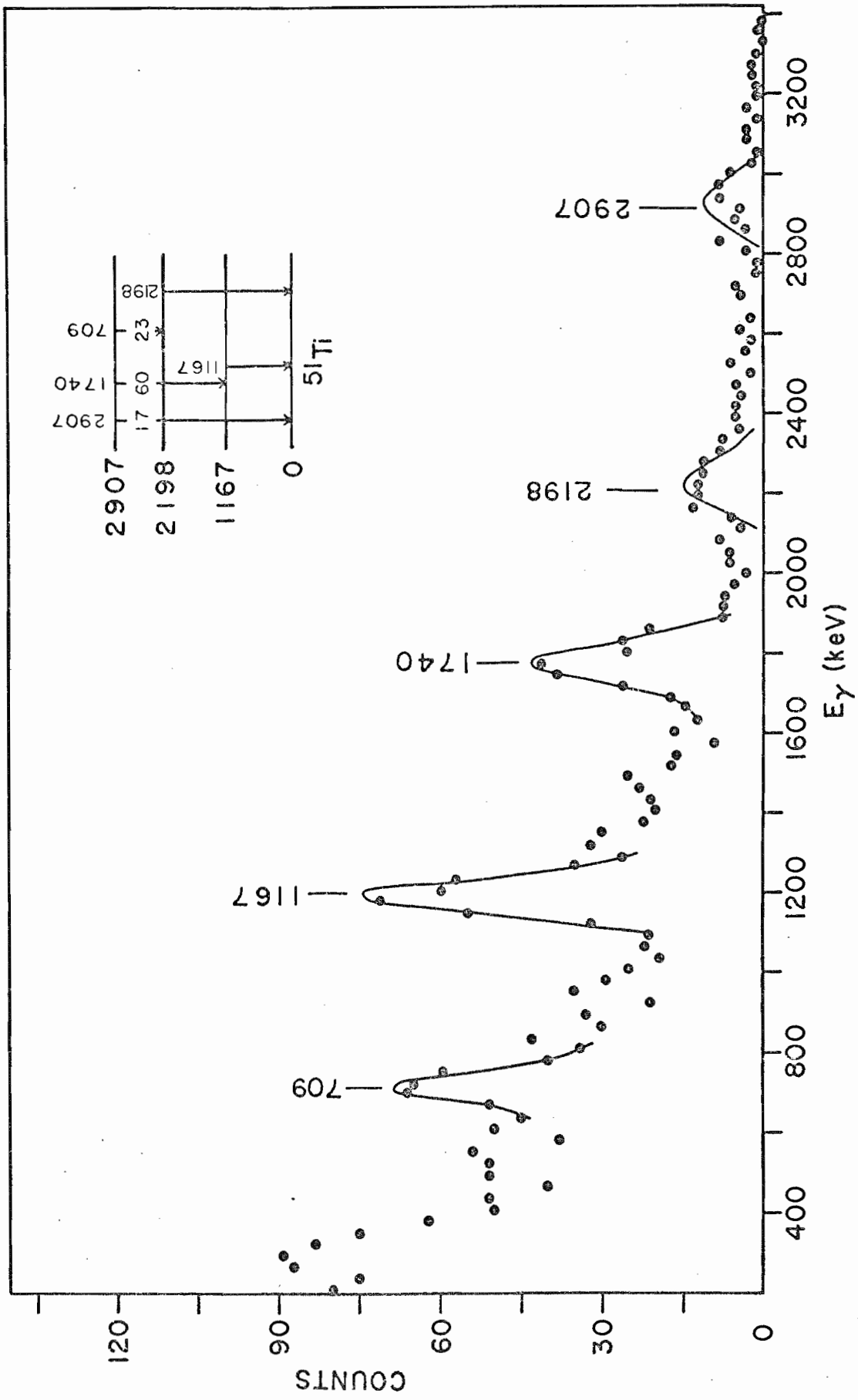
COUNTS
0
30
60
90
120
400
800
1200
1600
2000
2400
2800
3200
E_γ (keV)
709
1167
1740
2198
2907
^{51}Ti
2907
2198
1167
0
2907
17
1740
60
709
23
2198
1167

Figure 15. The γ-ray Spectrum in Coincidence with the Particles Leading to the ^{51}Ti 3174-keV Level. This spectrum is the sum of spectra taken at five angles. The solid lines are meant only to guide the eye. Contaminant γ-rays from the decay of the 4897-keV level of ^{49}Ti are seen. The experiment ^{48}Ti(d,pγ)^{49}Ti was performed with a target enriched to 99% ^{48}Ti. The γ-ray spectrum in coincidence with the particles leading to the ^{49}Ti 4897-keV level was obtained. By comparing the relative intensities of the 342-keV and 3174-keV γ-rays in these two spectra, it was determined that in the spectrum shown here, about one half of the 3174-keV γ-rays come from the 3174-keV level of ^{51}Ti and about one-half from the 4897-keV level of ^{49}Ti. Only a ground state decay from the 3174-keV level of ^{51}Ti is observed. The energy of the 3174-keV γ-ray of ^{51}Ti is that obtained from the ^{48}Ca(α,nγ)^{51}Ti experiment. The energies of the ^{49}Ti γ-rays are those deduced from the adopted level scheme of Raman (1970). All energies are given in keV.

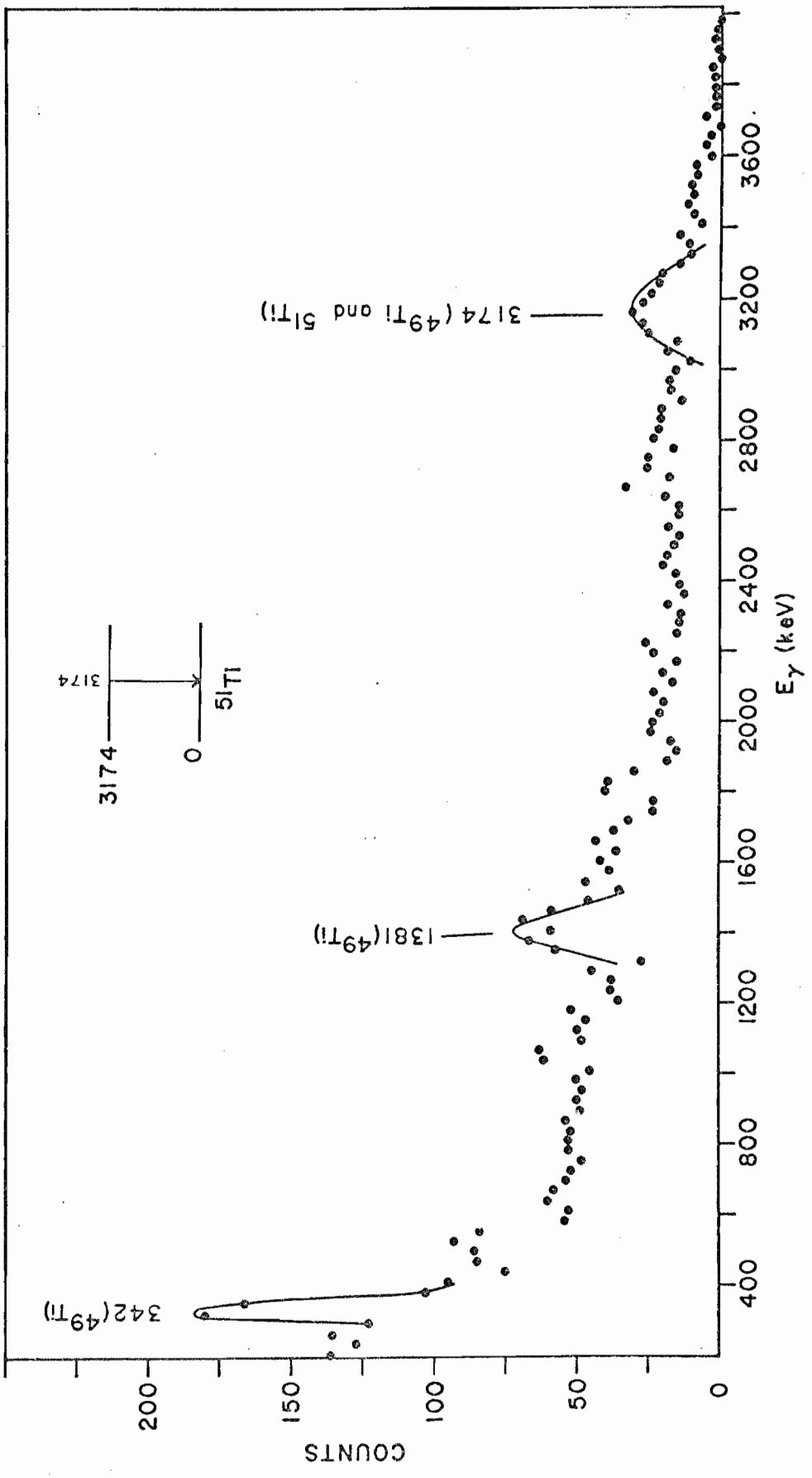
COUNTS
0
50
100
150
200
400
800
1200
1600
2000
2400
2800
3200
3600
E_γ (keV)
342(^{49}Ti)
1381(^{49}Ti)
3174 (^{49}Ti and ^{51}Ti)
3174
0
^{51}Ti

Figure 16. The γ-ray Spectrum in Coincidence with the Particles Leading to the ^{51}Ti 3774-keV Level. This spectrum is the sum of spectra taken at five angles. The solid lines are meant only to guide the eye. The 908-keV γ-ray could not be explained by a transition between any previously known levels. A new level was proposed at 2346-keV excitation and later confirmed by the results of the ^{48}Ca(α,nγ)^{51}Ti experiment. The branching ratio for the decay of the 3774-keV level was obtained by assuming that the 2346-keV level decays only to the 1438-keV level. The ratio of the intensities of the 908-keV and 2336-keV (including a correction for the detector efficiency and absorption in the target chamber walls) then gives the approximate branching ratio for the decay of the 3774-keV level. The number of counts in the 1430-keV peak is consistent with this branching ratio. All energies are given in keV. The energies of the γ-rays are taken from the results of the ^{48}Ca(α,nγ)^{51}Ti experiment.

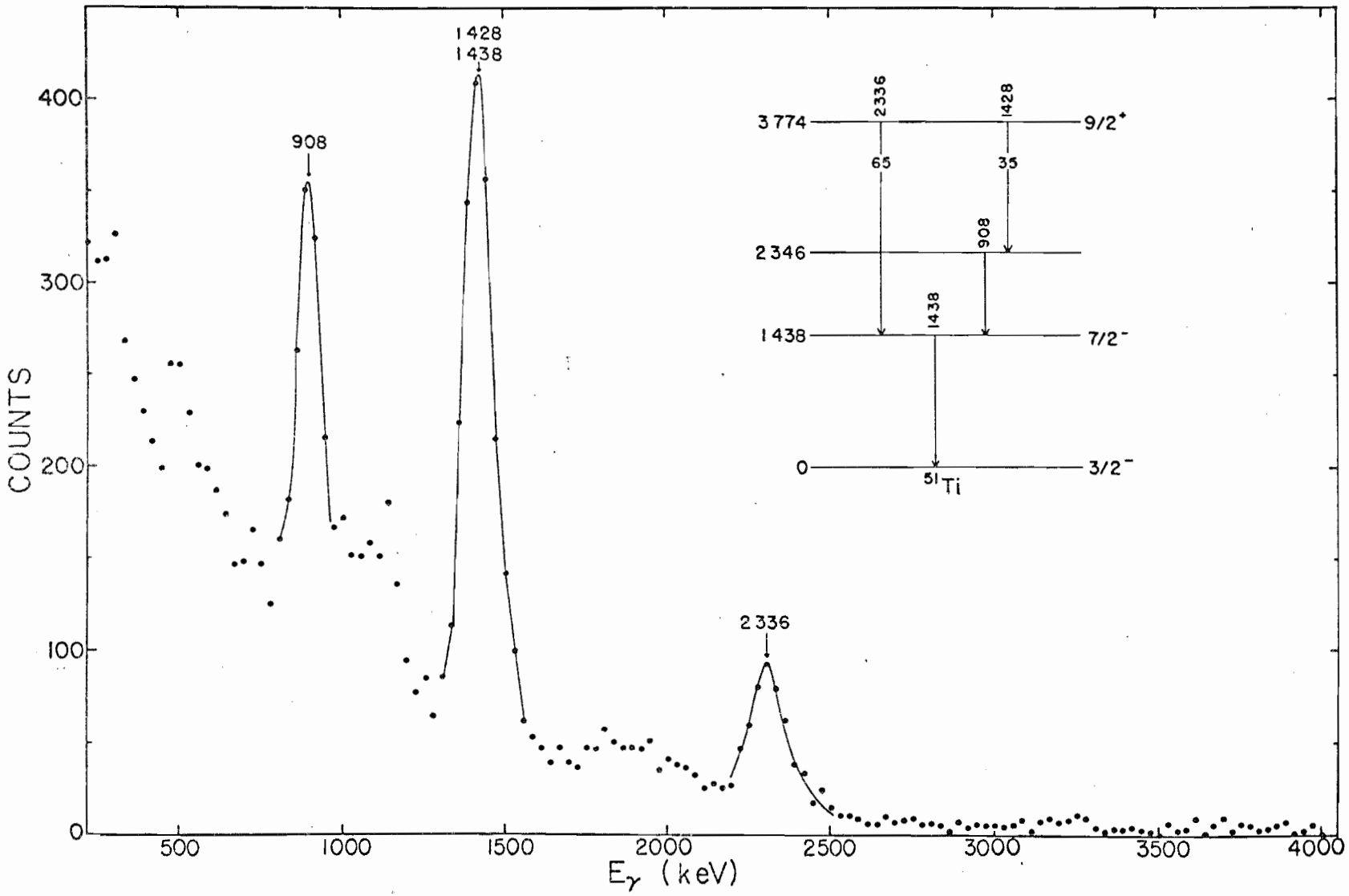
1428
1438
908
2336
400
300
200
100
0
COUNTS
500
1000
1500
2000
2500
3000
3500
4000
E_γ (keV)
3774
9/2+
2346
1438
7/2-
0
3/2-
65
35
908
1438
2336
1428
51Ti

γ-ray decay to a new level at 2346-keV which then decayed to the 1438-keV level by emission of a 908-keV level. Evidence obtained in the study of the $^{48}Ca(\alpha,n\gamma)^{51}Ti$ reaction (see Section IV B) indicates that the decay must be 3774→2346→1438→0. The 3774-keV level decays with a 65% branch to the 1438-keV level and a 35% branch to the new level at 2346-keV. Only a decay to the 1438-keV level is observed from the 2346-keV level.

A correlation was measured for the 3774→1438 transition. The results are shown in Figure 17. The $\ell_n = 4$ assignment by Barnes et al. (1964) rules out all but the 7/2 and 9/2 cases. If J = 7/2, then the M2/E1 mixing ratio is $\pm\infty$ or $1.04^{+1.24}_{-0.55}$. These values imply a strong M2 enhancement. If J = 9/2, then the M2/E1 mising ratio is $\pm\infty$ or -0.02 ± 0.31, that is, essentially pure M2 or pure E1. Appreciable M2/E1 mixing can occur only if there is an E1 retardation of $>10^8$ over the Weisskopf single-particle estimate of the half-life (Nuclear Data Group, 1970). This corresponds to a lifetime of $\geq$5.5 n.s. for the 3774-keV level. A lifetime on this order would have been observed as a appreciable shift of the peak of the time spectrum. No shift was observed. An assignment of $9/2^+$ with a mixing ratio of -0.02 ± 0.31 is made.

8) The 4162-keV Level

This level also has a ^{49}Ti contaminant and the correlation could not be performed. Only a ground state decay of this level was observed.

Figure 17. a) The Angular Correlation for the Photopeak of the 2336-keV γ-ray from the 3774-keV Level is Shown. The curve was calculated with the parameters corresponding to the minimum of χ^2 shown in (b) with J = 9/2. The data are plotted as a function of $\cos^2\theta$. The correlation was performed at E_d = 6.0 MeV.

b) Plots of χ^2 Versus Arctan x for J = 1/2, 3/2, 5/2, 7/2, 9/2, and 11/2 are Shown. An ℓ = 4 assignment by Barnes et al. (1964) rules out all but J = 7/2 and 9/2. If J = 7/2, then the M2/E1 mixing ratio is $\pm\infty$ or $1.04^{+1.24}_{-0.55}$. Both of these imply strong M2 enhancements which seem very unlikely. If J = 9/2, then the M2/E1 mixing ratio is $\pm\infty$ or -0.02 ± 0.31, that is, essentially pure M2 or pure E1. Again the pure M2 assignment seems very unlikely and an assignment of 9/2 with a mixing ratio of -0.02 ± 0.31 is made.

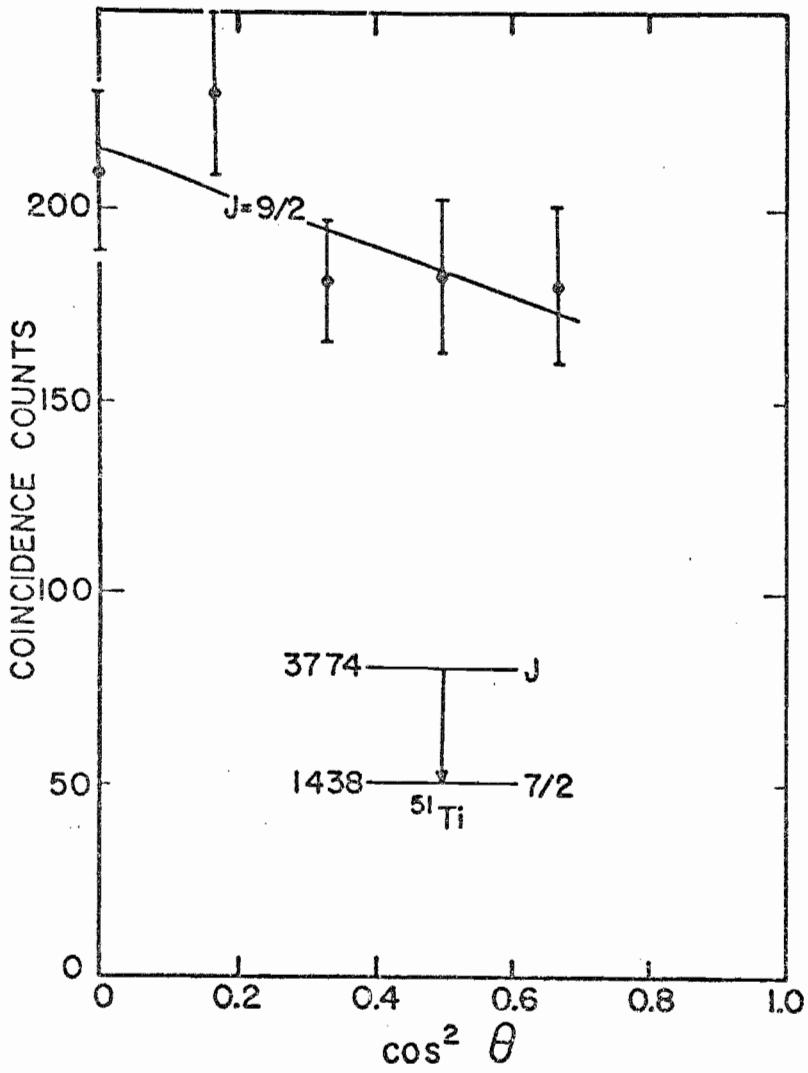
COINCIDENCE COUNTS
200
150
100
50
0
0
0.2
0.4
0.6
0.8
1.0
cos² θ
J=9/2
3774
J
1438
7/2
51Ti

(a)

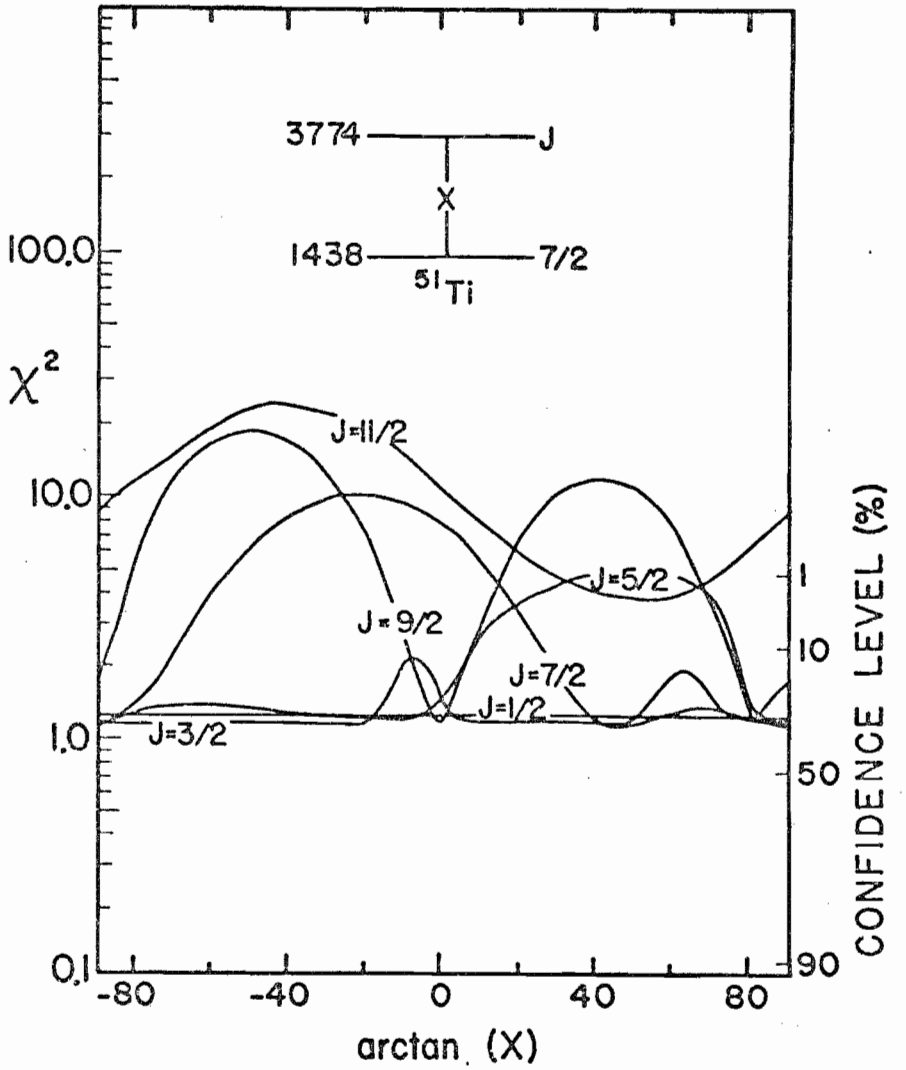
χ²
100.0
10.0
1.0
0.1
-80
-40
0
40
80
arctan (X)
CONFIDENCE LEVEL (%)
1
10
50
90
3774
J
X
1438
7/2
51Ti
J=11/2
J=5/2
J=9/2
J=7/2
J=1/2
J=3/2

(b)

9) The 4554- and 4592-keV levels

The 4592-keV level is the stronger member of this doublet, with the 4554-keV proton group showing up only as a shoulder. The γ-ray spectrum in coincidence with the proton group leading to the 4592-keV level is shown in figure 18. This level decays with a 90% branch to the ground state. The other branch is either a 3160-keV decay to the 1438-keV level or a 1430-keV decay to the 3174-keV level. The resolution of the NaI(Tℓ) crystal was not good enough to distinguish between these two possibilities.

A correlation was measured for the 4592→0 transition and the results are shown in Figure 19. The results give good fits for both J = 3/2 and J = 5/2. Both of these values are consistent with the ℓ_n = 2 assignment by Barnes et al. (1964) using the reaction $^{50}Ti(d,p)^{51}Ti$. No mixing ratio can be obtained for J = 3/2. If J = 5/2, then M2/E1 mixing ratios of $2.5^{+1.1}_{-0.6}$ or $0.38^{+0.29}_{-0.24}$ are obtained. The larger mixing ratio implies a strong M2 enhancement and therefore seems less likely.

10) The 4747-keV level

This state was weakly populated and a correlation could not be performed. The coincident γ-ray spectrum for this level is shown in Figure 20. As noted in the figure caption of Figure 20, the decay scheme of the 4747-keV level is still uncertain. Only a branch to the 2346-keV level is observed but the possibility of other decays from the 4747-keV level is quite possible.

Figure 18. The γ-ray Spectrum in Coincidence with the Particles Leading to the ^{51}Ti 4592-keV Level. This spectrum is the sum of spectra taken at five angles. The solid lines are meant only to guide the eye. A strong ground state decay is seen, as well as 1440-keV and 3170-keV γ-rays. The latter two γ-rays can be explained by either of the two decays indicated by dashed lines in the level diagram. The excitation energy of the 4592-keV level is not well known and the NaI(Tℓ) resolution does not allow a choice to be made between the two possible decays. This level was not populated by the ^{48}Ca(α,nγ)^{51}Ti reaction. All energies are given in keV. The energy of the 4592-keV level was taken from Barnes et al. (1964), and the energies of the 1438-keV and 3174-keV levels were taken from the results of the ^{48}Ca(α,nγ)^{51}Ti experiment.

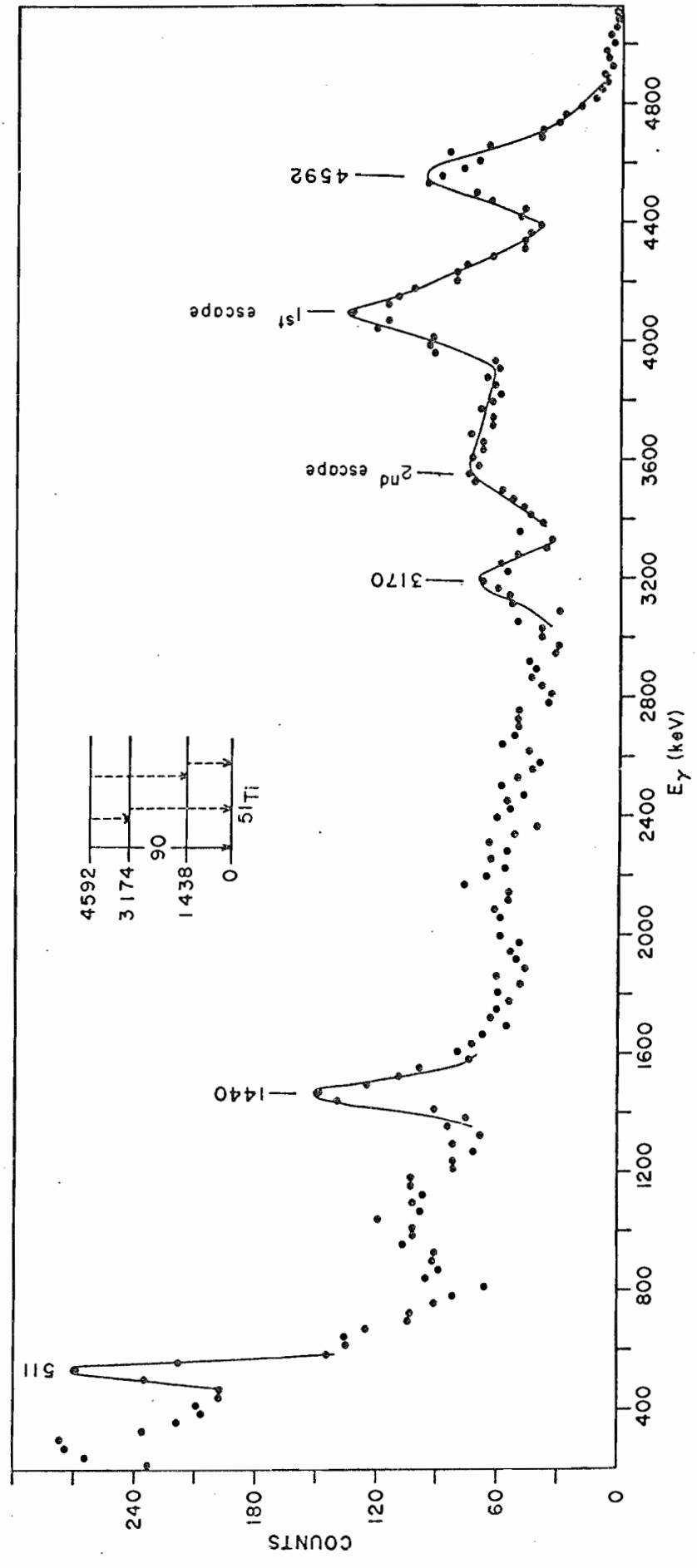
511
1440
3170
2nd escape
1st escape
4592
COUNTS
0
60
120
180
240
400
800
1200
1600
2000
2400
2800
3200
3600
4000
4400
4800
E_γ (keV)
4592
3174
90
1438
0
^{51}Ti

Figure 19. a) The Angular Correlation for the Photopeak and the First-escape Peak of the 4592-keV γ-ray is Shown. The curves were calculated with the parameters corresponding to the minima of χ^2 shown in (b) with J = 3/2 and 5/2. The data are plotted as a function of $\cos^2\theta$. The correlation was performed at E_d = 6.0 MeV.

b) Plots of χ^2 Versus Arctan x for J = 1/2, 3/2, 5/2, 7/2 are Shown. Only J = 3/2 and J = 5/2 fall below the 1% confidence level. No choice between the two is possible in this work.

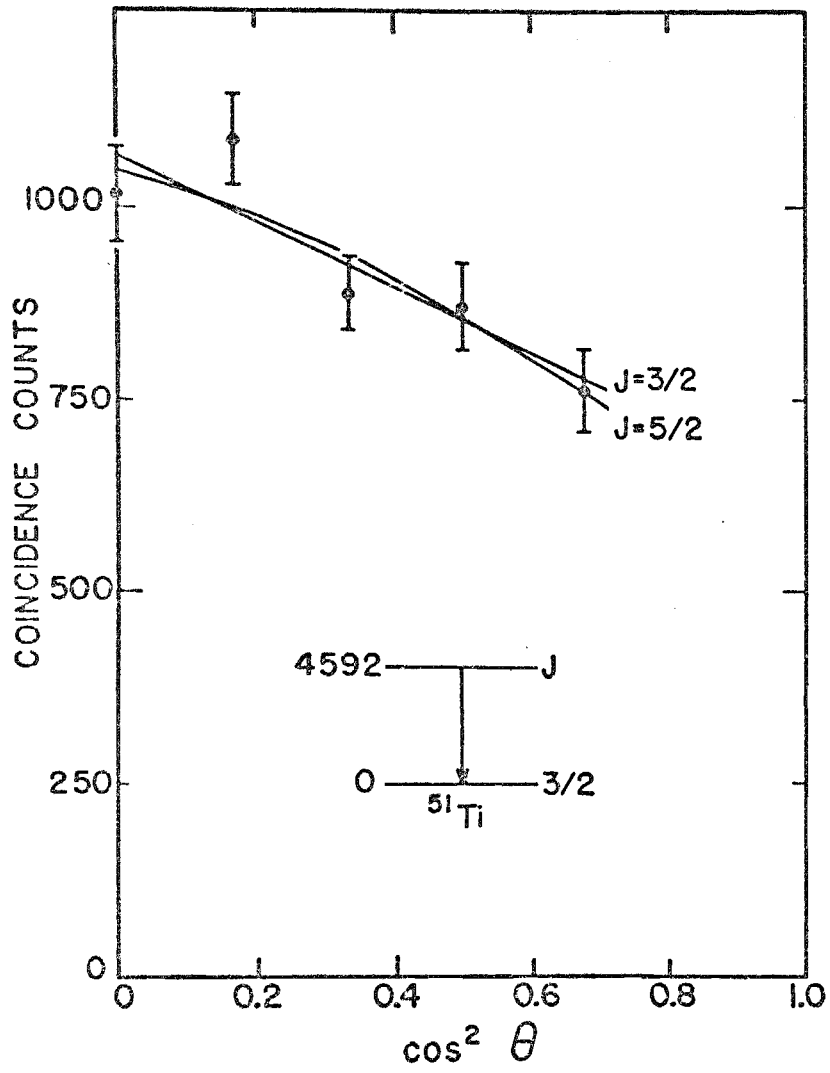
COINCIDENCE COUNTS
1000
750
500
250
0
0
0.2
0.4
0.6
0.8
1.0
cos² θ
J=3/2
J=5/2
4592
J
0
3/2
51Ti

(a)

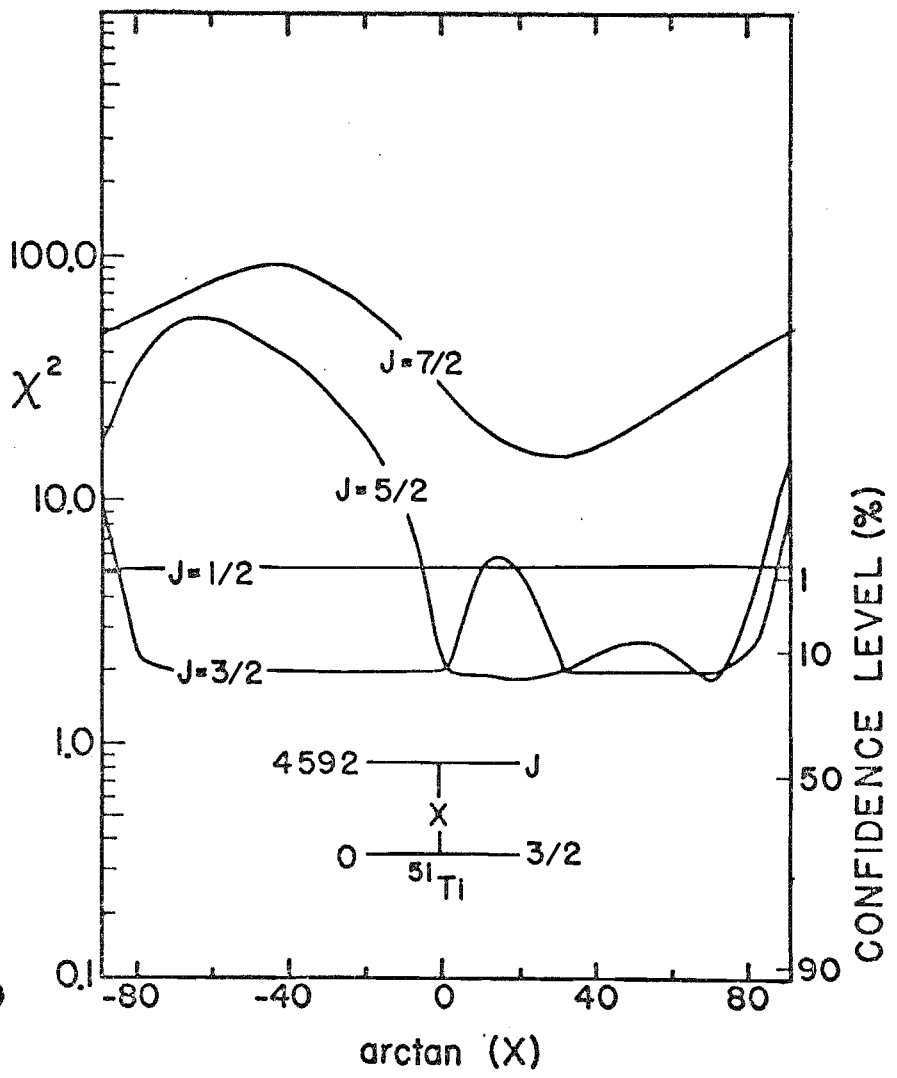
χ²
100.0
10.0
1.0
0.1
-80
-40
0
40
80
arctan (X)
J=7/2
J=5/2
J=1/2
J=3/2
4592
J
X
0
3/2
51Ti
CONFIDENCE LEVEL (%)
1
10
50
90

(b)

Figure 20. The γ-ray Spectrum in Coincidence with the Particles Leading to the ^{51}Ti 4747-keV Level. This spectrum is the sum of spectra taken at five angles. The solid lines are meant only to guide the eye. Energies are given in keV. A decay to the 2346-keV level and the γ-rays from the decay of that level are seen. However, the yield of the 2401-keV γ-ray (after efficiency correction) is not equal to the yield of the 908-keV and 1438-keV γ-rays. One explanation would be a strong correlation effect that would increase the yield of the 2401-keV γ-ray at 0°. The yield at that angle could not be measured in this experiment. Another explanation is that the 4747-keV level decays to a state that decays in turn to the 2346-keV level. The γ-rays from these transitions could be obscured by other peaks in the spectrum. One such possibility is a 4747→3774 transition. However, the 2336-keV γ-ray from the decay of the 3774-keV level is not seen.

The small peak near 1150-keV has not been identified. It may be a 1167→0 transition. It should also be noted that the background above the 2401-keV peak is very high, suggesting the existence of a higher energy photopeak. Such a peak was not observed. The energies of the 908-keV and 1438-keV γ-rays were taken from the ^{48}Ca(α,nγ)^{51}Ti experiment. The energy of the 2400-keV γ-ray was determined from the NaI(Tℓ) spectrum shown here.

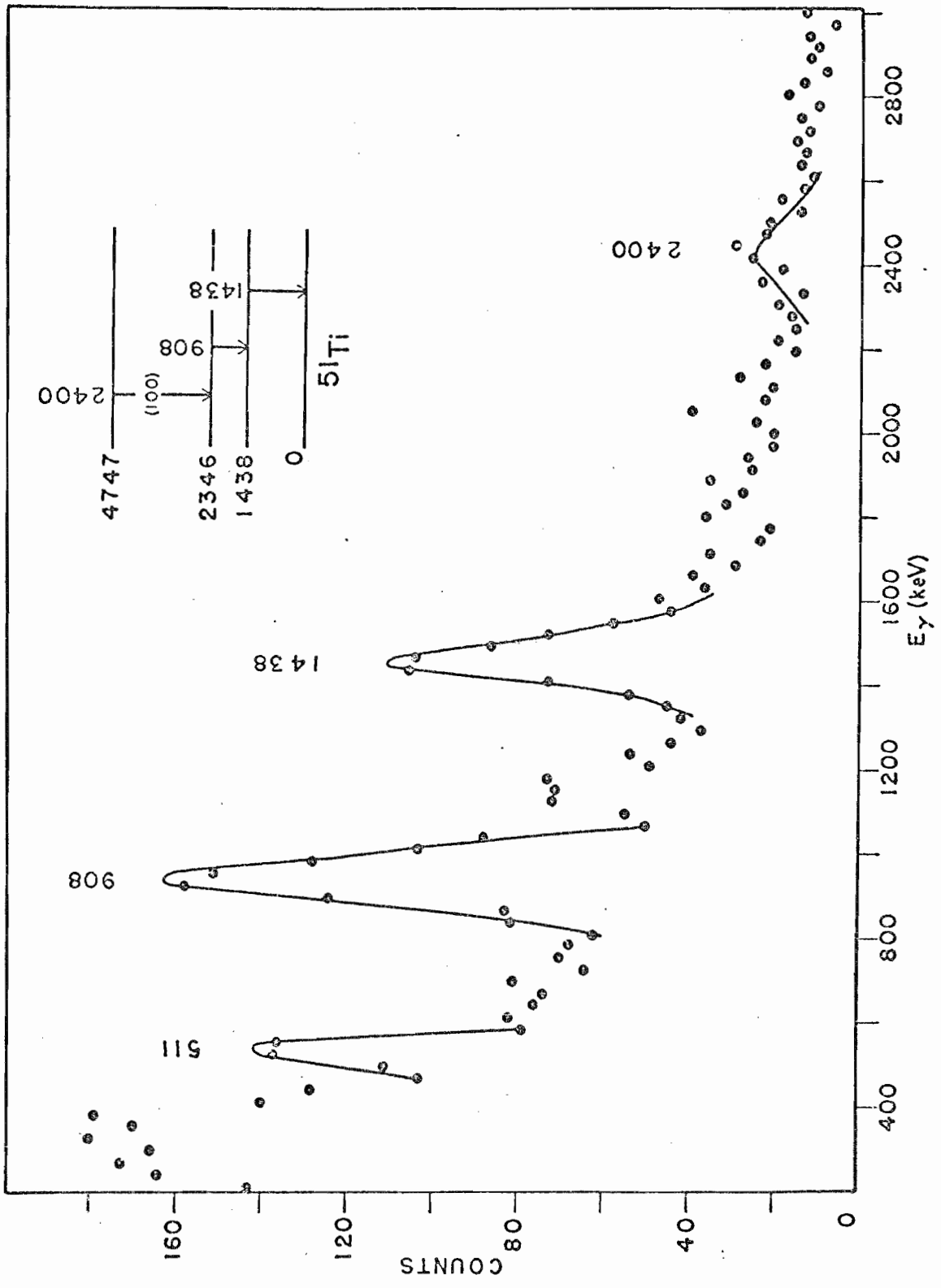
COUNTS
0
40
80
120
160
400
800
1200
1600
2000
2400
2800
E_γ (keV)
511
908
1438
2400
^{51}Ti
0
1438
908
2400
(100)
2346
4747

11) The 4810-keV Level

This state was weakly populated and a correlation was not obtained. This state decays principally to the ground state with less than an 8% branch to the first excited state.

12) The 4882-keV Level

This state was observed to have an 80% branch to the 2144-keV level and a 20% branch to the 1438-keV level. The coincident γ-ray spectrum for this level is shown in Figure 21. A correlation was measured for the decay to the 2144-keV and is shown in Figure 22. Barnes et al. (1964) report $\ell_n = 0$ for this level implying a spin of 1/2. Cosman et al. (1968), studying the analog states in ^{51}V of the low-lying ^{51}Ti states via the reaction ^{50}Ti(p,p)^{50}Ti, report the resonance corresponding to this level to be of f-wave character and suggest an $\ell = 3$ assignment for this level. This would imply possible spins of 5/2 or 7/2. The existence of the decay to the 7/2 level at 1438-keV makes the J = 1/2 assignment less likely although the correlation does give an acceptable fit for J = 1/2. If J = 5/2 then the E2/M1 mixing ratio is 0.32 ± 0.13 or $-5.8^{+2.9}_{-92.3}$. If J = 7/2 then the E2/M1 mixing ratio is -0.26 ± 0.11 or ±∞.

13) The 5139-keV Level

The coincident γ-ray spectrum for the 5139-keV level is shown in Figure 23. This level has a 97% branch to the ground state and a 3% branch to the first excited state. A correlation was measured for the ground state transition and is shown in

Figure 21. The γ-ray Spectrum in Coincidence with the Particles Leading to the ^{51}Ti 4882-keV Level. This spectrum is the sum of spectra taken at five angles. The solid lines are meant only to guide the eye. Transitions are seen to the 2144-keV and 1438-keV levels. The subsequent decays of these levels are also seen. The 3444-keV level was not seen in the ^{48}Ca(α,nγ)^{51}Ti experiment, but the 2738-keV γ-ray was seen in coincidence with the 2144-keV γ-ray. With the exception of the 3444-keV γ-ray, the energies of the γ-rays are those obtained from the results of the ^{48}Ca(α,nγ)^{51}Ti experiment. The energy of the 3444-keV γ-ray is deduced from the energies of the 4882-keV and 1438-keV levels. All energies are in keV.

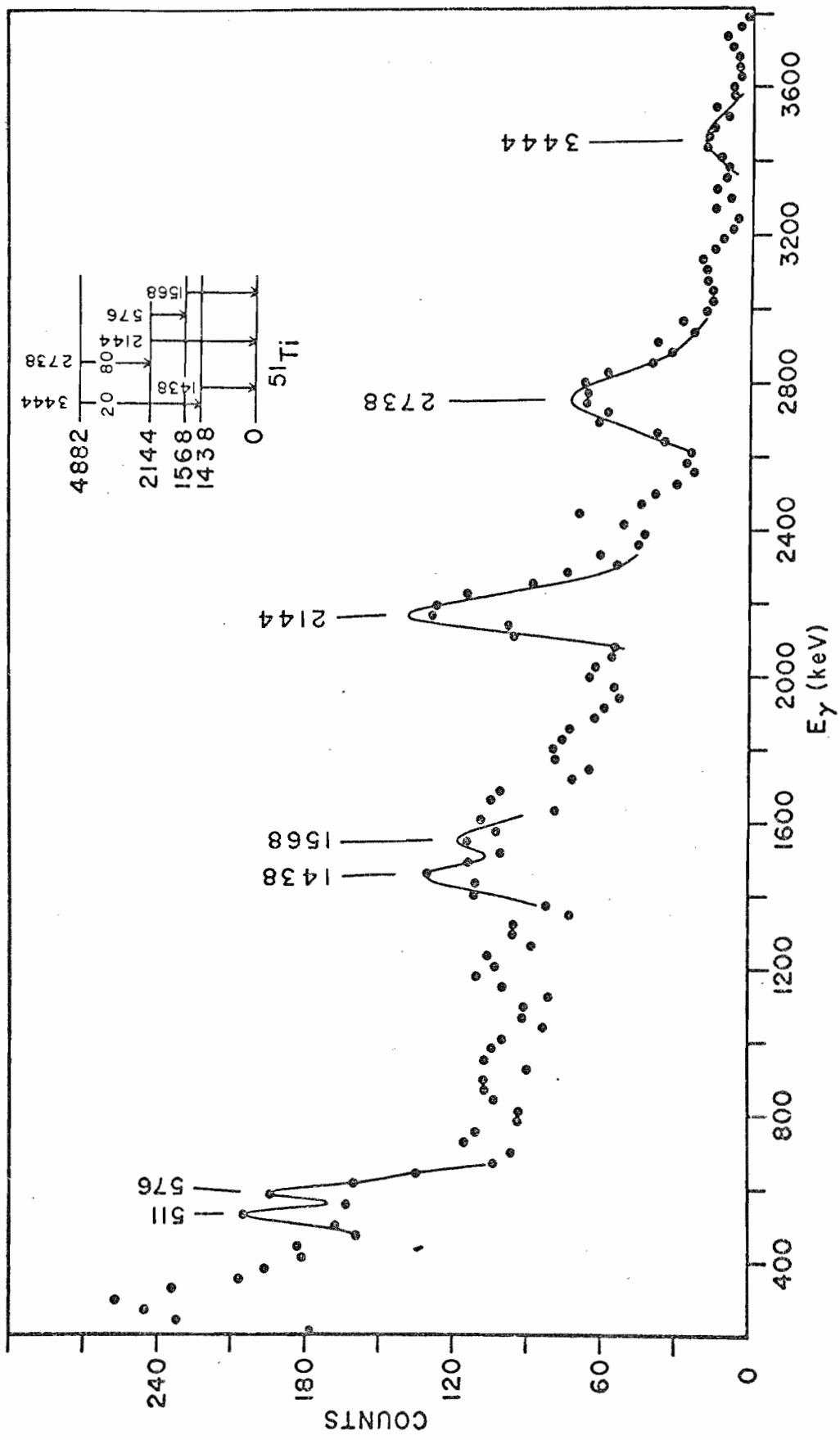
COUNTS
240
180
120
60
0
400
800
1200
1600
2000
2400
2800
3200
3600
E_γ (keV)
511
576
1438
1568
2144
2738
3444
^{51}Ti
4882
3444
2738
2144
1568
1438
0
20
80
576
1568

Figure 22. a) The Angular Correlation for the Photopeak of the 2738-keV γ-ray from the 4882-keV Level is Shown. The curves were calculated with the parameters corresponding to the minima of χ^2 shown in (b) with J = 5/2 and 7/2. The data are plotted as a function of $\cos^2\theta$. The correlation was performed at E_d = 6.0 MeV.

b) Plots of χ^2 Versus Arctan x for J = 1/2, 3/2, 5/2, 7/2, and 9/2 are Shown. Barnes et al. (1964) report an ℓ-value of 0 for this level implying a spin of $1/2^+$. Since this level decays to the $7/2^-$ level at 1438-keV, a $1/2^+$ spin in very unlikely. Cosman et al. (1968) report an ℓ = 3 assignment for this level, implying spins of 5/2 and 7/2. Both 5/2 and 7/2 give acceptable fits and no choice between the two is possible in this work.

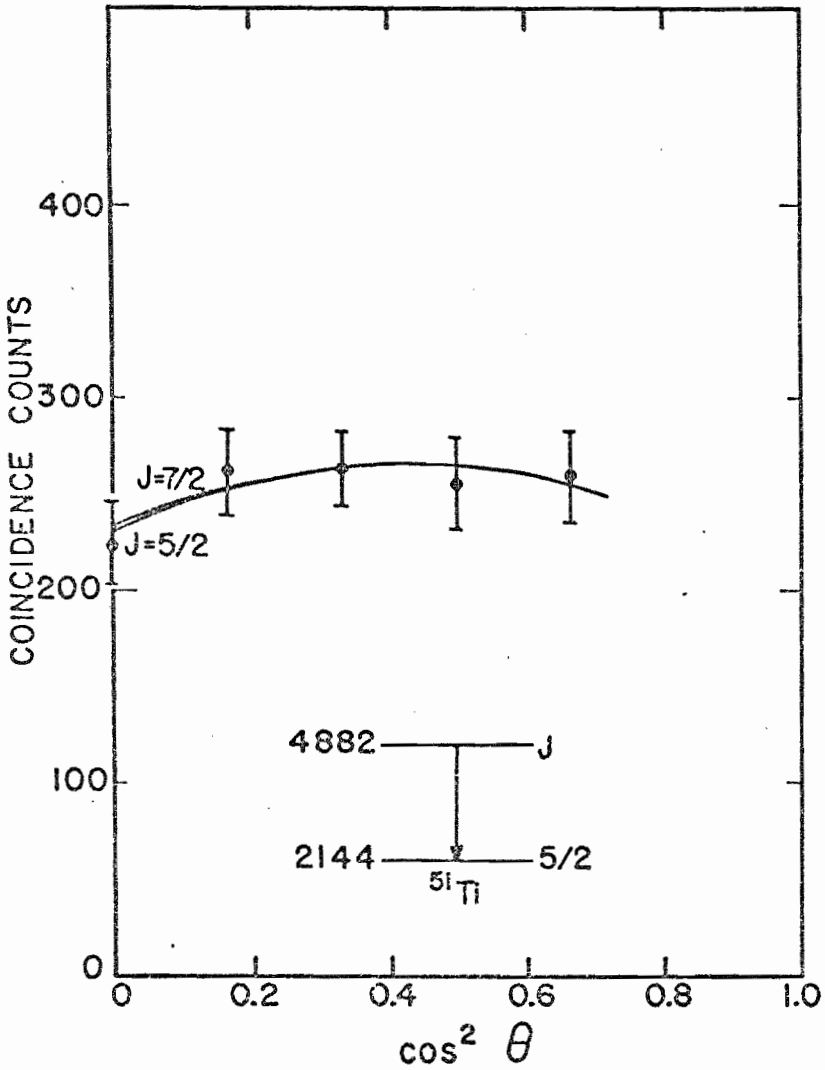
COINCIDENCE COUNTS
400
300
200
100
0
J=7/2
J=5/2
4882
J
2144
5/2
51Ti
0
0.2
0.4
0.6
0.8
1.0
cos² θ

(a)

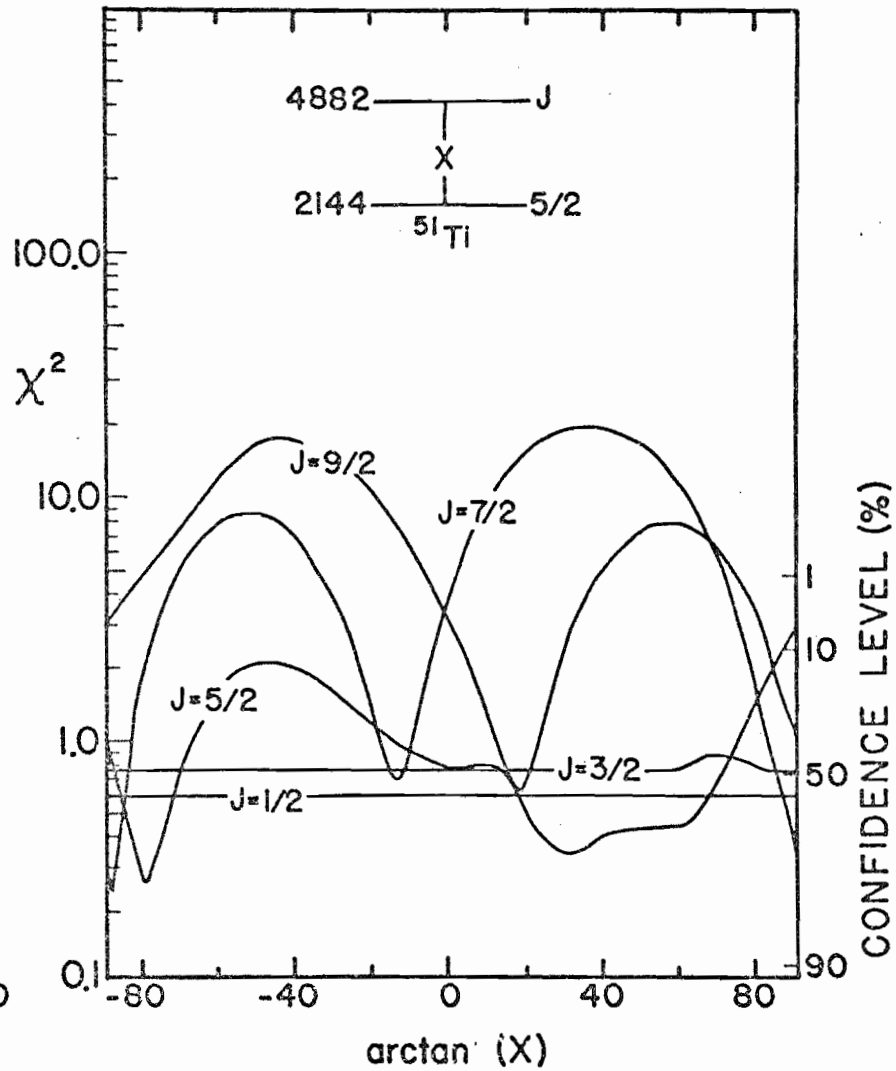
χ²
100.0
10.0
1.0
0.1
4882
J
X
2144
5/2
51Ti
J=9/2
J=7/2
J=5/2
J=3/2
J=1/2
-80
-40
0
40
80
arctan (X)
CONFIDENCE LEVEL (%)
1
10
50
90

(b)

Figure 23. The γ-ray Spectrum in Coincidence with the Particles Leading to the ^{51}Ti 5139-keV Level. This spectrum is the sum of spectra taken at five angles. The solid lines are meant only to guide the eye. Energies are given in keV. A strong ground state transition is observed as well as a weak branch to the 1167-keV level. The energies of the γ-rays are those deduced from the energies of the levels.

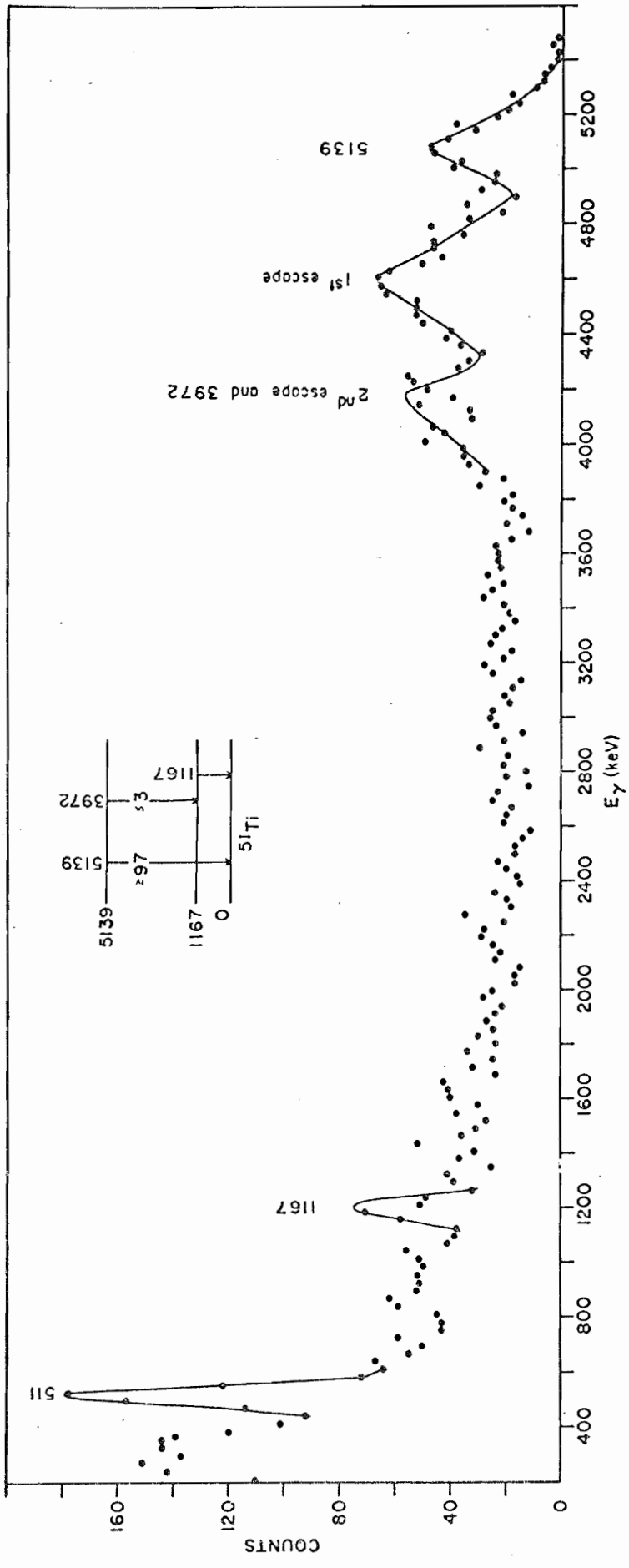
COUNTS
160
120
80
40
0
400
800
1200
1600
2000
2400
2800
3200
3600
4000
4400
4800
5200
E_γ (keV)
511
1167
2nd escape and 3972
1st escape
5139
5139
3972
1167
0
≤3
≥97
^{51}Ti

Figure 24. Barnes et al. (1964) report an $\ell = 3$ assignment for the proton distribution leading to this level from the $^{50}Ti(d,p)^{51}Ti$ reaction. This allows values of J = 5/2 or J = 7/2. If J = 5/2 then the E2/M1 mixing ratio is $-8.1^{+3.9}_{-6\ 3.0}$ or -0.30 ± 0.15. If J = 7/2 then the M3/E2 mixing ratio is $0.26^{+0.34}_{-0.29}$ or $1.5^{+19.4}_{-1.1}$. The latter value of the mixing ratio seems unlikely as it requires a strong M3 enhancement.

14) The 5214-keV Level

The coincident γ-ray spectrum for the 5214-keV level is shown in Figure 25. A strong ground state transition is observed. The possibility of a very weak branch to the 1167-keV level also exists. The γ-ray yield was too weak to obtain a reliable correlation.

15) The 5440-keV Level

This level probably corresponds with the level at 5427-keV reported by Cosman et al. (1969), studying the analog states in ^{51}V of the low-lying ^{51}Ti states via the reactions $^{50}Ti(p,p)^{50}Ti$ and $^{50}Ti(p,p')^{50}Ti$. They have tentatively assigned $\ell = 2$ for this level. The γ-ray yield was too weak to obtain a correlation but the coincident γ-ray spectrum (Figure 26) yielded 5440, 1438, and 1167-keV γ-rays. Since the intermediate transitions are not seen, a reliable decay scheme cannot be proposed. The principal decay is the ground state transition with a branching ratio of greater than 70%.

Figure 24. a) The Angular Correlation for the Photopeak of the 5139-keV γ-ray is Shown. The curves were calculated with the parameters corresponding to the minima of χ^2 shown in (b) with J = 5/2 and 7/2. The data are plotted as a function of $\cos^2\theta$. The correlation was performed at E_d = 6.0 MeV.

b) Plots of χ^2 Versus Arctan x for J = 1/2, 3/2, 5/2, and 7/2 are Shown. An ℓ = 3 assignment by Barnes et al. (1964) rules out all but J = 5/2 and 7/2. No choice between the two is possible in this work.

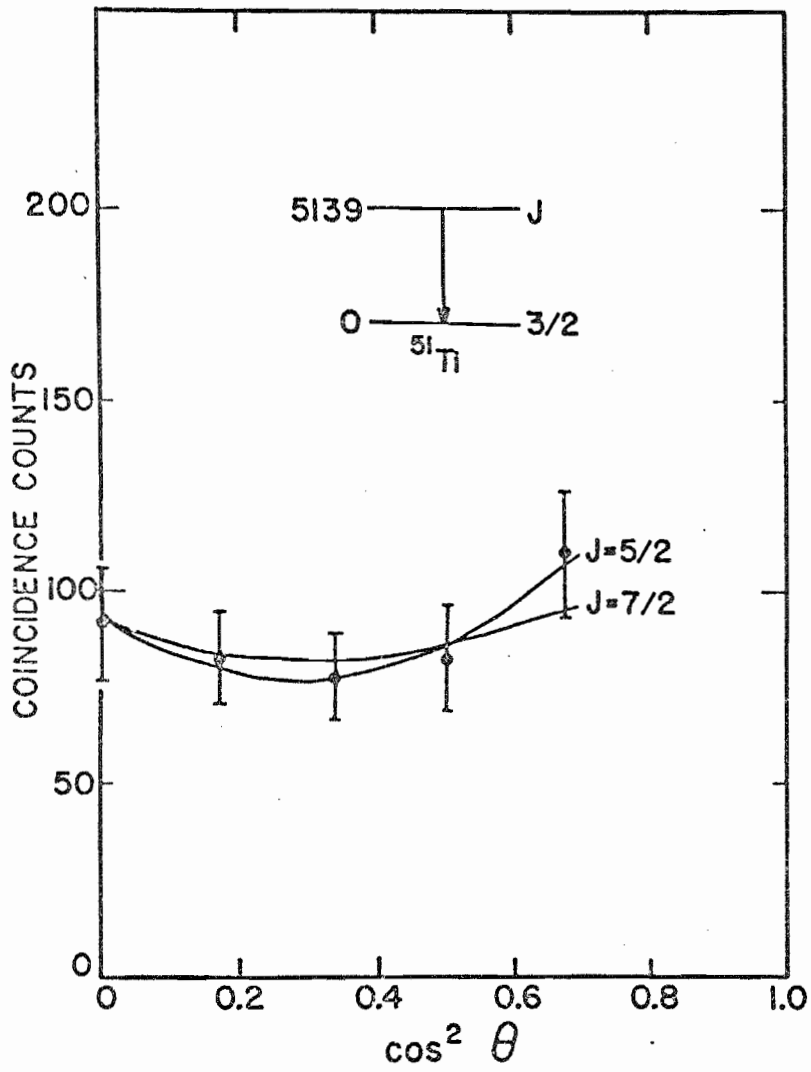
5139
J
0
3/2
51 In
200
150
100
50
0
COINCIDENCE COUNTS
J=5/2
J=7/2
0
0.2
0.4
0.6
0.8
1.0
cos² θ

(a)

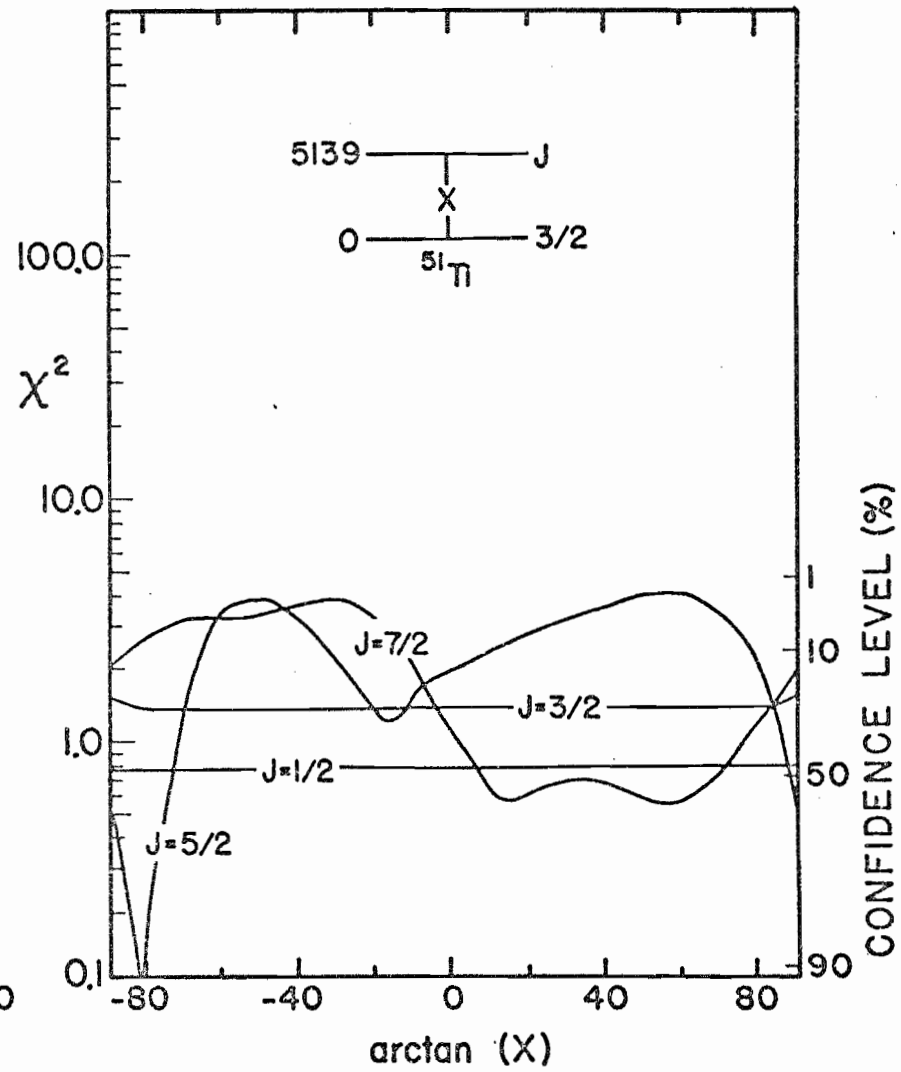
5139
J
X
0
3/2
51 In
100.0
10.0
1.0
0.1
χ²
J=7/2
J=3/2
J=1/2
J=5/2
-80
-40
0
40
80
arctan (X)
1
10
50
90
CONFIDENCE LEVEL (%)

(b)

Figure 25. The γ-ray Spectrum in Coincidence with the Particles Leading to the ^{51}Ti 5214-keV Level. This spectrum is the sum of spectra taken at five angles. The solid lines are meant only to guide the eye. Energies are given in keV. A strong ground state transition is observed. The possibility of a very weak branch to the 1167-keV level also exists. The energy of the 5214-keV γ-ray is deduced from the energy of the 5214-keV level, as reported by Barnes et al. (1964).

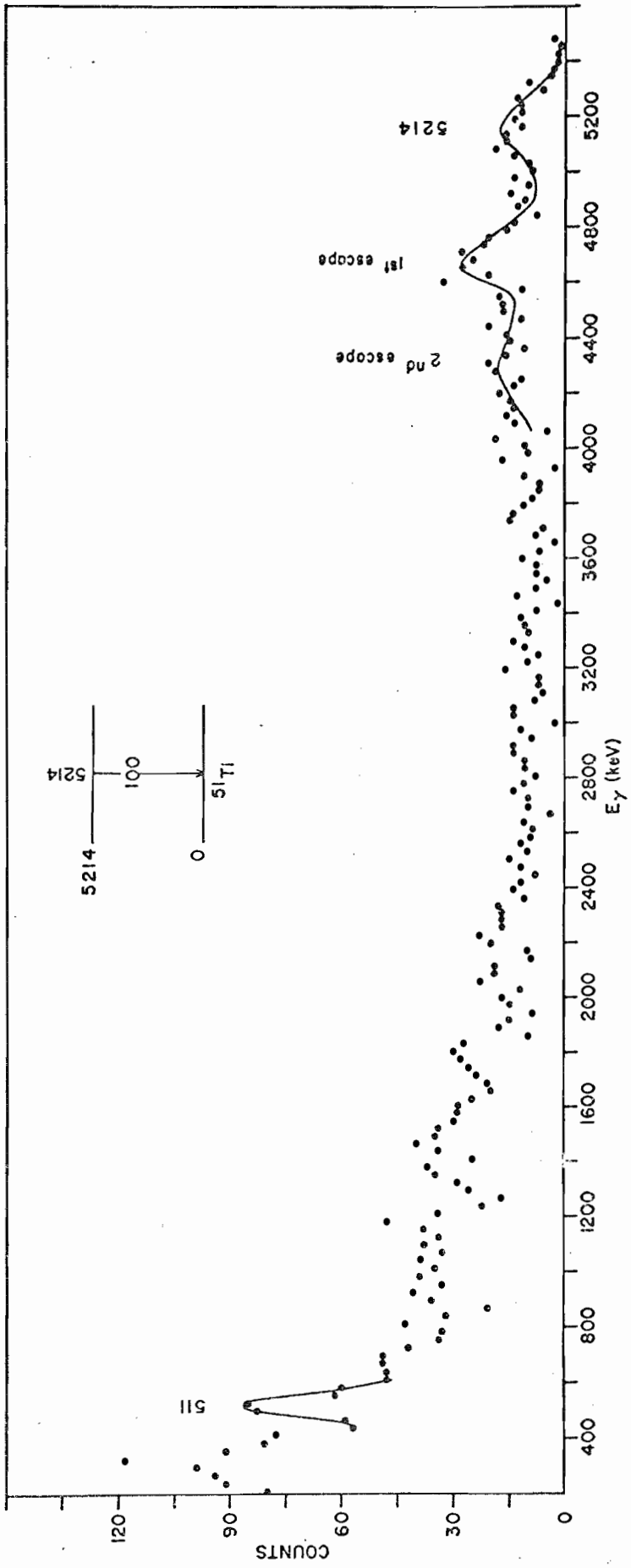
COUNTS
120
90
60
30
0
400
800
1200
1600
2000
2400
2800
3200
3600
4000
4400
4800
5200
E_γ (keV)
511
2nd escape
1st escape
5214
5214
100
^{51}Ti
5214
0

Figure 26. The γ-ray Spectrum in Coincidence with the Particles Leading to the ^{51}Ti 5440-keV Level. This spectrum is the sum of spectra taken at five angles. The solid lines are meant only to guide the eye. Energies are given in keV. This is a previously unreported level. The energy of the proton group as well as the energy of the photopeak of the ground state transition are consistent with a ^{51}Ti level at 5440 keV excitation. The existence in the spectrum of the 1167-keV and 1438-keV γ-rays is further evidence that this proton group is due to a ^{51}Ti level. Since the transitions to these levels are not seen, the complete decay scheme of this level cannot be proposed. The energy of the 5440-keV γ-ray is that measured with the NaI(Tℓ) crystal. The energies of the 1167-keV and 1438-keV γ-rays were taken from the results of the ^{48}Ca(α,nγ)^{51}Ti experiment. The two peaks near 1600 and 2250 keV have not been identified.

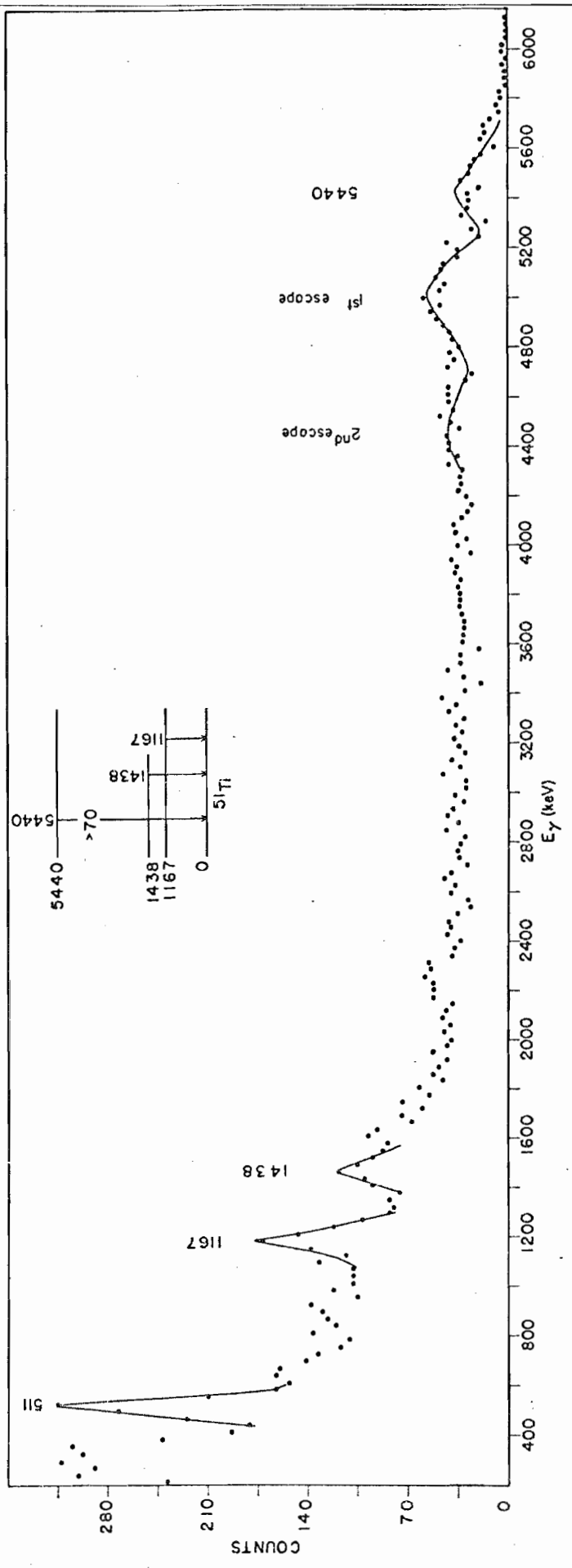
COUNTS
0
70
140
210
280
400
800
1200
1600
2000
2400
2800
3200
3600
4000
4400
4800
5200
5600
6000
E_γ (keV)
511
1167
1438
5440
2nd escape
1st escape
5440
>70
1438
1167
0
^{51}Ti
5440

B) $^{48}Ca(\alpha,n\gamma)^{51}Ti$ Measurements

Figure 27 shows the proposed decay scheme for levels populated by the $^{48}Ca(\alpha,n\gamma)^{51}Ti$ reaction. The levels at 2733 keV, 2755 keV, 2922 keV, 3235 keV, 3473 keV, 3619 keV, 3636 keV, and 5786 keV have not been previously reported. The evidence for several of these is not very firm, and these levels are indicated as dashed lines. Evidence for the new levels was obtained from both the γ-γ coincidence data and the neutron threshold data.

1) Neutron Threshold Results

In a neutron recoil spectra, neutron groups are not separated as are particle groups in a surface barrier detector. For each neutron of energy E_n, the detected energy can range from zero to E_n^{max}. The observed neutron spectra is then made up of a series of overlapping neutron spectra with the higher energy neutrons extending farther out on the E axis. By setting a lower limit or baseline on the E axis, low energy neutrons are eliminated. By raising the baseline to be greater than E_n^{max}, the entire neutron group of energy E_n is eliminated. When reading back the Ge(Li) spectra, a lower limit was placed on the neutron energy and this lower limit was then raised in small increments so that a series of γ-ray spectra was obtained with each spectra having a different neutron energy baseline. Figure 28 is the coincident γ-ray spectrum obtained with the baseline set at channel number 8. (See Figure 31 for neutron energy.) Figures 29a and 29b are the coincident γ-ray spectra obtained with the

Figure 27. The Proposed Decay Scheme for Levels Populated in the $^{48}Ca(\alpha,n\gamma)^{51}Ti$ Reaction. All levels below 4000-keV that were observed in the $^{50}Ti(d,p\gamma)^{51}Ti$ experiment were also seen in the $^{48}Ca(\alpha,n\gamma)^{51}Ti$ experiment. Previously unreported levels were observed at 2733, 2755, 2922, 3235, and 3636 keV excitation energies. Tentative assignments of new levels at 3473, 3619, and 5786 keV excitation were made. These latter levels are indicated by dashed lines. Uncertain transitions are also indicated by dashed lines. All energies are given in keV.

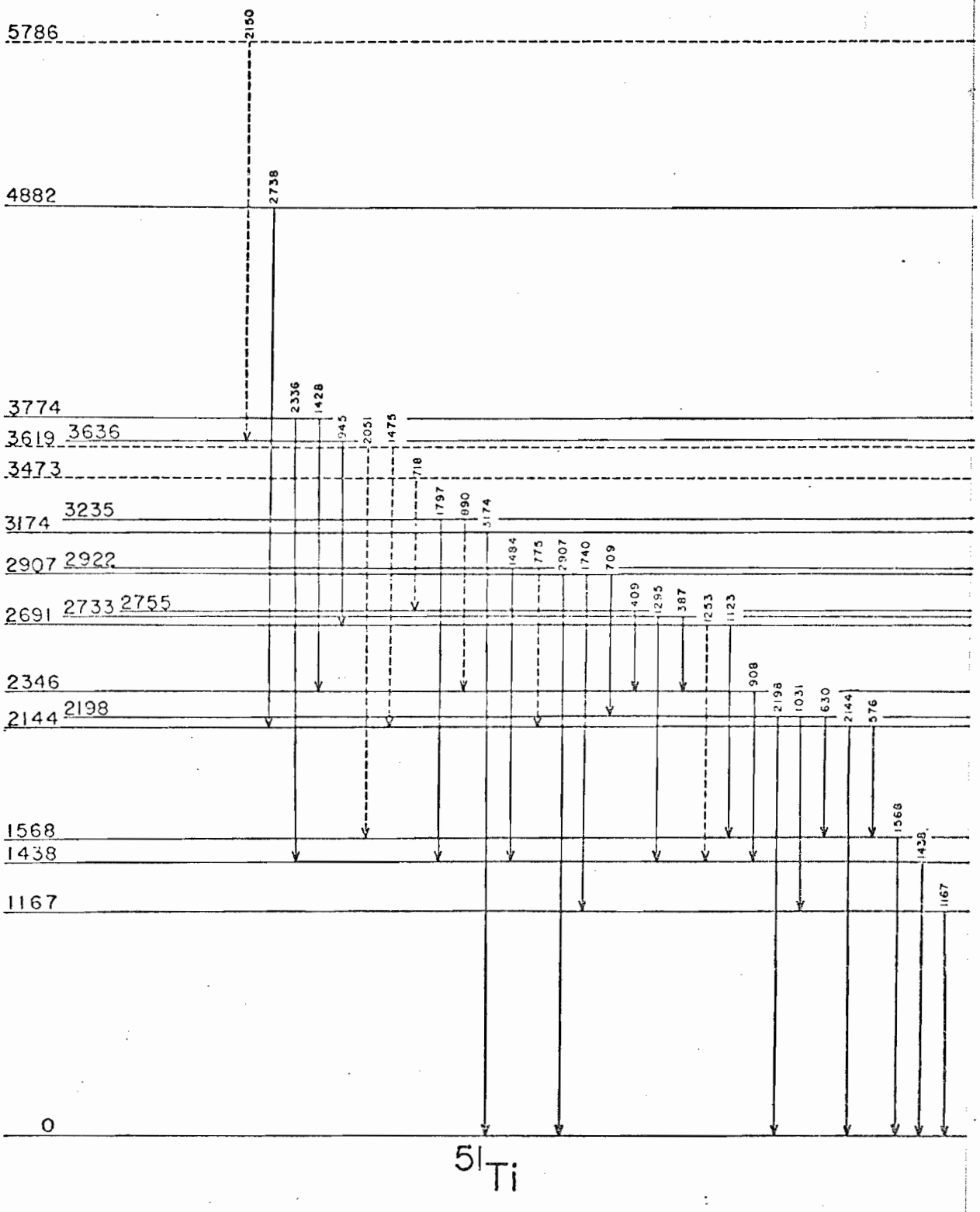
5786
4882
3774
3619
3636
3473
3235
3174
2922
2907
2755
2733
2691
2346
2198
2144
1568
1438
1167
0
2150
2738
2336
1428
945
2051
1475
718
1797
890
3174
1484
775
2907
1740
709
409
1295
387
1253
1123
908
2198
1031
630
2144
576
1568
1438
1167

^{51}Ti

Figure 28. The γ-ray Spectrum in Coincidence with Neutrons Detected at 0°. The neutron baseline was set at channel 8 (see Figure 31) for this spectrum. All energies are given in keV.

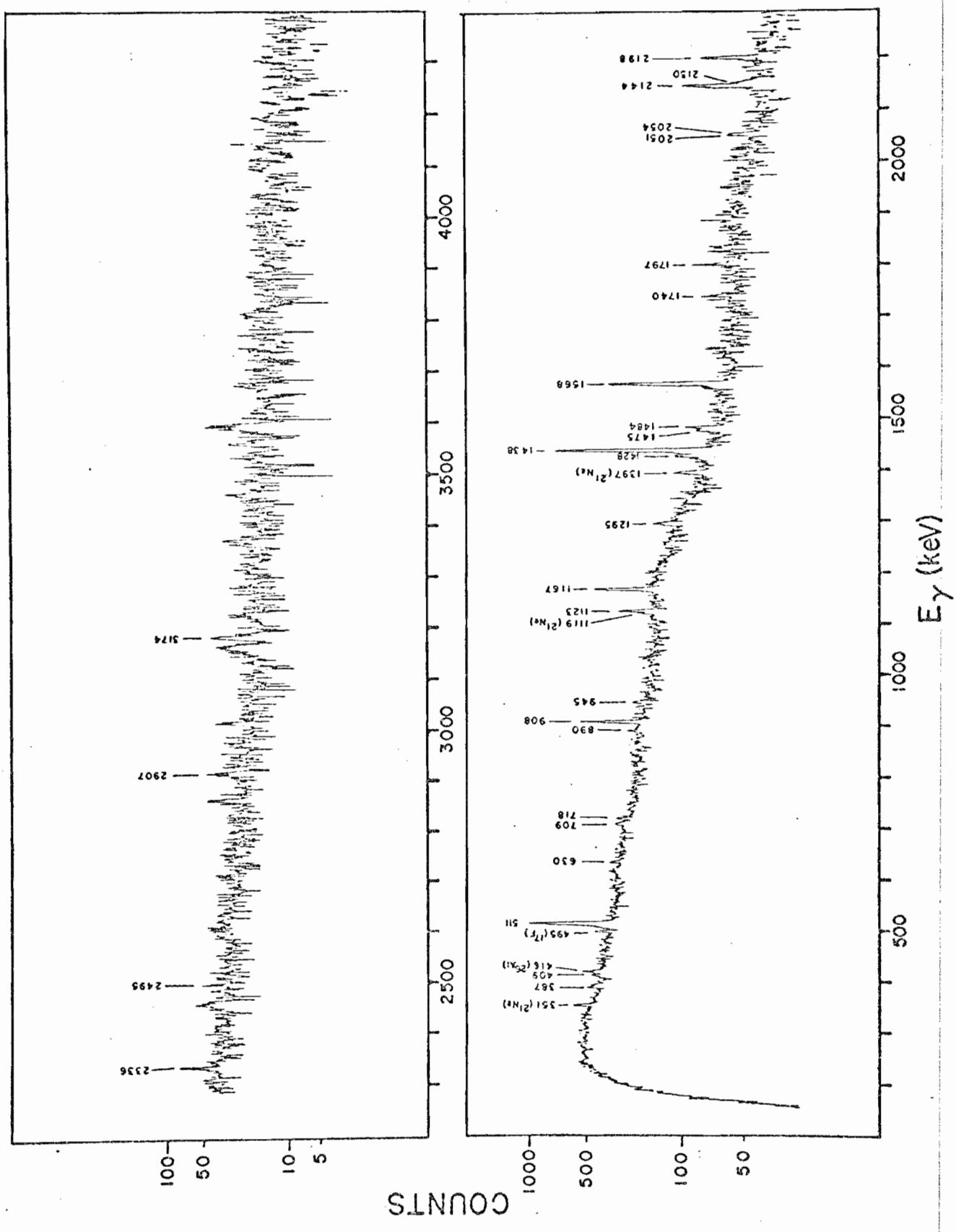
COUNTS
1000
500
100
50
100
50
10
5
2500
3000
3500
4000
500
1000
1500
2000
E_γ (keV)
2336
2493
2907
3174
351 (^{21}Ne)
387
405
416 (^{25}Al)
495 (^{17}F)
511
630
709
718
830
908
945
1119 (^{21}Ne)
1123
1167
1295
1397 (^{21}Ne)
1428
1438
1473
1484
1568
1740
1797
2051
2054
2144
2150
2198

Figure 29. a) The γ-ray Spectrum in Coincidence with Neutrons Detected at 0°. The neutron baseline was set at channel 34 (see Figure 31) for this spectrum. All energies are given in keV.

b) As above, except that the neutron baseline was set at channel 50 for this spectrum. Only five levels are seen, with the 2144-keV and 2198-keV γ-rays being very weak.

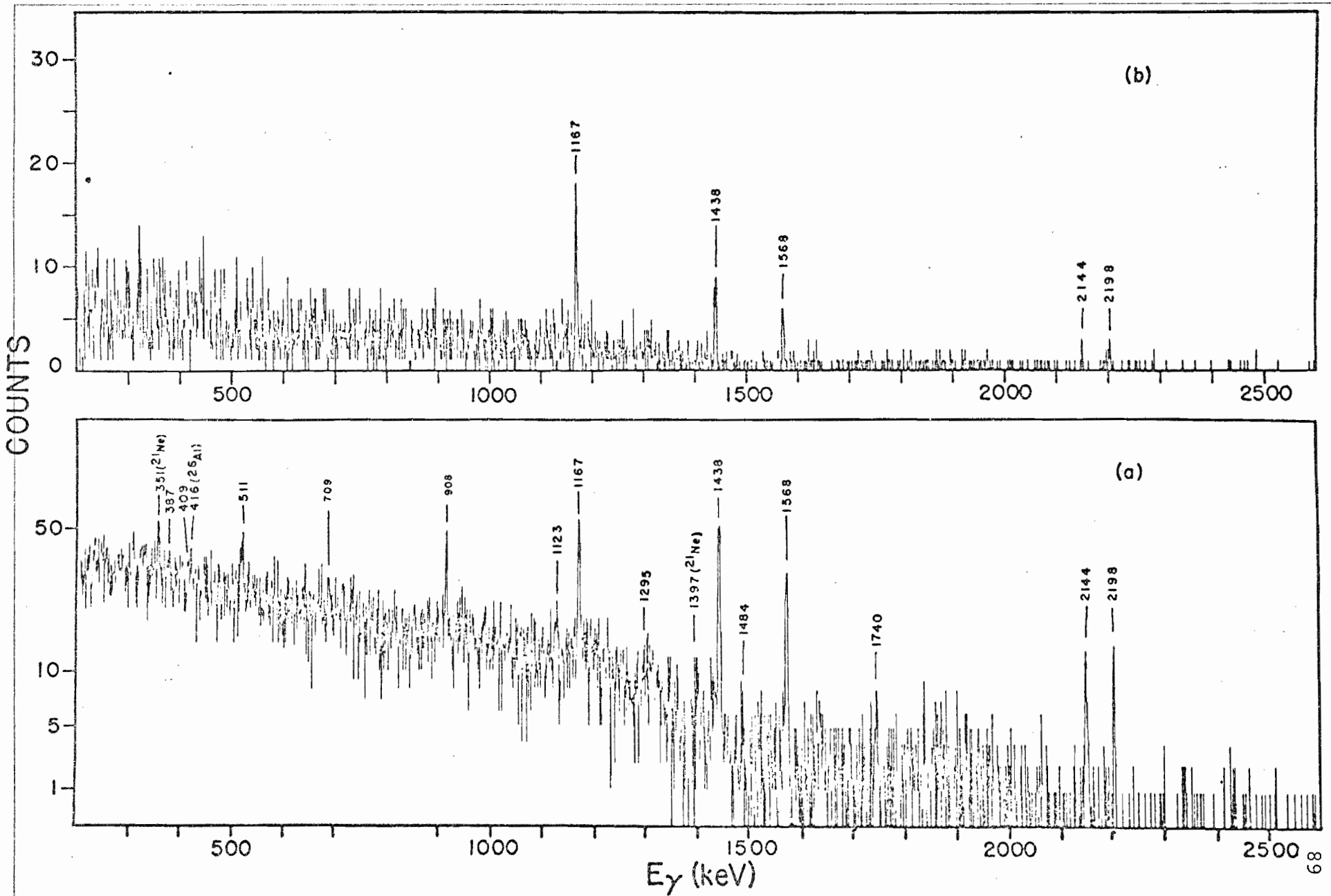
(b)
1167
1438
1568
2144
2198
(a)
351 (21Ne)
387
409
416 (26Al)
511
709
908
1123
1167
1295
1397 (21Ne)
1438
1484
1568
1740
2144
2198
COUNTS
Eγ (keV)

baseline set at channels 34 and 50, respectively. By plotting the yield of a γ-ray vs. the baseline, the approximate excitation energy could be obtained. Figure 30 shows such a plot for the 1167, 1438, and 908-keV γ-rays. When the yield of a γ-ray approached zero, this baseline was said to correspond with E_n^{max} and was called the neutron threshold for the γ-ray. The neutron threshold for each γ-ray was then plotted vs. the proposed energy level from which the γ-ray was thought to decay. This plot is shown in Figure 31. The solid line is the plot of E_n^{max} vs. the excitation energy where E_n^{max} has been calculated from the kinematics of the reaction. Most of the data points below 5000 keV excitation fall on or near this calibration line. Above 5000 keV, the detector response is non-linear and the straight line detector calibration is no longer valid. Since the point at which a γ-ray has no yield was not easily established, especially for the weaker γ-rays, accurate excitation energy determinations were not possible. However by placing the excitation energy to within ±300 keV as was done here and combining these results with the γ-γ data to be discussed below, the evidence for the new levels became fairly conclusive.

The investigation of the 351-keV (see Figure 28) γ-ray led to the discovery of a very interesting contaminant in the $^{48}Ca(NO_3)_2$ target. It was determined that this γ-ray was from the 351→0 transition in ^{21}Ne. This level was populated by the reaction $^{18}O(\alpha,n\gamma)^{21}Ne$. The natural abundance of ^{18}O is only 0.2%, but there are six Oxygen atoms in the target for every

Figure 30. Plots of γ-ray Yield Versus Neutron Baseline Channel Number for the 1167, 1438, and 908-keV γ-rays. For each data point, a spectrum of all γ-rays coincident with neutrons above the specified baseline was obtained. The photopeak of each γ-ray was then summed and plotted. The highest baseline at which a peak was discernible was called the threshold channel number for that γ-ray. In this figure, the 1438-keV γ-ray is seen to have the highest yield at low baselines. This is an indication of the number of higher levels that decay to the 1438-keV level. As the baseline was raised, the yield of the 1438-keV γ-ray decreased rapidly until the yield was less than that of the 1167-keV γ-ray. The thresholds of the 1167, 1438 and 908 keV γ-rays were determined to be channels 54 ± 2, 52 ± 2 and 44 ± 2 respectively.

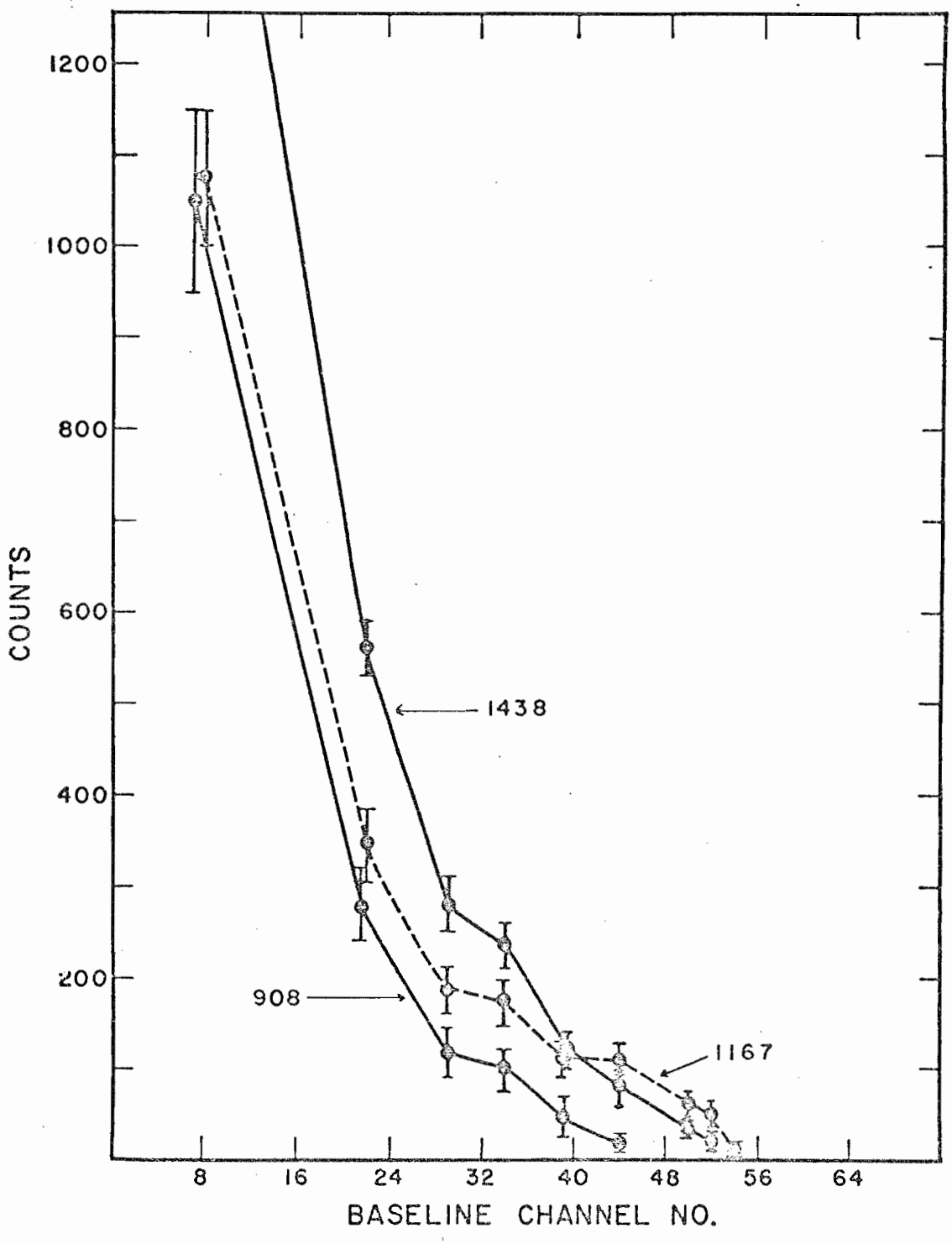
1200
1000
800
600
400
200
COUNTS
1438
908
1167
8
16
24
32
40
48
56
64
BASELINE CHANNEL NO.

Figure 31. Plots of Neutron Threshold Channel Number Versus Proposed Excitation Energy for the Level from which the Indicated γ-rays Decayed. The threshold for each γ-ray was obtained using the procedure discussed in the caption of Figure 30. The neutron energy (right vertical scale) corresponding to each threshold channel number was obtained using ^{60}Co and ^{137}Cs sources and assuming a linear calibration (see text). The straight line is a plot of neutron energy versus excitation energy and was obtained from the kinematics of the reaction. Above 5000 keV neutron energy, the assumption of a linear calibration of neutron energy versus threshold channel number is no longer valid. If a better calibration had been made, the line would curve upward and intersect more data points. With the exception of the 2150 γ-ray, all of the assignments of γ-rays to particular excitation energies are consistent with the neutron threshold data.

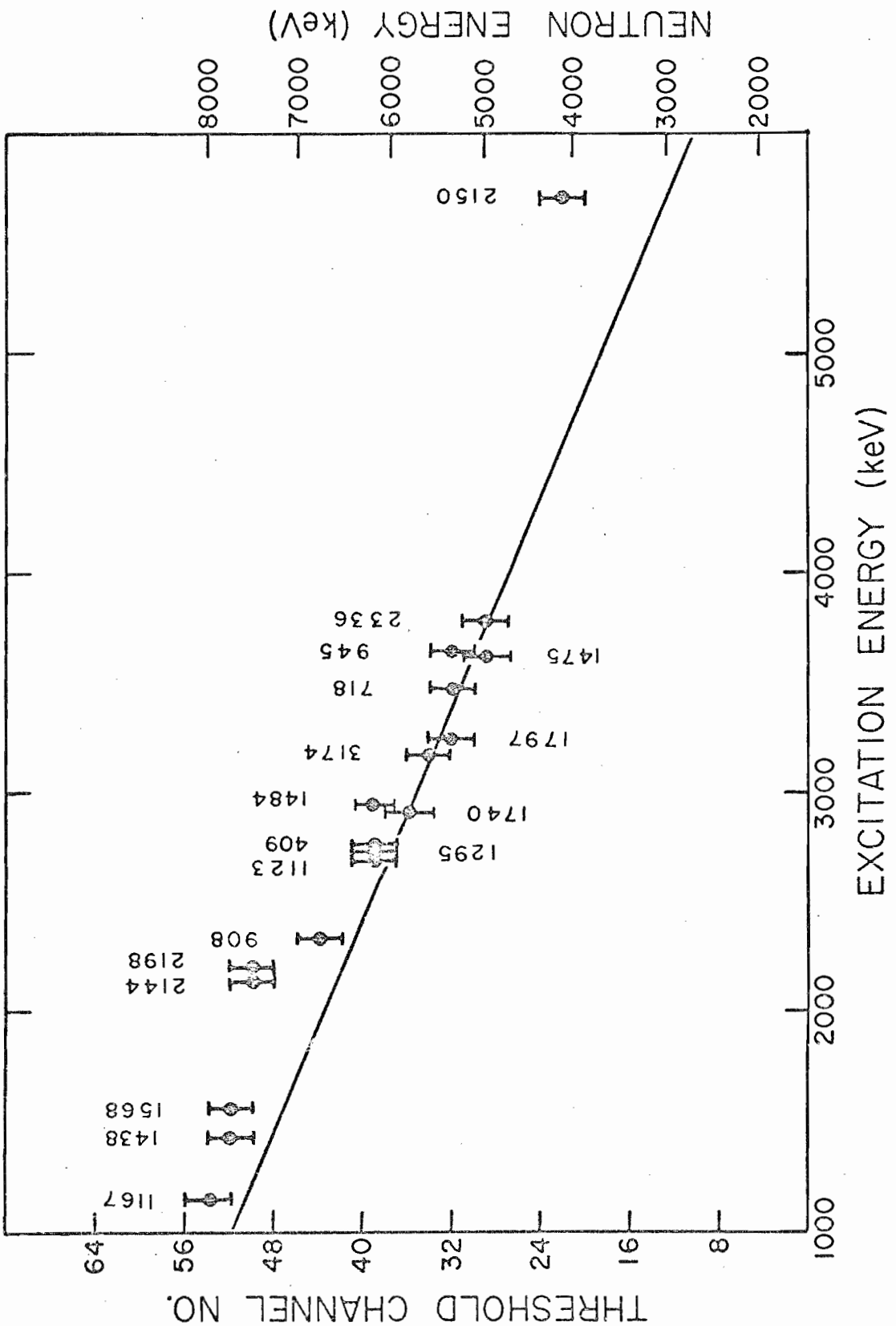
NEUTRON ENERGY (keV)
8000
7000
6000
5000
4000
3000
2000
2150
2336
945
1475
718
1797
3174
1484
1740
1295
409
1123
908
2198
2144
1568
1438
1167
THRESHOLD CHANNEL NO.
64
56
48
40
32
24
16
8
1000
2000
3000
4000
5000
EXCITATION ENERGY (keV)

^{48}Ca atom and the Coulomb barrier for an alpha particle incident on ^{18}O is much lower than for an alpha particle incident on ^{48}Ca. Three other γ-rays from ^{21}Ne were also seen: a 1119-keV γ-ray, a 1397-keV γ-ray, and a 1564-keV γ-ray. All of these are seen in coincidence with the 351-keV γ-ray. Since the 1119-keV and 1564-keV γ-rays were very near in energy to the 1123-keV and 1658-keV γ-rays respectively, the 351-keV γ-ray appeared in coincidence with both of the latter γ-rays leading to speculation that the 351-keV γ-ray was due to a new level in ^{51}Ti. However, by selecting smaller windows for these γ-rays, the 351-keV γ-ray was eliminated from the coincidence spectra.

Three γ-rays from the reaction ^{23}Na$(\alpha,n\gamma)^{26}$Al were also seen. These were the 416-keV, 1341-keV, and 1653-keV γ-rays. No reasonable explanation can be offered for the presence of ^{23}Na in the target.

2) The γ-γ Coincidence Results

Most of the γ-rays from levels below 4000 keV that were seen in the (d,p) experiment were also seen in the ^{48}Ca$(\alpha,n\gamma)^{51}$Ti experiment. Table 1 lists the transitions observed in the $(\alpha,n\gamma)$ experiment, and indicates the γ-rays that were observed in coincidence with some of the stronger transitions in the γ-γ measurements. Several of the ground state transitions, for example the 2907→0 and 3174→0, were not observed in the γ-γ coincidence experiment implying that these levels are not fed strongly from higher levels. The γ-rays from previously unreported levels are

Table 1. Summary of $^{48}Ca(\alpha,n\gamma)^{51}Ti$ Results

Level(keV)[a]	Transition[b]	Eγ(keV)	Coincident γ-rays from γ-γ measurements (keV)[c]
1167 ± 1	1167→0	1167	1031, 1740
1438 ± 1	1438→0	1438	(331), 387, 409, (575)^{VW}, 718, (890), 908^{S}, (1253), 1295, 1484, 1797, (1802), 2336^{VW}
1568 ± 1	1568→0	1568	576^{S}, 630^{S}, (900), 945, (1027), 1123^{S}, (1350)^{VW}, (1432)^{VW}, (2051)^{VW}
2144 ± 1	2144→0	2144	(775), (1475)^{VW}, 2738^{VW}
	2144→1568	576	
2198 ± 1	2198→0	2198	
	2198→1167	1031	
	2198→1568	630	
2346 ± 1	2346→1438	908	(331), 387^{S}, 409^{S}, (718), (890)^{VW}, (1280)^{VW}, 1428^{VW}, 1438^{S}
2691 ± 1	2691→1568	1123	945^{S}, (1298), 1568^{S},
	2691→1438	1253	(1637)^{VW}, (1790)^{VW}, (1809) (2054)^{VW}
2733 ± 2	2733→1438	1295	(331), 1438^{S}, (2308)^{VW}
	2733→2346	387	
2755 ± 2	2755→2346	409	(890)^{VW}, 908^{S}, 1438^{S}

a) Tentative level assignments in parentheses

b) Tentative transitions in parentheses

c) Gamma-rays in the 30 cm^3 detector in coincidence with gamma-ray window set on 80 cm^3 detector. Uncertain and unidentified γ-rays are in parentheses. ^{S} signifies a relatively strong peak and ^{VW} a relatively weak peak.

Table 1. (Continued)

Level(keV)[a]	Transition[b]	Eγ(keV)	Coincident γ-rays from γ-γ measurements (keV)[c]
2907 ± 1	2907→0	2907	
	2907→1167	1740	
	2907→2198	709	
2922 ± 2	2922→1438	1484	(770)^{vw}, (908)^{vw}, (1260)^{vw},
	(2922→2144)	775	1438^{s}
3174 ± 2	3174→0	3174	
3235 ± 2	3235→1438	1797	1438^{s}
	(3235→2346)	890	409^{s}, 908^{s}, 1438^{s}
(3473 ± 2)	(3473→2755)	718	(350), 409^{s}, 908^{s}, 1438^{s}, (1815)^{vw}
(3619 ± 2)	(3619→1568)	2015	
	(3619→2144)	1475	
3636 ± 2	3636→2691	945	1123^{s}, 1568^{s}, (2150)^{vw}
4882 ± 2	4882→2144	2738	
(5786 ± 3)	(5786→3636)	2150	

a) Tentative level assignmants in parentheses

b) Tentative transitions in parentheses

c) Gamma-rays in the 30 cm. detector in coincidence with gamma-ray window set on 80 cm. detector. Uncertain and unidentified -rays are in parentheses. ^{s} signifies a relatively strong peak and ^{vw} a relatively weak peak.

seen principally in coincidence with the 1438→0 transition or the 1568→0 transition. Figure 32 shows the γ-rays in coincidence with the 1167→0 transition. The two γ-rays at 1031 and 1740 keV have been previously observed with the (d,pγ) reaction and are transitions from the 2198- and 2907-keV levels, respectively.

a) The 2346-keV Level

Figures 33a and 33b show the γ-rays in coincidence with the 1438-keV and the 908-keV γ-rays respectively. Each of these is seen to be the strongest γ-ray in coincidence with the other. If there were an intermediate transition, it would be expected to be of comparable intensity. This, together with the neutron threshold data, is confirmation of the level at 2346-keV that was postulated in the ^{50}Ti(d,pγ)^{51}Ti experiment. Several other γ-rays are seen in coincidence with the 908-keV γ-ray indicating that the 2346-keV level is being fed by decays from higher states.

b) The 2691-keV Level

Figures 34a and 34b show the γ-rays in coincidence with the 1568-keV and 1123-keV γ-rays. Each of these γ-rays is seen to be very strong in the coincidence spectrum of the other. The 1123-keV γ-ray is assigned as the decay from the 2691-keV level to the 1568-keV level. This is consistent with the neutron threshold data for this level. Glover et al. (1968) using the reaction ^{49}Ti(t,p)^{51}Ti report a strongly populated $7/2^-$ level

Figure 32. The Spectrum of γ-rays in the 30 cm^3 Ge(Li) detector in Coincidence with the Photopeak of the 1167-keV γ-ray in the 80 cm^3 detector. Coincidences with events in the Compton distribution have been subtracted. All energies are given in keV. Only γ-rays corresponding to the 2198→1167 and 2907→1167 transitions are seen.

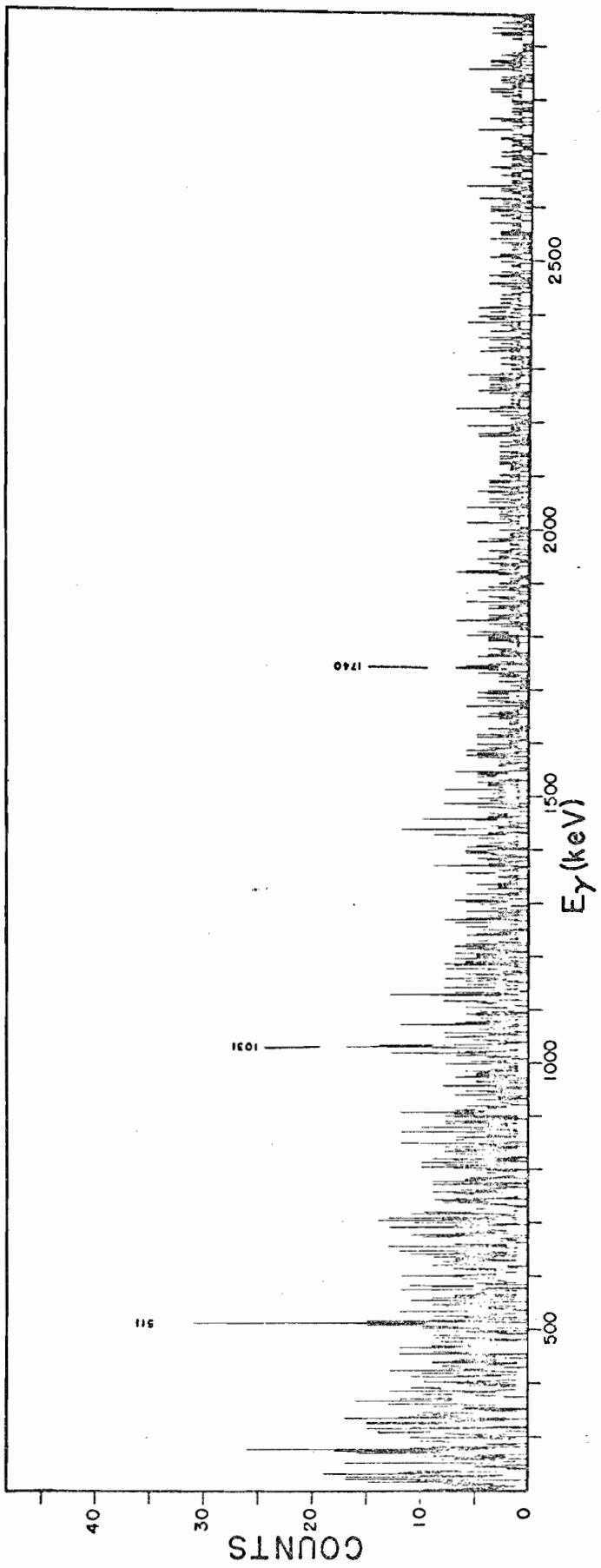
COUNTS
0
10
20
30
40
500
1000
1500
2000
2500
Eγ (keV)
511
1031
1740

Figure 33. a) The Spectrum of γ-rays in the 30 cm. Ge(Li) Detector in Coincidence with the Photopeak of the 1438-keV γ-ray in the 80 cm. Detector. Coincidences with events in the Compton distribution have been subtracted. All energies are given in keV. Many γ-rays are seen with the strongest being the 2346→1438 transition. The γ-rays of 331-keV and 1802-keV energy have not been identified.

b) The Spectrum of γ-rays in the 30 cm^3 Ge(Li) Detector in Coincidence with the Photopeak of the 908-keV γ-ray in the 80 cm^3 detector. Coincidences with events in the Compton distribution have been subtracted. All energies are given in keV. The strongest γ-ray is the 1438→0 transition. Several γ-rays are seen in this spectrum that are also in coincidence with the 1438-keV γ-rays. This implies that these γ-rays decay from levels above the 2346-keV level.

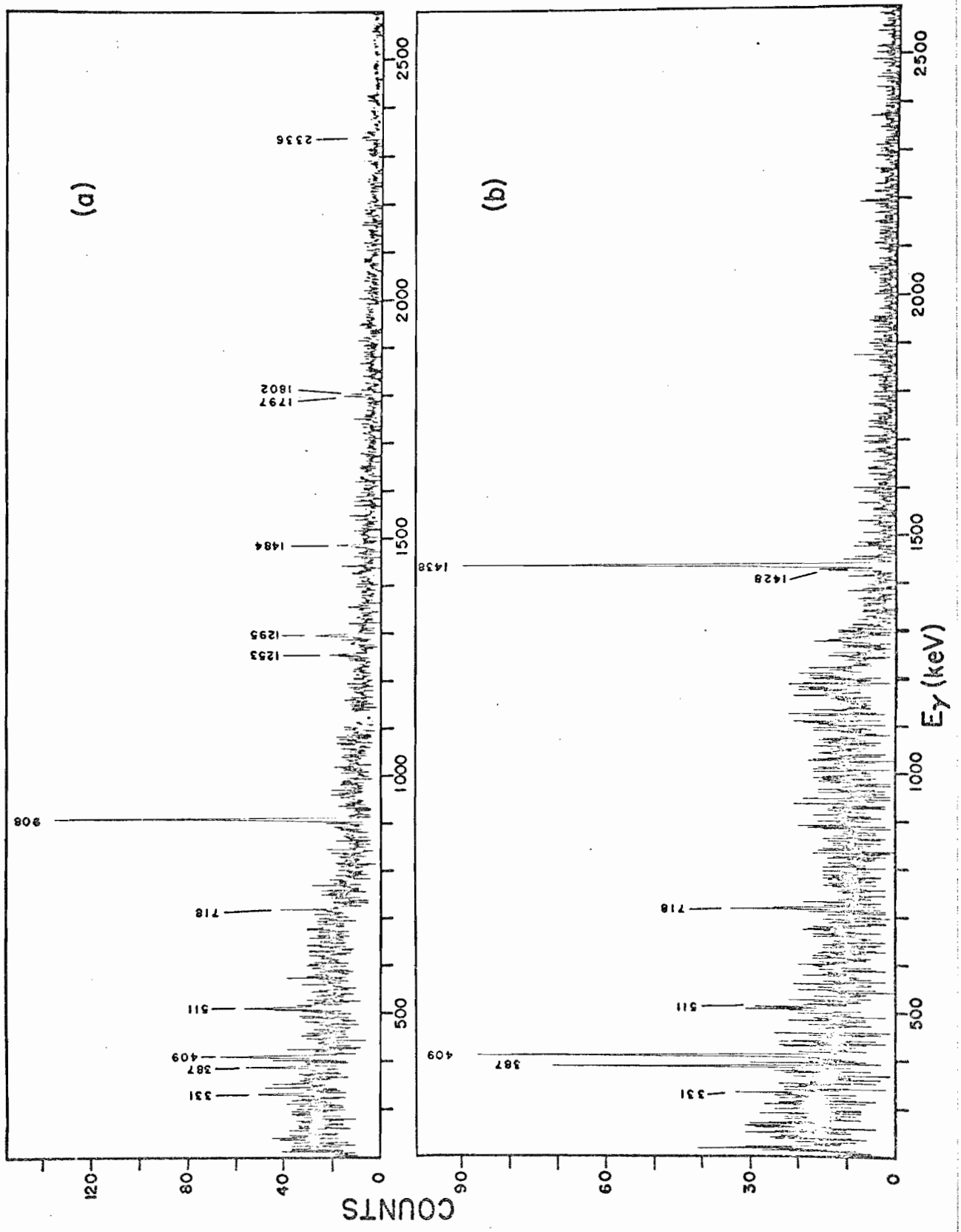
(a)
(b)
COUNTS
E_γ (keV)
331
387
409
511
718
908
1253
1295
1484
1797
1802
2336
1428
1438
0
500
1000
1500
2000
2500
30
60
90
40
80
120

Figure 34. a) The Spectrum of γ-rays in the 30 cm^3 Ge(Li) Detector in Coincidence with the Photopeak of the 1568-keV γ-ray in the 80 cm^3 detector. Coincidences with events in the Compton distribution have been subtracted. All energies are given in keV. Several γ-rays are seen with the strongest being the 2691→1568 transition. The γ-rays of 900 keV, and 1027 keV, have not been identified.

b) The Spectrum of γ-rays in the 30 cm^3 Ge(Li) Detector in Coincidence with the Photopeak of the 1123-keV γ-ray in the 80 cm^3 detector. Coincidences with events in the Compton distribution have been subtracted. All energies are given in keV. Several γ-rays are seen with the strongest being the 1568→0 transition. The 945-keV γ-ray has been identified as a transition from a level at 3636-keV to the 2691-keV level. The other peaks in this spectrum have not been identified.

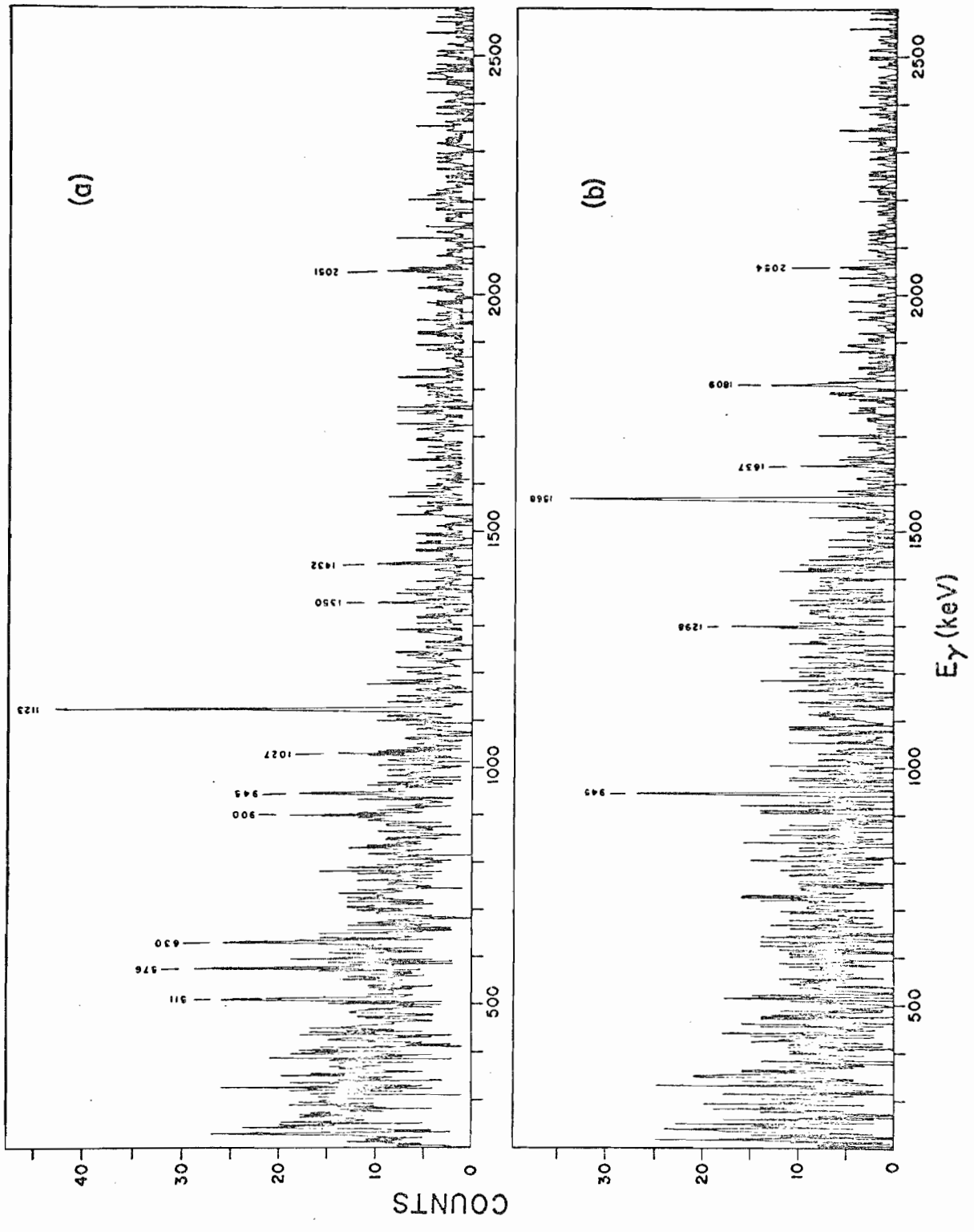
(a)
(b)
COUNTS
Eγ (keV)
511
576
630
900
945
1027
1123
1432
1550
2051
945
1298
1568
1637
1809
2054
0
10
20
30
40
500
1000
1500
2000
2500

at 2690 excitation and concluded that this state is primarily of 2p-1h nature. This level was not seen in the $^{50}Ti(d,p\gamma)^{51}Ti$ experiment. Another possible decay from this level is a 1253-keV γ-ray that is seen in coincidence with the 1438-keV γ-ray. The yield for this γ-ray is too weak to determine the excitation energy of the level from which it originates, and is shown as an uncertain transition in Figure 27.

c) The 2733-keV Level

A new level at 2733-keV is deduced from the existence of a 1295-keV γ-ray in coincidence with the 1438$\rightarrow$0 transition and a 387-keV γ-ray which is in coincidence with the 1438-keV and 908-keV γ-rays (see Figure 33). The neutron threshold data for the 1295-keV γ-ray is consistent with its assignment as a decay from a level at 2733-keV. The yield of the 387-keV γ-ray was so weak that the neutron threshold data is inconclusive for that γ-ray.

d) The 2755-keV Level

The 409-keV γ-ray is another strong γ-ray that is seen in coincidence with the 1438-keV and 908-keV γ-rays (see Figure 33). This coincidence data, together with the neutron threshold data makes possible the assignment of this γ-ray as a transition from a new level at 2755-keV to the 2346-keV level. No other decay from this level was seen.

e) The 2922-keV Level

The existence of a 1484-keV γ-ray in coincidence with the 1438-keV γ-ray leads to the assignment of a new level at 2922-keV. The neutron threshold data for this γ-ray indicates that the γ-ray decays from a level below 3000 keV excitation energy. A level at 2922 is the only candidate. A weak 775-keV γ-ray is seen in coincidence with the 2144→0 transition, but the 3 keV energy discrepancy makes this assignment suspect.

f) The 3174-keV Level

A 3174-keV γ-ray is observed in the $^{48}Ca(\alpha,n\gamma)^{51}Ti$ reaction. The neutron threshold data is consistent with its assignment as a decay from a level at 3174-keV. This γ-ray is not seen in any of the γ-γ coincidence spectra. This implies that it is not a decay to any of the low-lying levels of ^{51}Ti. This level is believed to correspond to the 3164-keV level reported by Barnes et al. (1964).

g) The 3235-keV Level

Principal evidence for this previously unreported level is a 1797-keV γ-ray in coincidence with the 1438-keV γ-ray, but which is not seen in coincidence with the 908-keV γ-ray. The neutron threshold data indicates that the 1797-keV γ-ray decays from a level of less than 4000-keV excitation. Therefore a 3235-keV to 1438-keV transition is the only candidate. An 890-keV γ-ray is seen in coincidence with the 2346→1438 transition. The neutron threshold data for this γ-ray is too weak to confirm

a 3235-keV to 2346-keV transition. Additionally, the 2755→2346 transition has an 890-keV γ-ray in coincidence with it. The possibility then exists that there are two 890-keV γ-rays or that there is no 3235→2346 transition.

h) The 3473-keV Level

A 718-keV γ-ray is being tentatively assigned as a transition from a new level at 3473-keV to the level at 2755-keV. In coincidence with the 718-keV γ-ray are seen the 1438-keV, 908-keV, and 409-keV γ-rays. The neutron threshold data shows the 718-keV γ-ray must decay from a level of less than 4000-keV excitation energy.

i) The 3619-keV Level

A tentative assignment is made of a new level at 3619-keV. A 2051-keV γ-ray is seen in coincidence with the 1568-keV γ-ray and a 1475-keV γ-ray is seen in coincidence with the 2144-keV γ-ray. The neutron threshold data for the 1475-keV γ-ray is consistent with its assignment as a decay from a level at 3619-keV excitation. The yield of the 2051-keV γ-ray is too weak to obtain an accurate threshold energy.

j) The 3636-keV Level

A 945-keV γ-ray is seen in coincidence with both the 1568-keV and 1123-keV γ-rays. This implies the existence of a level at 3636 keV. The neutron threshold data is consistent with this assignment. No other decays from this level were observed. This level may correspond with a level at 3640 keV reported by Glover

et al. (1968). They report this level to have 2p-1h characteristics. The decay of this level to the 2691-keV level is consistent with both states being of 2p-1h nature.

k) The 5786-keV Level

A tentative assignment of a new level at 5786-keV is made. Principal evidence for this level is a 2150-keV γ-ray in coincidence with the 3636→2691 transition. The neutron threshold data indicates that this γ-ray comes from a lower excitation energy. This suggests that this γ-ray could come from an unknown contaminant.

Chapter V

DISCUSSION

The decay scheme deduced in this work is shown in Figure 35. Because of the unknown population parameter in the $^{50}Ti(d,p\gamma)^{51}Ti$ reaction, the amount of information that could be extracted was limited. A summary of the results is given in Table 2. An isotropic distribution was obtained for the 1167-keV level. This is consistent with the shell model prediction of $1/2^-$ for this level. The 1438-keV and 1568-keV levels were weakly populated and no correlations could be obtained. Glover et al. (1968) report a $7/2^-$ assignment for the 1438-keV level and a probable $5/2^-$ assignment for the 1568-keV level. Correlation results for the 2144-keV level indicated that both $5/2^-$ or $7/2^-$ assignments were possible. The correlation result for the 2198-keV level was consistent with a spin assignment of $3/2^-$. No mixing ratio could be determined. A unique assignment of $9/2^+$ was made to the level at 3774-keV excitation. This level decays by a pure E1 transition to the 1438-keV level and also decays to a new level at 2346-keV. The 3774-keV level is thought to be the $1g_{9/2}$ single particle level which would explain why it is strongly excited in the (d,p) reaction. The results of 3/2 or 5/2 for the 4592-keV level and

Figure 35. The Level Scheme of ^{51}Ti Deduced in this Work. Tentative level assignments and uncertain transitions are shown as dashed lines. All energies are given in keV.

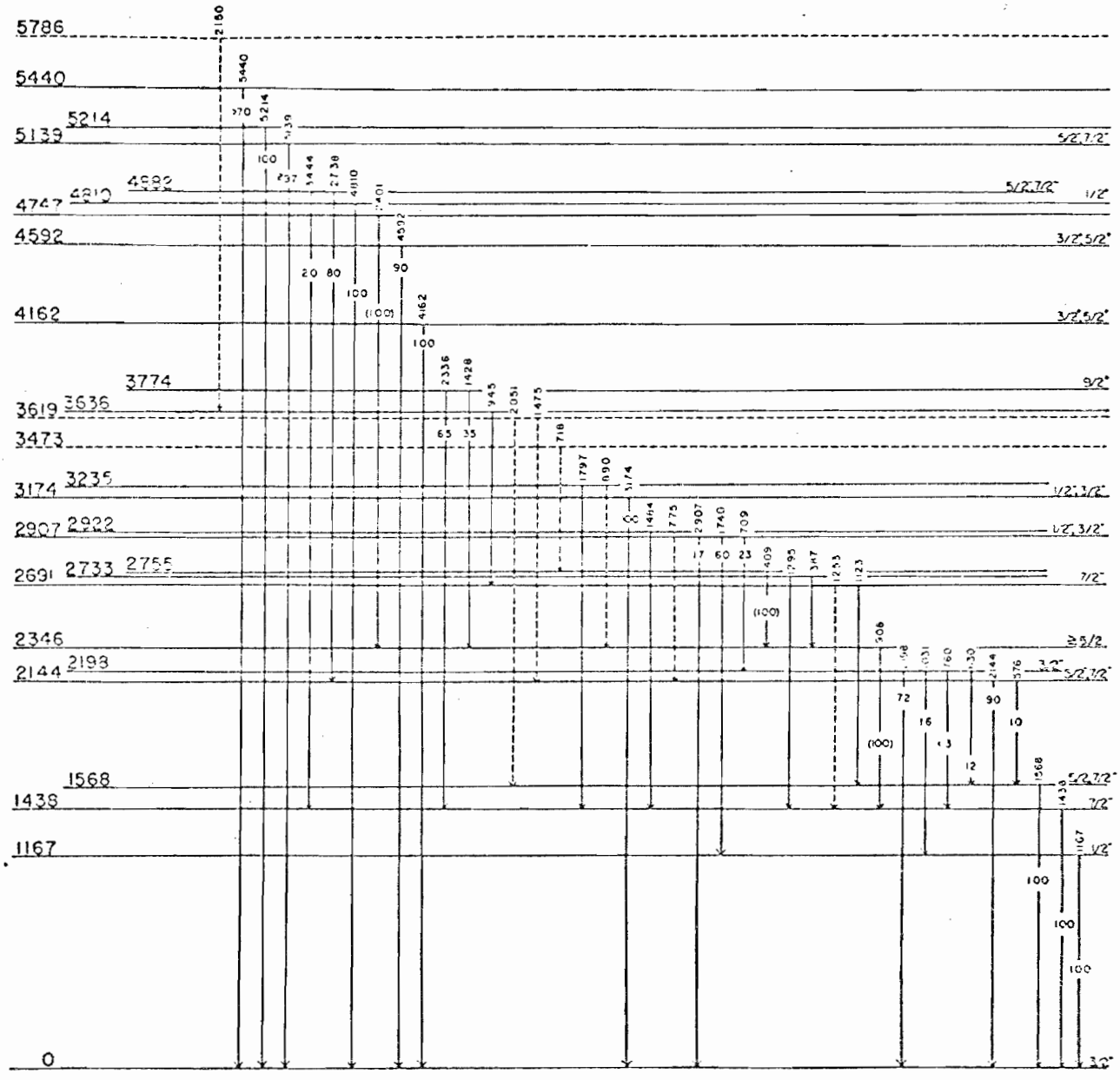
5786
5440
5214
5139
4992
4810
4747
4592
4162
3774
3636
3619
3473
3235
3174
2922
2907
2755
2733
2691
2346
2198
2144
1568
1438
1167
0
5/2,7/2
1/2
3/2,5/2
9/2
7/2
3/2

^{51}Ti

Table 2. Results of ^{50}Ti(d,pγ) Correlation Measurements

Transition (keV)	Branching Ratio (%)	Spin J_i^π	Combination J_f^π	Mixing Ratio[a]
1167→ 0	100	$1/2^-$	$3/2^-$	
		$3/2^-$	$3/2^-$	
2144→ 0	90± 5	$5/2^-$	$3/2^-$	± ∞
				or -0.21±0.07
		$7/2^-$	$3/2^-$	$0.3^{+0.5}_{-0.4}$
2144→1568	10± 5			
2198→ 0	72± 5	$3/2^-$	$3/2^-$	
2198→1167	16± 5			
2198→1568	12± 5			
2907→ 0	17± 5			
2907→1167	60± 5			
2907→2198	23± 5			
3174→ 0	100			
3774→1438	65±10	$9/2^+$	$7/2^-$	± ∞
				or -0.02±0.31
3774→2346	35±10			
4162→ 0	100			

a) The phase convention is that of Rose and Brink (1967)

Table 2. (Continued)

Transition (keV)	Branching Ratio (%)	Spin Combination J_i^π	J_f^π	Mixing Ratio[a]
4592→ 0	90± 5	$3/2^+$	$3/2^-$	
		$5/2^+$	$3/2^-$	$0.38^{+0.29}_{-0.24}$
				or $2.5^{+1.1}_{-0.6}$
4592→1438 or 4592→3174	10± 5			
4747→2346	(100)			
4810→ 0	100			
4810→1167	< 8			
4882→1438	20±10			
4882→2144	80±10	$5/2^-$	$(5/2)^-$	0.32±0.13
				or $-5.8^{+2.9}_{-92.3}$
		$7/2^-$	$(5/2)^-$	-0.26±0.11
				or ± ∞
5139→ 0	≥ 97	$5/2^-$	$3/2^-$	$-8.1^{+3.9}_{-63.0}$
				or -0.30±0.15
		$7/2^-$	$3/2^-$	$0.26^{+0.34}_{-0.29}$
				or $1.5^{+19.4}_{-1.1}$

a) The phase convention is that of Rose and Brink (1967)

Table 2. (Continued)

Transition (keV)	Branching Ratio (%)	Spin Combination J_i^π	J_f^π	Mixing Ratio[a]
5139→1167	≤ 3			
5214→ 0	100			
5440→ 0	> 70			

a) The phase convention is that of Rose and Brink (1967)

5/2 or 7/2 for the 5139-keV level were consistent with ℓ-value assignments made by Barnes et al. (1964). No unique spin determinations could be made. The decay scheme for the 4882-keV level is not consistent with a spin of $1/2^-$ for this level. This made the $\ell = 0$ assignment by Barnes et al. (1964) suspect and was more in agreement with an $\ell = 3$ assignment by Cosman et al. (1968). Branching ratios for many of the levels of ^{51}Ti were also determined by the ^{50}Ti(d,pγ)^{51}Ti experiment.

In order to confirm some of the decays observed in the ^{50}Ti(d,pγ)^{51}Ti experiment and also to confirm the new level at 2346-keV, the reaction ^{48}Ca(α,nγ)^{51}Ti was studied. Using the techniques of n-γ and γ-γ coincidence measurements the new level at 2346-keV was confirmed and more accurate values were established for the excitation energies of many of the previously known levels of ^{51}Ti. Additionally, several previously unreported levels were deduced. These are the levels at 2733 keV, 2755 keV, 2922 keV, 3236 keV, and 3636 keV. Three other levels were also suggested by the data of this experiment but the evidence for these is less firm. In each of these latter cases the evidence for the level came from the γ-γ experiment, but could not be confirmed by the n-γ results. The γ-γ results were thought to be more reliable and hence tentative assignments were made.

Although spin assignments for these new levels could not be made, the results do allow some discussion about the spins of these levels. In general, states of high spin are not seen

in the (d,p) reaction on even-even targets. It should be noted that the 1438-keV ($7/2^-$) and 1568-keV ($5/2^-$) levels were only weakly populated at 6.0 MeV deuteron energy and the $7/2^-$ level at 2691-keV was not seen at all in the $^{50}Ti(d,p)^{51}Ti$ reaction. (The $9/2^+$ level at 3774-keV was an exception to this rule, its strength most probably due to its single particle nature.) Hence the fact that the new levels are seen in the $^{48}Ca(\alpha,n\gamma)^{51}Ti$ reaction implies that these levels may have spins of 5/2 or greater. Also, the new levels decay principally to the 1438-keV ($7/2^-$) and 1568-keV ($5/2^-$) levels or to other new states. These new levels were not seen to decay to the $3/2^-$ ground state or to the $1/2^-$ first excited state. States of low spin would be expected to decay to these levels.

Several states of high spin have been seen in the other N = 29 nuclei, ^{53}Cr and ^{55}Fe, Figure 36 compares the energy spectra of the N = 29 nuclei, ^{49}Ca, ^{51}Ti, ^{53}Cr, ^{55}Fe, and ^{57}Ni. In ^{53}Cr, there is a possible $11/2^-$ level at 2172-keV, a possible $9/2^-$ level at 2227-keV, and a possible $15/2^-$ level at 3083-keV. In ^{55}Fe there are two $9/2^-$ levels at 2211-keV and 2301-keV and a probable $11/2^-$ level at 2542-keV excitation energy. Sawa (1970) reported a possible $13/2^-$ level at 2814-keV and a $15/2^-$ level at 3420-keV excitation energy. Since these nuclei are very similar, high spin states should also be observed in ^{51}Ti.

It is interesting to compare the energy spectra of the five N = 29 odd nuclei. The nuclei ^{49}Ca and ^{57}Ni are seen to differ appreciably from the other three. This indicates the

Figure 36. Level Diagrams for States of Less than 4000 keV Excitation Energy of Five N = 29 Nuclei are Compared. The ^{49}Ca results are from Kashy et al. (1964) and Arnell et al. (1969). The ^{51}Ti results are from this work. The ^{53}Cr results are taken from Carola et al. (1970) and Carola (1971). The ^{55}Fe results are from Robertson et al. (1970) and Sawa (1970). The ^{57}Ni results are from Gould (1969), Gould et al. (1970), and Bertin and Hirko (1971). The dashed lines indicate levels that should have similar structures.

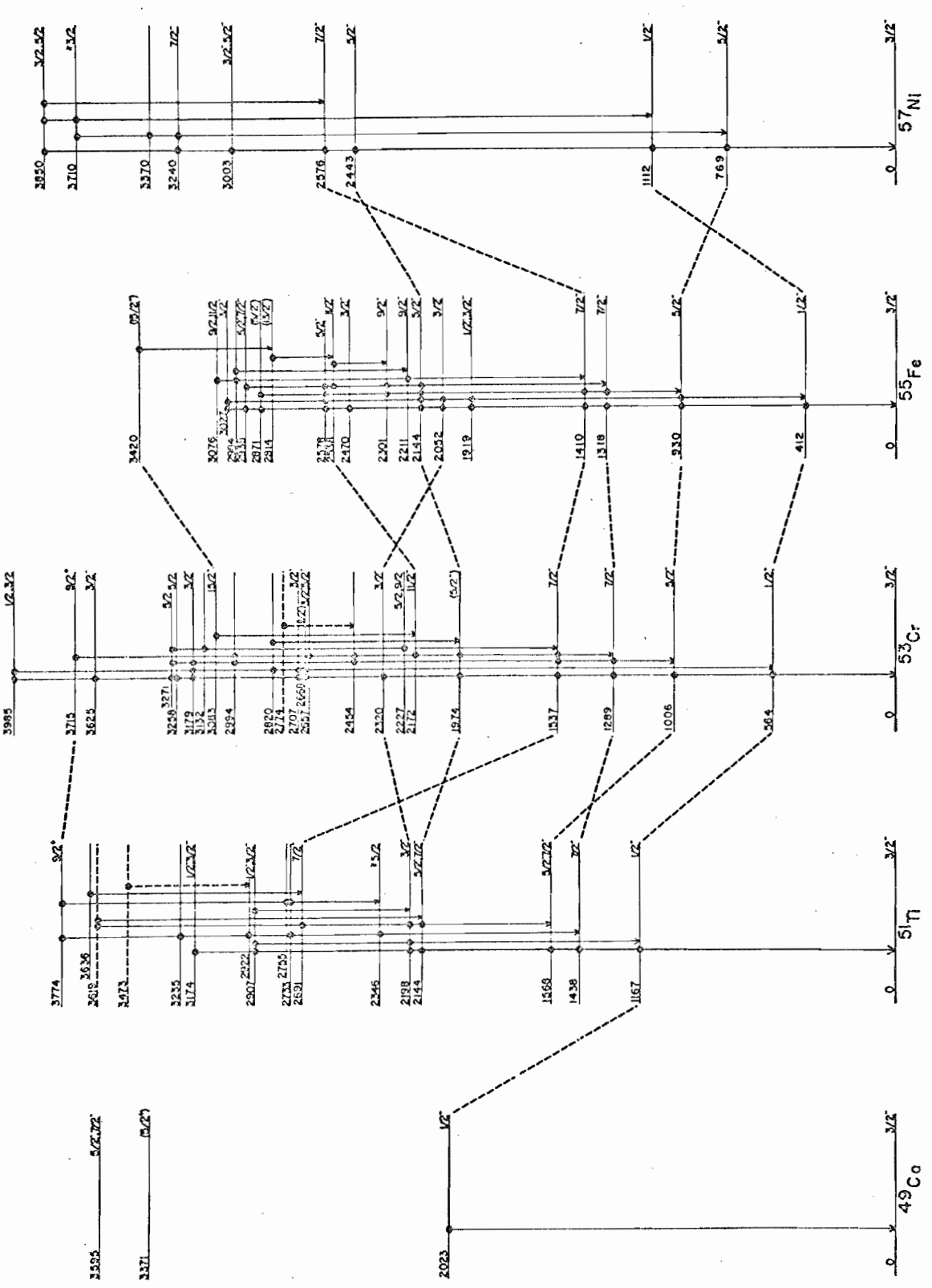
57Ni
55Fe
53Cr
51Ti
49Ca

remarkably strong effect of the shell closures at Z = 20 and Z = 28. The spectra of ^{51}Ti, ^{53}Cr, and ^{55}Fe are very similar but there are some differences. The first $5/2^-$ and $7/2^-$ levels of ^{51}Ti are in opposite order than are those of ^{53}Cr and ^{55}Fe. Also the second $7/2^-$ level which is usually interpreted as a 2p-1h state is at 2691-keV in ^{51}Ti while it is at 1536-keV and 1410-keV in ^{53}Cr and ^{55}Fe respectively. Caution must therefore be exercised when making comparisons between these nuclei.

The 2346-keV level of ^{51}Ti decays by a 100% branch to the lowest $7/2^-$ level. The $11/2^-$ level at 2172-keV excitation in ^{53}Cr decays by a 100% branch to the lowest $7/2^-$ level while the possible 9/2 level at 2227-keV decays by a 100% branch to the second $7/2^-$ level. In ^{55}Fe, the $9/2^-$ level at 2211-keV decays by a 100% branch to the second $7/2^-$ level, and the $9/2^-$ level at 2301-keV decays to the lowest $5/2^-$ and $7/2^-$ levels. The $11/2^-$ level at 2538 keV decays to the lowest $7/2^-$ level and also to the $9/2^-$ level at 2301 keV. The decay of the ^{51}Ti 2346-keV level is then more similar to the decays of the $11/2^-$ levels of ^{53}Cr and ^{55}Fe than to the decays of the $9/2^-$ levels of those nuclei. However, since the suggested 2p-1h $7/2^-$ state occurs at such a high excitation energy (2691 keV) in ^{51}Ti, it is difficult to compare the decays of these three nuclei.

Since there has been no evidence to date on the location of states of ^{51}Ti with spins of 9/2 or greater, most theoretical papers have not attempted to predict the energy levels or properties of these states. Ohnuma (1966) predicted $9/2^-$ levels

at 2698 keV and 3219 keV excitation energies, an $11/2^-$ level at 2778 keV and a $15/2^-$ level at 3271 keV.

Recent calculations by Divadeenam (1971) suggest that there should be several low-lying states with spins of 9/2 or greater. These calculations were made using the same model as Divadeenam and Beres (1969) except that core states of 0^+, 2^+, 4^+, and 6^+ were now considered. Figure 37 compares the calculations of Ohnuma (1966) and Divadeenam (1971) with the experimental energy spectra. Both models predict low-lying $9/2^-$ and $11/2^-$ levels as well as states of higher spin.

Ohnuma's calculations predict the energy of the $1/2^-$ first excited state very well. The order of the $5/2^-$ and $7/2^-$ levels are reversed as are the order of the $3/2^-$ and second $5/2^-$ levels. Divadeenam closely predicts the energies of the first $1/2^-$ and $7/2^-$ levels as well as the 2p-1h $7/2^-$ level at 2691 keV. However, the $5/2^-$ energy levels are not well reproduced. Ohnuma's calculations suggest the spin of the 2346-keV level to be $5/2^-$, $9/2^-$, or $11/2^-$, while Divadeenam's calculations favor an $11/2^-$ assignment. Above the energy of the 2346-keV level, comparisons with the models would not be useful at this time, except to note that the models help to account for the number of new levels seen.

Much more information on the properties of this nucleus is needed. One possible experiment that could be performed is a Method I correlation (Litherland and Ferguson, 1961) using the reaction $^{48}Ca(\alpha,n\gamma\gamma)^{51}Ti$. Another possible experiment

Figure 37. The Experimental Energy Spectrum of ^{51}Ti is Compared with Two Different Model Calculations. Only negative parity levels below 4000 keV are considered. Calculation (a) is a shell model type calculation by Ohnuma (1966). Calculation (b) is an excited-core model calculation by Divadeenam (1971). Both of these calculations are discussed briefly in Chapter 1.

Calculation (a) predicts four states of spin $J \geq 9/2$, and calculation (b) predicts five states of spin $J \geq 9/2$. Several of the experimental levels of unknown spin undoubtedly correspond to these states.

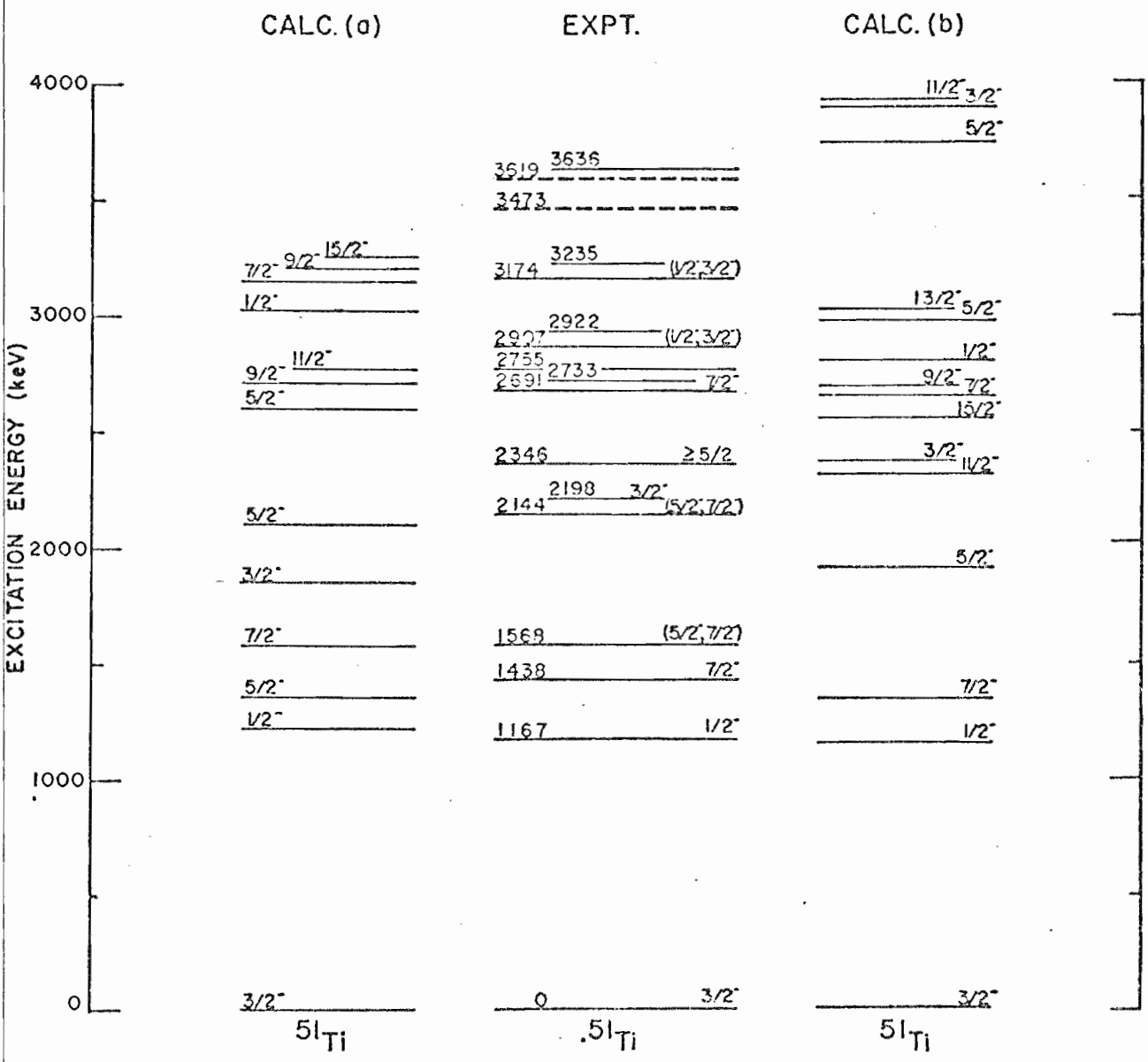
CALC. (a)
EXPT.
CALC. (b)
EXCITATION ENERGY (keV)
4000
3000
2000
1000
0
7/2⁻ 9/2⁻ 15/2⁻
1/2⁻
9/2⁻ 11/2⁻
5/2⁻
5/2⁻
3/2⁻
7/2⁻
5/2⁻
1/2⁻
3/2⁻
51Ti
3619 3636
3473
3174 3235 (1/2,3/2)
2907 2922 (1/2,3/2)
2755
2591 2733 7/2⁻
2346 ≥5/2
2144 2198 3/2⁻ (5/2,7/2)
1568 (5/2,7/2)
1438 7/2⁻
1167 1/2⁻
0 3/2⁻
51Ti
11/2⁻ 3/2⁻
5/2⁻
13/2⁻ 5/2⁻
1/2⁻
9/2⁻ 7/2⁻
15/2⁻
3/2⁻ 11/2⁻
5/2⁻
7/2⁻
1/2⁻
3/2⁻
51Ti

would be to use neutron time-of-flight techniques to resolve the neutron groups from the reaction $^{48}Ca(\alpha,n)^{51}Ti$. Either of these experiments might result in spin assignments of some of the new levels and mixing ratios of the resultant decays.

LIST OF REFERENCES

LIST OF REFERENCES

S. E. Arnell, R. Hardell, Ö. Skeppstedt, and E. Wallander, in Proc. Int. Symp. on Neutron Capture Gamma-ray Spectroscopy, Studsvik, Sweden, 1969 (International Atomic Energy Agency, Vienna, Austria, 1969) p. 183.

P. D. Barnes, C. K. Bockelman, O. Hansen, and A. Sperduto, Phys. Rev. 136B, (1964) 438.

M. C. Bertin and R. G. Hirko, Particles and Nuclei 1, (1971) 359.

L. C. Biedenharn, G. B. Arfken, and M. E. Rose, Phys. Rev. 83, (1951) 586.

A. M. Bizzeti-Sona, R. Messlinger, and H. Morinaga, Z. Naturforschg. 21a, (1966) 906.

T. P. G. Carola, Private Communication (1971).

T. P. G. Carola and H. Ohnuma, Nucl. Phys. A165, (1971) 259.

T. P. G. Carola, W. C. Olsen, D. M. Sheppard, B. D. Sowerby, and P. J. Twin, Nucl. Phys. A144, (1970) 53.

D. J. Church, Private Communication (1969).

E. R. Cosman, D. C. Slater, and J. E. Spencer, Phys. Rev. 182, (1969) 1131.

S. Devons and L. J. B. Goldfarb, in Handbuch der Physik, S. Flugge, Ed., (Springer-Verlag, Berlin, 1957) Vol. 42, p. 362.

M. Divadeenam and W. P. Beres, Phys. Letters 30B, (1969) 598.

M. Divadeenam, Private Communication (1971).

R. N. Glover, A. Denning and G. Brown, Phys. Letters 27B, (1968) 434.

C. R. Gould, Ph.D. dissertation, Univ. of Pennsylvania (1969).

C. R. Gould, E. C. Hagen, R. V. Poore, N. R. Roberson, G. E. Mitchell, and D. R. Tilley, Phys. Rev. Letters 25, (1970) 463

E. Kashy, A. Sperduto, H. A. Enge, and W. W. Buechner, Phys. Rev. 135B, (1964) 765.

T. T. S. Kuo and G. E. Brown, Nucl. Phys. A114, (1968) 241.

L. L. Lee and J. P. Schiffer, Phys. Rev. 154, (1967) 1097.

A. E. Litherland and A. J. Ferguson, Can. J. Phys. 39, (1961) 788.

J. R. Maxwell and W. C. Parkinson, Phys. Rev. 135B, (1964) 82.

J. B. McGrory, B. H. Wildenthal, and E. C. Halbert, Phys. Rev. C 2, (1970) 186.

Nuclear Data Group, Nucl. Data Sheets 4, (1970) V.

H. Ohnuma, Nucl. Phys. 88, (1966) 273.

A. R. Poletti and E. K. Warburton, Phys. Rev. 137B (1965) 595.

N. H. Prochnow, Ph.D. dissertation, Duke University (1971).

K. Ramavataram, Phys. Rev. 132, (1963) 2255.

B. C. Robertson, T. P. G. Carola, D. M. Sheppard, and W. C. Olsen, Nucl. Phys. A160, (1970) 137.

H. J. Rose and D. M. Brink, Rev. Mod. Phys. 39, (1967) 306.

F. Sawa, Progr. Report, Research Inst. for Phys., Stockholm, (1970) 1160.

T. Stammbach, Private Communication (1969).

J. Tenenbaum, R. Moreh, Y. Wand, and G. Ben-David, Phys. Rev. C 3, (1971) 663.

V. K. Thankappan and W. W. True, Phys. Rev. 137B, (1964) 793.

C. K. Tripathi, P. H. Blichert-Toft, and S. Boreving, in Proc. Int. Symp. on Neutron Capture Gamma-ray Spectroscopy, Studsvik, Sweden, 1969 (International Atomic Energy Agency, Vienna, Austria, 1969) p. 183.

J. Vervier, Nucl. Phys. 78, (1966) 497.

BIOGRAPHY

Name: George Paul Lamaze

Date of Birth: January 15, 1945

Place of Birth: Algiers, Algeria

Colleges Attended:

The Florida State University	B.A. in Physics	1965
Duke University	Ph.D.	1972

Publication:

An Angular Correlation Study of the Low-Lying Levels of ^{29}P (with Gould, Moss, Roberson, and Tilley). Nucl. Phys. A158 (1970) 43.

Abstracts:

Study of ^{29}P from the $^{32}S(p,\alpha\gamma)^{29}P$ Reaction (with Gould, Moss, Poore, Roberson, and Tilley). Bull. Am. Phys. Soc. 15 (1970) 565.

Study of ^{51}Ti from the $^{50}Ti(d,p\gamma)^{51}Ti$ and $^{48}Ca(\alpha,n\gamma)^{51}Ti$ Reactions (with Gould, Roberson, and Tilley). Bull. Am. Phys. Soc. 16 (1971) 556.

Positions Held:

Teaching Assistant at Duke University	1966-67
Research Assistant at Duke University	1967-71